Medizinische Fakultät

der

Universität Duisburg-Essen

Aus dem Augenzentrum am St. Franziskus-Hospital Münster

Alteration in bone marrow derived macrophage and trabecular meshwork cell reactions under increased hydrostatic pressure

I n a u g u r a l – D i s s e r t a t i o n

zur

Erlangung des Doktorgrades der Medizin

durch die Medizinische Fakultät

der Universität Duisburg-Essen

Vorgelegt von

Bo Wang

aus Wuhan, P.R. China

2019

DOI: 10.17185/duepublico/72087
URN: urn:nbn:de:hbz:464-20200729-064814-8

Dekan: Herr Univ.-Prof. Dr. med. J. Buer

1. Gutachter: Herr Prof. Dr. med. C. Heinz

2. Gutachter: Frau Priv.-Doz. Dr. Med. H. Westekemper

Tag der mündlichen Prüfung: 23. Juni 2020

Publications

Publications:

1. Kasper M, Walscheid K, Laffer B, Bauer D, Busch M, Wildschütz L, **Wang B**, Loser K, Vogl T, Grajewski RS, Langmann T, Heiligenhaus A. The phenotype of monocytes in anterior uveitis depends on the HLA-B27 status. Front Immunol. 2018 Jul 30;9:1773. doi: 10.3389/fimmu.2018.01773.

Posters:

1. **Bo Wang**, Dirk Bauer, Björn Laffer, Maren Kasper, Solon Thanos, Arnd Heiligenhaus, Carsten Heinz. Increased hydrostatic pressure enhances inflammation and promotes M1 polarization in macrophages. Jahrestagung der Deutschen Ophthalmologischen Gesellschaft 2019.
2. **Bo Wang**, Dirk Bauer, Björn Laffer, Maren Kasper, Martin Busch, Susanne Wasmuth, Arnd Heiligenhaus, Solon Thanos, Carsten Heinz. Increased hydrostatic pressure may alter macrophage function in vitro. Jahrestagung der Deutschen Ophthalmologischen Gesellschaft 2018.
3. Maren Kasper, Karoline Walscheid, Björn Laffer, Dirk Bauer, Martin Busch, Lena Wildschütz, **Bo Wang**, Karin Loser, Thomas Vogl, Rafael S Grajewski, Thomas Langmann, Arnd Heiligenhaus. Monozytensubpopulationen bei Patienten mit HLA-B27-assoziierter akuter anteriorer Uveitis versus HLA-B27-negativer idiopathischer anteriorer Uveitis. Jahrestagung der Deutschen Ophthalmologischen Gesellschaft 2018

Contents

1 Introduction

1.1 The human eye and the anterior chamber

The human eye is a sensory organ that responds to light and provides vision. The eye globe consists of three layers that surround the various anatomical structures. The outermost layer is called fibrous tunic and consists of the cornea, a transparent tissue allowing the light to enter the eye, and the sclera, which is responsible for maintaining eye shape and protecting eye contents. The middle layer, called the vascular tunic or uvea, is composed of the choroid (blood vessel-rich tissue that provides oxygen and nutrients to the retina), and located in the anterior cavity of the eye the ciliary body (accommodation of the lens, secretion of aqueous humor (AH)) and iris (adjust the amount of light entering the eye by controlling the pupil size). In the posterior cavity behind the lens the vitreous is located and adjacent to the this is the retina, which is responsible light perception. The photoreceptors in the retina can transform the light into electrical signals and send the visual information to the brain. To protect the sensitive ocular tissue from damage by pro-inflammatory processes, the eye is also known as an immune privileged organ. The blood-retina barrier and a blood aqueous barrier inhibit the entrance of peripheral immune cells or proteins, and inhibitory ocular micro-environment (immunosuppressive factors in the eye, such as transforming growth factor-beta (TGF-β), FasL, α-MSH, and others), modulating residential macrophages and infiltrated activated immune cells to maintain the immune privilege of the eye (Cone and Pais 2009; Zhou and Caspi 2010).

Inside the eye, the AH is located between the cornea and the lens. The anterior chamber (AC)(Fig. 1) is the cavity bounded by the cornea, iris and lens, and the angle of the AC is located at the edge, surrounded by the corneal limbus (the anterior wall), ciliary body and iris root (the posterior wall). The anterior boundary of the AC angle is called the Schwalbe line. The scleral spur protrudes to the AC and is the attachment point of the ciliary muscle. The trabecular meshwork (TM) is located on the inner side of the Schlemm's canal (SC), between the Schwalbe line and the scleral spur. The AC angle is the main passage for AH, anatomical or cellular changes of this area are associated with the progression and treatment of various types of glaucoma.

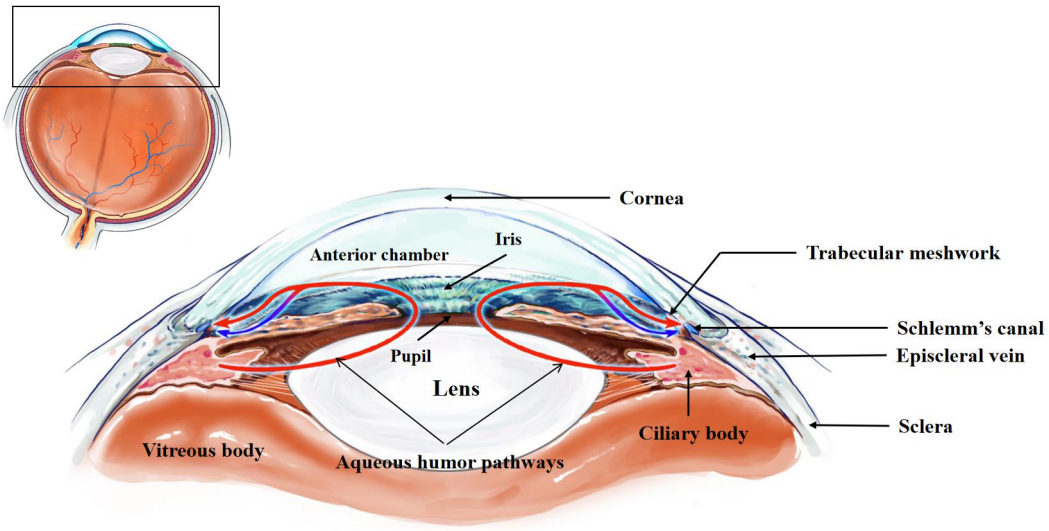

Figure 1 The human eye and the structure of the anterior chamber angle
Arrows represent aqueous humor outflow pathway. Figure was drawn by Zhiqiang Liu and permission is granted.

1.2 Aqueous humor and intraocular pressure

AH is produced by the ciliary body and flows through the pupil to the AC. The outflow pathways of the AC are divided into a trabecular outflow through the meshwork which accounts in normal uninflamed conditions for the majority of outflow and an uveoscleral outflow which capacity is used by anti-glaucomatous medication as prostaglandins or under inflammatory conditions (Fig. 2). Besides, small amount of AH flows via the iris, back into the posterior chamber and is cleared through the retina (Civan and Macknight 2004).

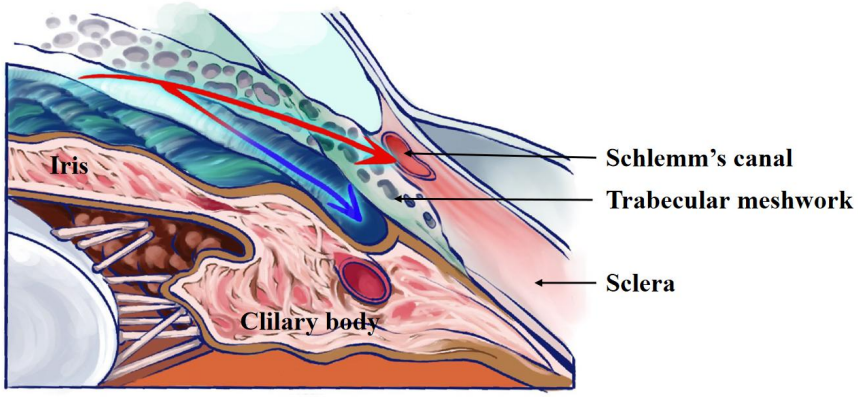

Figure 2 The AH outflow pathway
The red arrow showing the trabecular outflow pathway and the blue arrow showing the uveoscleral outflow pathway. AH=aqueous humor. Figure was drawn by Zhiqiang Liu and permission is granted.

The homeostatic balance between AH production and outflow rate determine the intraocular pressure (IOP). In healthy individuals, the secretion rate of the AH is almost equal to the draining rate, the IOP variations are in a small range and do not cause persistently elevated pressures. The balance of IOP is of great importance to the whole eye health and function. Disruption of this homeostasis may contribute to ocular hypertension (OHT) or glaucoma. Elevated IOP does not result from increased production of AH but rather from reduced aqueous outflow (Kwon et al. 2009). The resistance of the AH outflow is the main factor determining the IOP and it is generated mainly by the hydraulic conductivity of cells or surrounded extracellular matrix (ECM) in TM and the inner wall endothelium of SC. The elevated resistance is a primary factor for the increase IOP associated with glaucoma (Overby et al. 2009).

1.3 Trabecular meshwork in health and disease

TM is an avascular, structurally complex connective tissue that connects Schwalbe's line, scleral spur and ciliary muscle, spanning the entire length of the SC. The TM can be divided into four parts (from inside to outside): (1) the uveal meshwork, which is located close to the anterior chamber, consistent of TM cells covering a network of collagen and elastin, to form a large "open space" between the layers. (2) The corneoscleral meshwork which is located in the middle, consisting of TM cells and perforated collagen and elastin plates. (3) The juxtacanalicular (JCT) TM is a loose connective tissue composed of TM cells and the surrounded ECM. These three parts are regarded as the “filtering” TM, because they are located directly over the SC. Furthermore, (4) there is an “insert” part, which is considered as “non-filtering” TM. To ensure effective generation and regulation of outflow resistance (and thus IOP), the AH first passes through the uveal and corneoscleral TM, which act as a self-cleaning filter (functioning together with other cells, e.g. macrophages) that intercepts cell debris before reaching the JCT TM and inner wall of SC.

The TM cells in conventional outflow tissue have two different morphologies. The internal TM cells have macrophage-like activity, and take up and digest cell debris

before it reaches the deep part of the TM, therefore providing scavenger function (Grierson and Lee 1973). In order to keep the outflow pathway clean, the inner TM cells are functioning as endothelial cells, producing large amounts of heparin sulfate and tissue plasminogen activator. Like endothelial cells, the internal TM cells may mediate inflammation, by producing a variety of inflammatory cytokines like interleukin (IL)-8, chemokine ligand (CXCL)-6 and monocyte chemoattractant protein (MCP)-1 with or without any further pro-inflammatory stimulation (Shifera et al. 2010). According to the duty of IOP resistance generation, cells in the JCT region have fibroblastic and smooth muscle-like properties. Furthermore, TM cells can secrete large amount of ECM proteins, their homologous degrading matrix metalloproteinase (MMPs) and tissue inhibitor of MMP (TIMP) to support the remodeling of ECM (Kelley et al. 2009).

The composition of ECM, the contractile properties of TM itself and other factors together control the size of the spaces between the trabecular sheets, thereby controlling the outflow resistance. The dysfunction in TM can disturb the outflow, and thereby cause elevated IOP, which may induce damage to optical nerve head (ONH) in the retina, as commonly seen in glaucoma. Various IOP-regulating molecules and mediators affect the outflow through different mechanism. Nitric oxide (NO) is thought to be involved in the regulation of TM and have IOP-lowering effect (Chuman et al. 2000). The change in MMP/TIMP balance influences the ECM turnover, thereby influence the outflow resistance and IOP (Bradley et al. 2003). Activated TGF-β1 in TM can promote MMP-2 synthesis and enhance outflow facility temporarily, but the continuous activation may cause abnormal increased production of ECM in TM (Liton et al. 2005).

1.4 Glaucoma

Glaucoma is a group of chronic optic neuro-degenerative diseases, which is one of the leading causes of blindness all over the world. Worldwide, the glaucoma-caused progression of visual loss is expected to affect 111.8 million people by 2040 (Tham et al. 2014). Although family history, age, and ethnicity may have an impact on glaucoma, the most important risk factor is elevated IOP (Paul et al. 2000). Glaucoma is characterized by ONH damage, loss of optic nerve axons and retinal ganglion cells (RGCs) due to

high pressure in the eye (Nickells 2007). According to the different appearance of the anterior chamber angle, glaucoma can be classified into open-angle glaucoma (OAG) and angle closure glaucoma (ACG). They can be further divided into primary and secondary types. The global prevalence of primary OAG (POAG) (3.1%) was six times more than that of primary angle-closure glaucoma (PACG), but the PACG has a poor prognosis because of that the bilateral blindness related to glaucoma was more common in PACG than in POAG (Tham et al. 2014). In OAG, the AH is able to path through the TM and SC, but there is an increase of outflow resistance. Optic-nerve damage can develop even with a normal level of IOP in OAG (Kwon et al. 2009). The AH outflow pathway is obstructed in patients with CAG due to mechanical blockage of the outflow pathway by the peripheral iris.

An unstable or inadequate ocular blood supply and the following ischemia or reperfusion injury may cause damage to the ONH during glaucoma (Reinhard et al. 2017). Neuroinflammation are also thought to play an essential role in the process of glaucoma (Williams et al. 2017). During the pathogenesis of glaucoma, the activated astrocyte/microglia/macrophages and the released ILs and inflammatory cytokines cause damage to ganglion cell axons (responsible for neurotropic support) and apoptotic death of RGCs (Nickells 2012). These primary dying RGCs can also activate macroglia and microglia, producing tumor necrosis factor (TNF)-α and other pro-inflammatory cytokines, which can directly or indirectly induce apoptosis, affecting neighbor RGCs and eventually leading to the disappearance of RGCs and the loss of neural tissue (Williams et al. 2017).

IOP measurement is important for glaucoma diagnosis and follow-up. Although IOP is not a primary criterion for diagnosis, it is the major, controllable risk factor and is still the main goal for the glaucoma treatment. Perimetry visual-field test is also an important technique for diagnosing and tracking optic nerve damage in glaucoma (Paul et al. 2000). Although visual field loss can confirm the diagnosis of glaucoma, 20%-50% of RGCs may be lost before the loss of visual field are detectable in the standard test (Harwerth et al. 2010). The standard method of detecting glaucoma is to examine the glaucomatous changes in ONH and the retinal nerve fiber layer, including

the enlargement and deepening of the optic cup, thinning of the retinal nerve fiber layer and optic disc hemorrhages (Zhang et al. 2016). These changes can be measured by ophthalmoscopy or, more reliable, by optical coherence tomography.

Reducing IOP is the only proven way to treat or slowing the progression of glaucoma (Boland et al. 2013). Topical medication, such as prostaglandin analogues, miotics, β-adrenergic blockers, α-adrenergic agonists and carbonic anhydrase inhibitors can efficiently lower IOP (Yasuda et al. 2017). However, they may have some local or systemic adverse effects (such as pigmentation, bradycardia and arrhythmias). Laser or incisional glaucoma surgeries (such as trabeculectomy and implant drainage device) can be performed when medical treatment cannot achieve adequate IOP reduction, but a risk of complications (inflammation, low IOP, etc.) and reduced long-term success because of the fibrotic response at the surgical site, are still major clinical problems (Rulli et al. 2013).

1.5 Macrophages

Macrophages are a group of cells with strong plasticity, heterogeneity, and varied immunological functions, which are closely related to various physiological and pathological processes. According to the different functions, activated macrophages can be involved in both inflammatory and repair processes. They can be divided into classical activated (M1) or alternative activated (M2) macrophages (Martinez et al. 2008; Murray et al. 2014).

Interferon (IFN)-γ and lipopolysaccharide (LPS) stimulate M1 activation, which results in acute pro-inflammatory response and inflammatory clearance by secreting large amount of pro-inflammatory cytokines such as TNF-α, IL-1β/6/12/23, NO and reactive oxygen species (ROS), highly express CD40, CD80, CD86, CCR2, and inducible nitric oxide synthase (iNOS). Activation of M2 is mediated by IL-4, IL-10, and IL-13, and macrophages highly express Dectin-1, CD163, CD206 and CX3CR1 on their surface. M2 macrophages usually produce high level of IL-10, arginase-1 (Arg-1), and low level of IL-12, with little or no secretion of pro-inflammatory cytokines, increased secretion of anti-inflammatory cytokines, inhibit inflammatory response and

promote would healing and angiogenesis (Mantovani et al. 2004; Gordon and Martinez 2010).

Macrophages are widely distributed in various tissues and organs, including the eye. Recently, related studies have suggested that neuroinflammation is closely related to the pathogenesis of all types of glaucoma (Soto and Howell 2014) and macrophages/monocytes play an important role in the development and progression of glaucoma (Williams et al. 2017). Studies showed that number of macrophages was increased in the TM of human eyes after selective laser trabeculoplasty, and infusing macrophages into the anterior chamber of a rabbit model could increase AH outflow (Alvarado et al. 2010). Increased infiltration of macrophages in the iris and ciliary body was found in LPS-induced acute anterior endotoxin-induced uveitis in mice, and the depletion of macrophages in the anterior chamber significantly suppressed the clinical and histological manifestations of uveitis (Pouvreau et al. 1998). Infiltration of macrophages/monocytes into the AH outflow pathway, which is a common process in neurodegenerative diseases, has been shown to be closely associated with the development of glaucoma in DBA/2J mice, as DBA/2J mice lacking infiltrating monocytes do not develop glaucoma after irradiation (Howell et al. 2012). These findings suggest that macrophages/monocyte infiltration may be related with the development of glaucoma. Moreover, IFN-γ, and numbers of cytokines related to macrophages are known to influence the outflow facility and neuroinflammation in glaucoma (Williams et al. 2017).

Various experimental studies have shown that macrophages infiltrate the eye and the retina during development of glaucoma and macrophage depletion reduces RGC loss, suggesting a detrimental effect of macrophages during experimental glaucoma (Huang et al. 2007). Therefore, macrophages might be considered as a novel therapeutic target to the treatment of evaluated IOP in the eye.

1.6 Uveitis, intraocular hypertension and secondary glaucoma

Uveitis is a group of ocular inflammatory diseases that may involve uvea, retina or vitreous. Uveitis may develop in all ages, races and occur frequently in young and

middle-aged adults. Uveitis is often prone to recurrence, finally leading to serious complications, including secondary cataract, secondary glaucoma, cystoid macular edema (CME), retina scars and optic neuropathy, visual impairment and blindness. In fact, uveitis is the fourth common cause of blindness worldwide (Rothova et al. 1996; Acharya et al. 2013).

Uveitis can be idiopathic, and can also be associated with infectious or systemic diseases. Uveitis is usually classified into anterior uveitis (iritis, iridocyclitis or anterior cyclitis), intermediate uveitis (para planitis, posterior cyclitis or hyalitis), posterior uveitis (focal, diffuse choroiditis, chorioretinitis, retinitis or neuroretinitis) and panuveitis (two or more of these segments affected) according to the anatomical location of the inflammation (Jabs et al. 2005). Anterior uveitis is the most common form of uveitis (Deschenes et al. 2008).

Glaucoma with elevated IOP may occur in up to 41.8% of patients with uveitis (Herbert et al. 2004). The mechanism of raised IOP in uveitis is complex: trabeculitis and clogging of the TM with inflammatory cells (most commonly seen in viral uveitis) may lead to a reduced AH outflow and acute IOP elevation with open angles; pupillary block and forward movement of the iris root or lens often cause acute and closed-angle IOP elevation; chronic inflammation may cause damage to TM, which then develops to chronic and open-angle IOP elevation, and synechial closure usually cause chronic IOP elevation with close angles; iatrogenic factor, such as the use of corticosteroids to manage intraocular inflammation, is also important for IOP elevation in uveitis (Din et al. 2012).

The majority of uveitis glaucoma (UG) patients suffer from secondary OAG (SOAG) while only few of them have angle closure (Heinz et al. 2009). The chronic changes in the TM outflow pathway (ECM deposition, alternation of the structure or function in TM cells) by inflammatory activity, and the corticosteroids treatment may influence the development of uveitis glaucoma (Bauer et al. 2018).

The clinical management of uveitis include the controlling of the intraocular inflammation, controlling increased IOP, and treating for potential systemic disease. Corticosteroids are the mainstay of therapy and can be used, depending on the anatomic

subtype of uveitis, topically, periocularly, intravitreally or systemically. Due to the potential side effects of long-term use of corticosteroids, such as cataract, glaucoma or local immunosuppression, corticosteroid-free drugs (such as methotrexate, mycophenolate mofetil, T-cell suppressors, cytotoxic agents and TNF inhibitors) or less effective corticosteroids should be slowly replaced if long-term anti-inflammatory therapy or drugs is required (Fini et al. 2017).

1.7 Glucocorticoids induced glaucoma

Glucocorticoids (GCs) are the main treatment for various ocular diseases. Topical ocular or intravitreal injections (including subconjunctival, subtenon, retrobulbar, or peribulbar) are the most common routes of administration for GCs, and long-term GCs treatment (weeks to months) can increase IOP in some individuals painlessly, which can later lead to glaucomatous optic neuropathy if left untreated (Fini et al. 2017). The properties of the GC, the way of administration, the duration of treatment and the susceptibility of the individual may play roles in GC-induced OHT. About half of individuals experienced with high intraocular concentration of GCs have OHT, and almost all glaucoma patients are responsive (developing increased IOP during therapy) to steroid (Clark et al. 2005).

Besides individual susceptibility, GCs can change the structure and function of TM cells, including reorganizing cytoskeleton (Raghunathan et al. 2015), inhibiting phagocytosis (Zhang et al. 2007), inhibiting cell proliferation or migration (Stamer and Clark 2017) and increasing the deposition of ECM (e.g. fibronectin and collagen) (Kasetti et al. 2017). As a result, the aqueous outflow resistance increased and IOP elevated, which can also be found in POAG patients. The exact mechanism of GC-induced OHT is not fully understood and cases of GC-OHT are normally treated with IOP lowering medication or surgery.

1.8 The pressure chamber system

Direct application of mechanical stress (sheer force or hydrostatic pressure (HP)) to the human eye, tissues or TM cells *in vitro* can be used as a model to study high IOP in humans. A great number of studies have documented changes in outflow pathways

under the influence of changed IOP using perfused enucleated eyes or anterior chamber systems applied with different pressures for varying time periods.

In this study, an already described pressure chamber system (Böhm et al. 2016) was used to incubate cell cultures under different hydrostatic pressure (Fig. 3). The chambers are out of rust-free steel, 15cm in diameter and 10cm deep with lids. Each chamber is connected to two external pressure meters, one is for measuring the internal pressure constantly and the other is for pressure adjustment. Various kinds of culture plates, flasks or petri dishes can be placed into the chambers. The chamber system can be used to reproducible generate various HP conditions *in vitro* and are able to keep constant pressures for several days.

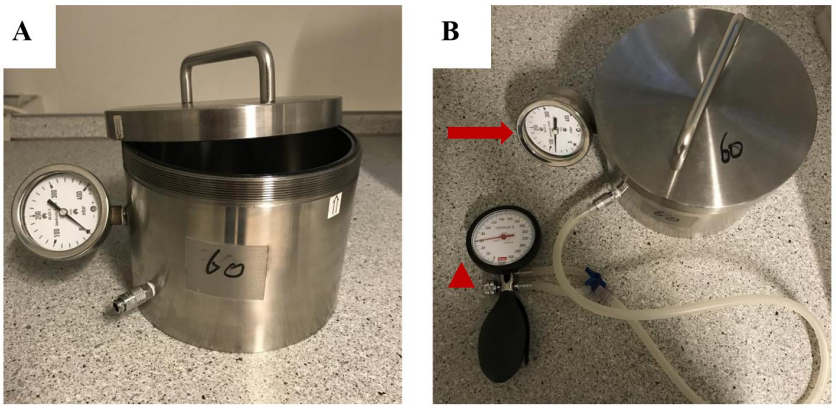

Figure 3 Pressure chamber system
(A) Basic structure of the pressure chamber system. (B) The system can establish and keep a constant pressure. Arrow shows the external pressure meter which can control and generate the internal pressure, triangle shows another external pressure meter which can adjust and measure the internal pressure.

1.9 Aims of the study

Elevated IOP is the most important and the only modifiable risk factor in glaucoma. For inflammatory eye diseases, like uveitis, elevated IOP, which later may develop to secondary glaucoma, is one of the most sight-threatening complication and difficult to treat. GCs are commonly used to treat cases of uveitis, however, GCs are also known to have a major impact on TM. The TM plays a major role in the AH outflow facility. The alterations of the micro-environment in TM (inflammation- or GC-related changes in TM) may influence the functions of TM, which is related to the development of increased IOP. As GCs are widely used in the treatment of uveitis, and with regard to

their known impact on TM, GC-related alteration of TM might also plays a role in GC-induced OHT. Resident macrophages and the infiltration of macrophages in the TM outflow pathway during inflammation modulate the TM outflow facility. In dependence to environmental factors, macrophages are able to polarize in M1 or M2 phenotypes, and modulate pro- or anti-inflammatory responses. The exact role of macrophages or TM cells under increase IOP or GC-induced OHT are not fully understood. Therefore, in this thesis, BMDMs and HTM cells were studied under increased HP with or without GC, generated *in vitro* by a pressure chamber system, to answer the following questions:

(1) Studying the role of increased HP on the M1/M2 polarization of BMDMs and their effector response (production of cytokines, NO, ECM, et al.) during pro-inflammatory or Dexamethason-treated conditions, explaining the role of macrophage under elevated IOP and GC-induced OHT;

(2) Studying the influence of increased HP on HTM cells (production of TNF-α, NO, ECM, et al.) when cultured under increased hydrostatic pressure during pro-inflammatory, Dex-treated, or Adalimumab-treated conditions, explaining the role of HTM cells under elevated IOP and GC-induced OHT;

(3) Comparing the reaction of HTM cells with the reaction of BMDMs under different conditions, finding possible similarities or synergistic effect leading to elevated IOP and GC-induced OHT.

2 Materials and Methods

2.1 Materials

2.1.1 Chemicals

Name	Company
Accutase	Biowest, Nuaillé, France
Acetic acid	Carl Roth, Karlsruhe
Amphotericin B	VWR International, Darmstadt
Aqua bidest	Carl Roth, Karlsruhe
Bluing solution	Shandon GmbH, Frankfurt
Demethylsulfoxid (DMSO)	Sigma-Aldrich, Taufkirchen
Eosin Y alcoholic	Shandon GmbH, Frankfurt
Ethanol≥99.5%	Carl Roth, Karlsruhe
Ethylendiamintetraacetat (EDTA)	Sigma-Aldrich, Taufkirchen
Formaldehyde (37%)	Carl Roth, Karlsruhe
Glycerin	Carl Roth, Karlsruhe
Hematoxylin	Shandon GmbH, Frankfurt
Hoechst 33342	Sigma-Aldrich, Tqufkirchen
Hydrochloric acid 6N standard solution (HCL)	Carl Roth, Karlsruhe
Methanol	Carl Roth, Karlsruhe
3- (4,5-Dimethylthiazol-2-yl) -2,5-diphenyltetrazolium bromide (MTT)	Carl Roth, Karlsruhe
Mowiol	Sigma-Aldrich, Taufkirchen
N, N-dimethylformamide (DMF)	Sigma-Aldrich, Taufkirchen
N- (1-naphthyl) ethylenediamine	Sigma-Aldrich, Taufkirchen
Paraformaldehyde (PFA)	Sigma-Aldrich, Taufkirchen
Penicillin / Streptomycin (Pen / Strep)	PAA Laboratories, Pasching
Phosphate-buffered saline (PBS) powder	Carl Roth, Karlsruhe
Sodium azide (NaN_3)	Merck, Darmstadt
Sodium carbonate (Na_2CO_3)	Carl Roth, Karlsruhe
Sodium chloride (NaCl)	Carl Roth, Karlsruhe
Sodium hydrogencarbonate ($NaHCO_3$)	Carl Roth, Karlsruhe
Sodium hydroxide solution (NaOH)	Carl Roth, Karlsruhe
Sulfuric acid (H_2SO_4)	Carl Roth, Karlsruhe
Sulphanilic acid 99% A.C.S Reagent	Sigma-Aldrich, Taufkirchen
Surgipath Paraplast Plus (paraffin)	Carl Roth, Karlsruhe
TRIS-HCl	Carl Roth, Karlsruhe
Triton X-100	Merck, Darmstadt
Trypan blue	Bio-Rad, Hercules, CA, USA
Tween 20	Carl Roth, Karlsruhe
Xylene	Carl Roth, Karlsruhe

2.1.2 Medium and serum

Name	Company
DMEM/Ham's F-12	Biochrom, Berlin
Fetal Bovine Serum (FBS)	Biochrom, Berlin
RPMI 1640	Biochrom, Berlin

2.1.3 Experimental consumables

Name	Company
Cell Counting Slides for TC20	Bio-Rad, Kauwenhoven, the Netherlands
Cell culture flask 75cm^2 with filter screw caps	TPP, Trasadingen, Switzerland
Cell culture plates 6-, 12-, 24-, 96-well, flat bottom	TPP, Trasadingen, Switzerland
Centrifuge tube 15ml, 50ml	Biochrom, Berlin
Chamber Slide (Millicell) EZ Slide	Merck Millipore,Darmstadt
Cover slips	Carl Roth, Karlsruhe
Disposable latex gloves	Carl Roth, Karlsruhe
Eppendorf tubes 1.5ml and 2ml	Carl Roth, Karlsruhe
Greiner round bottom tubes 1.3ml	Greiner Bio One, Frickenhausen
Nunc-Immuno Plate, 96-well microtiter plate (ELISA plate)	Thermo Scientific, Schwerte
Parafilm	Sigma-Aldrich, Taufkirchen
Petri dishes	Thermo Fisher, Dreieich
Pipette tips 10µl, 200µl, 1000µl	Sarstedt, Numbrecht
Serological pipettes 10ml	VWR International, Darmstadt
SuperFrost Plus Microscope Slides	Thermo Scientific, Schwerte
Terumo Syringe without Needle 1ml	Terumo, Eschborn
Test Tube, 12x75mm, blue	Beckman Coulter GmbH, Krefeld
Tissue Tek Cryomold (chamber)	Sakura Finetek, Tokyo, Japan

2.1.4 Instruments

Name	Company
Apotome 2	Carl Zeiss, Jena
Easypet	Eppendorf AG, Hamburg
Elisa Reader MRX-ELISA	Dynatech Laboratories, Sussex, UK
Eppendorf-Zentrifuge	Heraeus Holding, Hanau
Flow Cytometry CytoFLEX	Beckman Coulter GmbH, Krefeld
Fluorescence microscope Axio Imager M2	Carl Zeiss, Jena
Freezers -20°C	Liebherr-Baumaschinen, Dortmund

Freezer -80°C	Heraeus Holding, Hanau
Fridges 4°C	Heraeus Holding, Hanau
Heating & drying ovens Memmert	Dunn laboratory technology, Asbach
Hera Cell Incubator	Heraeus Holding, Hanau
Heraeus Multifuge 3SR Plus	Heraeus Holding, Hanau
HERAsafe Safety Cabinets	Heraeus Holding, Hanau
Inverted microscope CK40	Olympus Germany, Hamburg
Magnetic stirrer hot plate	Heidolph Instrument, Kelheim
Microscope Olympus BX40 F4	Olympus Germany, Hamburg
Multipette M4	Eppendorf AG, Hamburg
NANOpure Diamond	Wilhelm Werner, Leverkusen
Olympus Binocular Microscope SZ-PT	Olympus Europe SE & Co. KG, Hamburg
Paraffin stove	Memmert, Schwabach
Pipette, 10-, 200-, 1000µl	Eppendorf AG, Hamburg
SERVA BlueShake 3D	SERVA Electrophoresis GmbH, Heidelberg
TC20 Automated Cell Counter	Bio-Rad, Kouwenhoven, Netherland
Vacuum pump, KNF	Laboport, Village-Neuf, France
Vortex mixer	Marienfeld, Mergentheim
Water bath	Haake Germany, Vreden

2.1.5 Test systems

Name	Company
Arginase Test System QuantiChrom	Biotrend Chemicals, Cologne
ELISA MAX Standard Test System Mouse IL-6	BioLegend, Koblenz
ELISA MAX Standard Test System Mouse IL-10	BioLegend, Koblenz
ELISA MAX Standard Test System Mouse TNF-α	BioLegend, Koblenz
ELISA Max Standard Test System Human TNF-α	BioLegend, Koblenz

2.1.6 Reagents

2.1.6.1 Buffer and medium:

Reagent	Component
DMEM/F12	17.12g/L DMEM/Ham's F-12 Powder 17.12g/L $NaHCO_3$, pH 7.2 add 1000ml with A.dest.(Stir 2h)
PBS, 10x	9.55 g/L PBS powder in 5L A.dest. dissolve
RPMI 1640	10.43g/L RPMI 1640 powder 2g/L $NaHCO_3$, pH 7.2 add 1000ml with A.dest.(Stir 2h)

2.1.6.2 Cell culture medium:

Reagent	Component
Cell culture medium for HTM cells	DMEM/F12 10% FBS 1% Pen/Strep
Cell culture medium for L929 cells	RPMI 1640 10% FBS 1% Pen/Strep 1% Amphotericin B
Cell culture medium for macrophages	RPMI 1640 10% FBS 15% L929 supernatant 1% Pen/Strep 1% Ciprofloxacin
FBS	Was heated in a water bath at 56°C for 30 minutes to inactivate complement factors and stored at -20°C until use

2.1.6.3 Stimulation reagents:

Reagent	Company
Brefeldin A solution (BFA), 1000x	Thermo Fisher (eBioscience), Dreieich
Dexamethasone D4902 (Dex)	Sigma-Aldrich, Taufkirchen
Lipopolysaccharide (LPS) solution, 500x	Thermo Fisher (eBioscience), Dreieich
HUMIRA® 40mg	AbbVie Biotechnology, Ludwigshafen

2.1.6.4 Reagents for MTT test:

Reagent	Component
MTT solution	Dissolve 5mg/ml MTT in 1xPBS Sterile filtered Storage protected from light at 4°C
Stop solution	50% A.dest. 50% DMF 0.3M SDS Stored at room temperature (RT)

2.1.6.5 Reagents for Immunofluorescence (IF):

Reagent	Component/Company

Fixation solution	4% paraformaldehyde in 1xPBS
Goat serum	Sigma-Aldrich, Taufkirchen
Hoechst 33342	Stock: 1 mg/ml Use: 1 µg/ml (1: 1000) Diluted in 1xPBS
IF washing buffer	1% FBS in 1xPBS
Mowiol (mounting medium)	12g Mowiol 30g glycerol 30ml A. dest. 60ml 0.2M TRIS-HCl buffer
Permeabilization buffer (macrophages)	Permeabilization buffer (10x) Thermo Fisher (eBioscience), Dreieich Diluted 1:10 with A.dest.

2.1.6.6 Reagents for flow cytometry:

Reagent	Company
Cleaning solution Cytoflex "Flow Clean"	Beckman Coulter, Krefeld
Fixation and permeabilization concentrate and diluent	Thermo Fisher (eBioscience), Dreieich
Intracellular fixation buffer	Thermo Fisher (eBioscience), Dreieich
Pass buffer Cytoflex "Sheath Fluid"	Beckman Coulter, Krefeld
Permeabilization buffer (10x)	Thermo Fisher (eBioscience), Dreieich
Washing buffer	1xPBS pH 7.4

2.1.6.7 Reagents for ELISA:

Reagent	Component/Company
Assay diluent solution	10% FBS in 1xPBS
Avidin-horseradish peroxidase (Avidin-HRP)	Thermo Fisher (eBioscience), Dreieich
Coating buffer	8.4g $NaHCO_3$ 3.56g of Na_2CO_3 Add 1.0L A.dest., pH 9.5 Sterile filtered
Coating buffer for IL-10	1xPBS pH 7.4
ELISA-Washing buffer	0.05% Tween 20 in 1xPBS
Stop solution	2M H_2SO_4
3.3', 5.5'-tetramethylbenzidine (TMB) substrate kit	Thermo Fisher (eBioscience), Dreieich TMB Substrate Solution A: TMB Substrate solution B=1:1

2.1.6.8 Reagents for NO-test:

Reagent	Component
Sodium nitrite (NaNO2) standard	10mM
Sulfanilic acid solution	1% sulphanilic acid in 4N hydrochloric acid
N- (1-Naphthyl) ethylene diamine solution	1% N-(1-naphthyl) ethylenediamine in absolute methanol

2.1.6.9 Reagents for Arginase Assay:

Reagent	Component/Company
Arginine buffer	Biotrend Chemicals, Cologne
Leupeptin	Sigma-Aldrich, Taufkirchen
Lysis buffer	10mM Tris-HCL, pH 7.4 1µM Pepstatin A 1µM Leupeptin 0.4 % Triton X-100
Mn solution	Biotrend Chemicals, Cologne
Pepstatin A	Sigma-Aldrich, Taufkirchen
Substrate buffer, 5x	Arginine buffer Mn solution (4:1, v/v)
Tris-HCL 10mM (pH 7.4)	0.3152g Tris-HCL Add 200ml A. dest. Adjust to pH 7.4 with NaOH in A. dest.
Urea reagent	Biotrend Chemicals, Cologne Reagent A:Reagent B=1:1
Urea standard	Biotrend Chemicals, Cologne Stock concentration: 50ng/dL

2.1.7 Fluorochromes

Conjugate	Full name	Laser line	Excitation / Emission (nm)
AF488	Alexa Fluor 488	488	495/519
APC	Allophycocyanin	638	645/660
FITC	Fluorescein-5-isothiocyanate	488	493/525
FVD eFluor 780	Fix viability dye eFluor780	638	633/780
PE	R-phycoerythrin	488	495/575
PerCP/Cy5.5	Tandem fluorochrome peridinin-chlorophyll protein with cyanine 5.5	488	482/690

PE Cy7	Tandem fluorochrome r-phycoerythrin with cyanine 7	488	496/774
Strep/AF 594	Streptavidin / Alexa Fluor 594	488	590/617
PerCP eFluor710	Tandem fluorochrome peridinin-chlorophyll protein eFluor710	488	482/690

2.1.8 Antibodies

2.1.8.1 Antibodies for IF (macrophages):

Name	Source / clone	Conjugate	Company
Anti-mouse F4/80	Rat/BM8	Unconjugated	OriGene
Anti-mouse IL-6	Rat/MP5-32C11	Biotin	eBioscience
Anti-mouse IL-10	Rat/JES5-2A5	Biotin	eBioscience
Anti-mouse TNF-α	Rat/MP6-XT3, MP6-XT22	Biotin	eBioscience
Anti-mouse/human Arg-1	Sheep Polyclonal	PE	R&D System
Anti-mouse/human fibronectin	Rabbit Polyclonal	Unconjugated	Invitrogen
Anti-mouse/human/rat Arg-2	Rabbit Polyclonal	AF488	Bioss
Anti-mouse/human/rat collagen IV	Rabbit Polyclonal	Unconjugated	Invitrogen
Anti-mouse/human/rat iNOS	Rabbit Polyclonal	Unconjugated	GeneTex
Anti-mouse/human/rat smooth muscle actin (SMA)	Rabbit/17H19L35	Unconjugated	Invitrogen

2.1.8.2 Antibodies for IF (HTM cells)

Name	Source / clone	Conjugate	Company
Anti-human collagen IV	Mouse/CIV22	Unconjugated	DAKO
Anti-human Fibronectin	Rabbit Polyclonal	Unconjugated	DAKO
Anti-human myocilin	Rabbit Polyclonal	Unconjugated	SantaCruz
Anti-human/mouse Arg-1	Sheep Polyclonal	PE	R&D System
Anti-human/mouse/rat iNOS	Rabbit Polyclonal	Unconjugated	Invitrogen
Anti-human/mouse/rat/ chicken/pig α-SMA	Rabbit Polyclonal	Unconjugated	Abcam
Anti-human/mouse/rat/	Rabbit Polyclonal	Unconjugated	Invitrogen

canine/bovine eNOS				
Anti-human/mouse/rat/ rabbit/bovine nNOS	Rabbit Polyclonal	Unconjugated	Invitrogen	

2.1.8.3 Antibodies for flow cytometry

Name	Source / clone	Conjugate	Isotype	Company
Anti-mouse CD206	Rat/C068C2	PE	IgG2a, κ	BioLegend
Anti-mouse CD86	Rat/GL-1	PE Cy7	IgG2a, κ	BioLegend
Anti-mouse F4/80	Rat/BM8	PE Cy7	Rat IgG1	BioLegend
Anti-mouse IL-10	Rat/JES5-16E3	AF488	Rat IgG2b, κ	BioLegend
Anti-mouse iNOS	Rat/CXNFT	PerCP eFluor 710	IgG2a, κ	eBioScience
Anti-mouse TNF-α	Rat/MP6-XT22	PE Cy7	Rat IgG1	BioLegend
Anti-human/mouse Arg-1	Sheep Polyclonlal	PE	IgG	R&D System

2.1.9 Mice

C57BL/6J wild type (WT) (Charles River Laboratories, Wilmington, USA) were housed in standard animal rooms under a 12-hour light/dark cycle with food and water provided ad libitum. Mice were housed in the animal facility of the eye clinic at the University of Cologne (approval document number: AZ 2015.A011).

2.1.10 Primary cells and cell lines

HTM cells used in this study were isolated from donor corneoscleral rims which were used for human cornea transplantation (document number: Ethikkommission der Ärztekammer Westfalen-Lippe und der Universität Münster 2018-574-f-N). All experiments involving human tissues or cells were followed the tenets of the Declaration of Helsinki.

The murine L929 cells were from NCTC clone 929 (L cell, L-929, derivative of strain L) (ATCC CCL-1) provided by the German Collection of Microorganisms and Cell

Cultures.

2.1.11 Software

Name	Company
EndNote X9	Thomson ResearchSoft, Stamford, Connecticut, USA
GraphPad PRISM 6	GraphPad Software, La Jolla, California, USA
ImageJ 1.80	National Institutes of Health, USA
Kaluza Analysis 2.1	Beckman Coulter, Indianapolis, USA
Microsoft Excel 2010	Microsoft, Redmond, Washington, USA
Microsoft PowerPoint 2010	Microsoft, Redmond, Washington, USA
Microsoft Word 2010	Microsoft, Redmond, Washington, USA
ZEN lite V2.3	Carl Zeiss, Jena, Thuringia, Germany

2.2 Methods

2.2.1 Experimental flow chart

Bone marrow-derived cells were obtained from C57BL/6 mice (age from 2- to 14 days). After cultured in macrophage complete medium (RPMI containing 10% FBS, 15% L929 supernatant, 1% Pen-Strep and 1% ciprofloxacin) for 1 week, cells were stimulated with medium, LPS, Dex or LPS+Dex separately. Cells after 24-hour stimulation were used for immunofluorescence. After 48h or 1 week stimulation, supernatant from the cells were used for enzyme-linked immunosorbent assay (ELISA) or nitric oxide (NO)-test (Griess-reaction), cells were used for flow cytometry, and the cell lysates were used for arginase activity test (Fig. 4A).

Primary HTM cells were isolated from donor corneoscleral rims for human cornea transplantation and cultured with complete medium. HTM cells from passage four were stimulated differently. Immunofluorescence was performed to cells after 24-hour stimulation. After 48h stimulation, supernatant from the cells were used for ELISA or NO-test, and the cell lysates were used for arginase activity test (Fig. 4B).

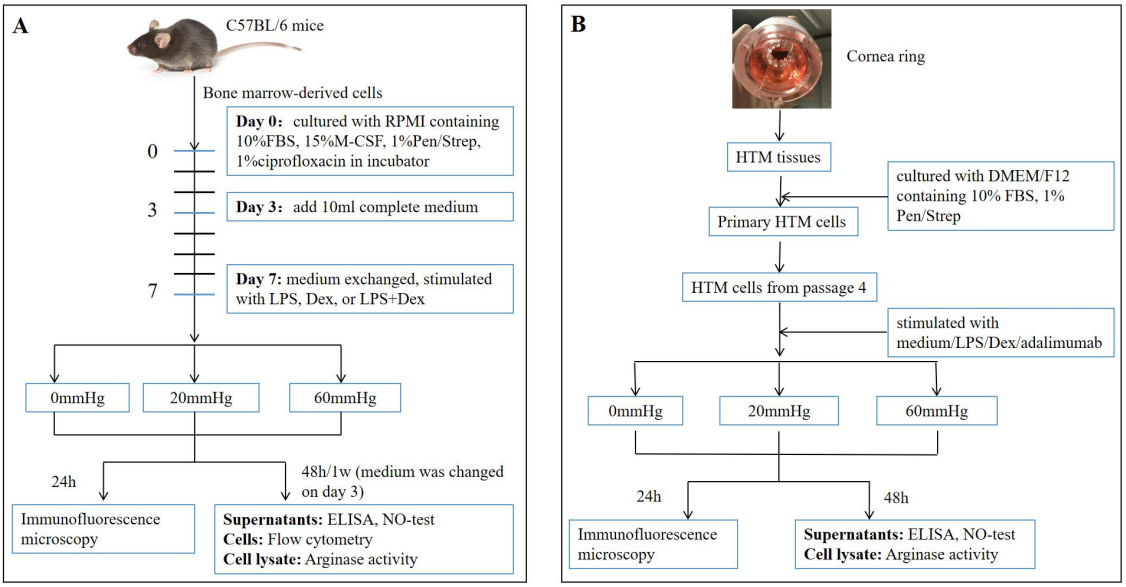

Figure 4 The experimental flow charts

Primary cells were stimulated with different treatments and HPs. After 24h, 48h, or 1w cells and / or cell culture supernatants were subjected to analysis via different immunological assays.The flow charts for experiments of BMDMs (A) and HTM cells (B). BMDMs=bone marrow derived macrophages; HTM=human trabecular meshwork; FBS= fetal bovine serum; M-CSF=macrophage colony-stimulating factor; LPS=lipopolysaccharide; Dex=dexamethasone; ELISA=enzyme-linked immunosorbent assay; NO=nitric oxide.

2.2.2 Isolation and culture of cells

2.2.2.1 Isolation and culture of bone marrow-derived macrophages (BMDMs)

Bone marrow-derived cells were isolated as described previously (Zhang et al. 2008). All forceps and scissors were soaked in 70% ethanol for 5 min before use. Mice were euthanized by CO_2 inhalation, bathed with 70% ethanol, and skin was pealed from the top of the hind leg and down to the foot. Hind legs were cut off with scissors at the hip joint and femurs were left intact.

Femurs were placed in plastic petri dish containing sterile 1xPBS. Excess muscle and other tissues were removed with forceps and scissors. Then the femurs were removed from each joint. 1ml syringe were attached to 27-G needle and filled in with cold sterile RPMI 1640 medium. The needle was inserted into bone marrow cavity of the femurs and bone marrow was flushed 3-5 times with 1ml medium into a 50ml round bottom polypropylene tube until the bone cavity appeared white. Bone marrow suspension was piped up and down to get a single cell suspension.

Cell suspension was centrifuged for 10min at 500g at RT. Supernatant was discarded and cells were re-suspended in macrophage complete medium (RPMI 1640 medium containing 10% fetal bovine serum (FBS), 15% L cell-conditioned medium (sterile filtered supernatant harvested from L929 cells), 1% ciprofloxacin and 1% Pen/Strep). Cells were counted with a hemocytometer and were adjusted to a concentration of $5x10^5$/ml in complete culture medium. 10ml cell suspensions were added into sterile petri dish ($5x10^6$ cells/per dish) and incubated in 37°C, 5% CO_2, humidified incubator.

10ml complete medium was added to each plate on day 3. After 7-days of culturing, more than 90% of the adherent cells were F4/80+ according to a flow cytometry analysis. The BMDMs on day 7 were used for all experiments in which macrophages were used.

2.2.2.2 Stimulation of BMDMs

After 7-day culturing, supernatant was discarded, and adherent cells were washed once with sterile 1xPBS. For immunofluorescence mycroscopy, ELISA, NO test and arginase activity assay, the BMDMs were randomly divided into 2 groups: LPS group and medium (control) group. For LPS group, 10ml complete BMDMs culture medium containing 100ng/ml LPS was added per plate. For control group, only 10ml complete BMDMs culture medium was added per plate. The BMDMs were then continued to be cultured at different pressures.

For flow cytometry detecting CD206 and CD86, macrophages were randomly divided into 4 groups: medium (control) group, LPS group, Dex group and LPS+Dex group. The control group and LPS group were the same as the above, and for Dex group, 10ml complete BMDMs culture medium containing 200ng/ml Dex was added per plate. For LPS+Dex group, 10ml complete BMDMs culture medium containing 100ng/ml LPS and 200ng/ml Dex were added per plate (the concentrations of LPS and Dex were used according to (Kim et al. 2017)). The BMDMs were then cultured under different pressures.

2.2.2.3 Isolation and culture of human trabecular meshwork (HTM) cells

Primary HTM cells were isolated as described previously (Keller et al. 2018). Corneoscleral rims were placed in a sterile plastic petri dish with the corneal endothelium side showing up. Iris and pigment attached on the corneal endothelium side was peeled off carefully with sterile forceps. Under the microscope, the TM tissue could be located between the Schwalbe line and the scleral spur (Fig. 5). TM tissue could be dissected with sterile forceps.

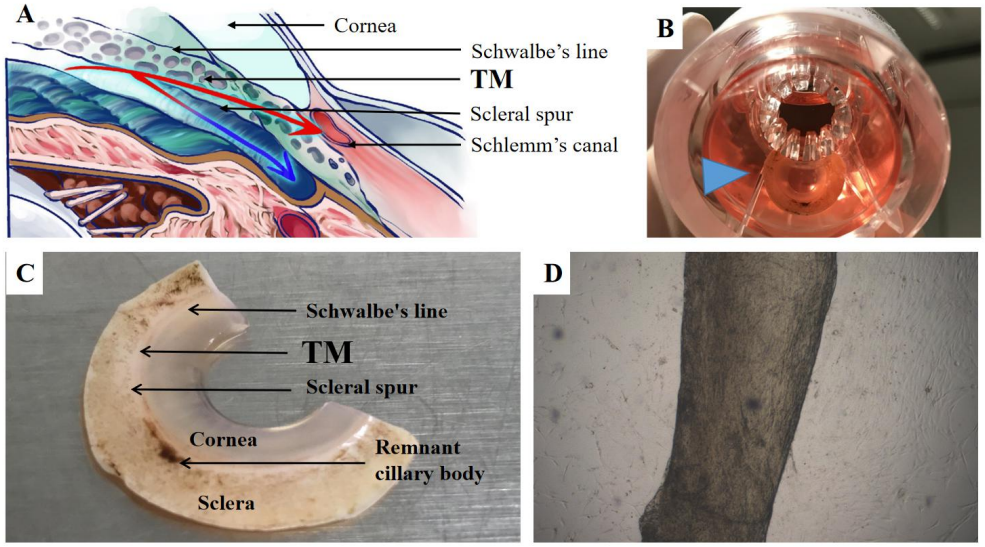

Figure 5 Corneoscleral rim and the TM structure
(A) The structure of the TM tissue in the AC angle. Figure was drawn by Zhiqiang Liu, permission granted. (B) Corneoscleral rim from a human donor. Blue triangle shows the corneoscleral rim. (C) The location of TM in the corneoscleral rim. (D) Cells grown out of TM tissue. TM=trabecular meshwork; AC=anterior chamber.

TM tissues were then placed in a 6-well plate. Sterile cover glasses were put onto the tissues and 2ml Dulbecco's modified Eagle's medium/Nutrient Mixture (DMEM/F12) containing 10% FBS and 1% Pen/Strep was added into each well. The plate was left undisturbed in 37°C, 5%CO_2, in a humidified incubator for 7-14 days.

After observing of an initial cell growth out of the TM (Fig. 5D), medium was exchanged twice a week until cells were grown to colonies which begin to grow together. TM tissues were then removed, the growing cells were maintained and cultured with complete medium. Medium was changed twice a week. After cells approached 90% confluency, medium was discarded and attached cells were washed 3 times with sterile 1xPBS. Cells were then incubated in a standard incubator with 0.25%

trypsin solution (500µl/well) for 5min. 3ml/well complete medium was added and cells were washed away by gently pipetting. Cell suspension was collected into sterile tube and centrifuged for 10min at 500g at RT. Supernatant was discarded and cells were resuspended and adjusted to a concentration of $1x10^6$/ml with complete medium. Cell suspension was dispensed into cell culture flasks. Medium was changed twice a week and cells were subcultured after approaching to 90%. Cells from passage four were used for all experiments.

To characterize the primary cells as TM cells, cells were immunostained with antibodies against fibronectin, collagen IV and Dex-induced myocilin (refer to 2.2.5.2) to characterize them as TM cells (Clark et al. 2001; Stamer and Clark 2017).

2.2.2.4 Stimulation of HTM cells

Cells from passage four were harvested and adjusted to a concentration of $2x10^5$/ml with complete HTM cell culture medium, and cultured in flat cell culture plates for 2 days. After removal of non-attached cells, cells were cultured with serum free medium for 3 days. Cells were then randomly divided into 6 groups. Each group was treated with medium, 1000ng/ml Adalimumab, 100ng/ml LPS, 100ng/ml LPS+1000ng/ml Adalimumab, 100nM Dex and 100ng/ml LPS+100nM Dex separately. The HTM cells were then continued to be cultured under different pressures.

2.2.3 Increased hydrostatic pressure as an *in vitro* model for increased IOP

The pressure chamber system has been described in 1.6. Before using the pressure chamber, the chambers were placed, lid opened, in the humidified incubator (37°C, 5% CO_2) for 1 hour to adapt culture conditions. Cell culture plates were then placed into the different pressure chambers (0mmHg, 20mmHg or 60mmHg), with still opened chambers for 3-4 hours. The chambers were then carefully closed to allow pressure build up. The pressure in the system was adjusted to 0mmHg, 20mmHg or 60mmHg separately. Chambers were incubated in a humidified incubator at 37°C, 5%CO_2 and the pressure was checked every 2 hours in the first 6 hours and then every 12 hours each day.

2.2.4 MTT cell viability assay

BMDMs or HTM cells were harvested and cell suspension was centrifuged at 500g for 5min at 4°C. The supernatant was discarded and cells were washed once by cell culture medium. After centrifugation, cell concentration was adjusted to $1x10^5$ cells/ml in culture medium. 100µl of cell suspension was added per well in 96-well plates and cultured in a standard incubator for 24h. The outermost circle of the plate was filled with sterile 1xPBS only (without cells). After the cells recovered and reattached, supernatant was removed carefully and 100µl/well different medium with different stimulation (BMDMs: medium or 100ng/ml LPS; HTM cells: medium, 1000ng/ml Adalimumab, 100ng/ml LPS, 100ng/ml LPS+1000ng/ml Adalimumab, 100nM Dex or 100nM Dex+100ng/ml LPS) was added to the cells. Each stimulation was repeated six times per plate and medium group was repeated 12 times and served as cell-based controls. The PBS in the wells from the left most column was discarded and replaced with 100µl culture medium (as blank controls). After different cell culture time periods (BMDMs: 48h or 1w; HTM cells: 48h) and different HP conditions in the pressure chambers, 10µl MTT reagent was added into each well. Plates were incubated at 37°C for 4h and purple precipitate could be clearly visible under the microscope. 100µl of stop solution was added to each well and plates were incubated at 37°C in the dark overnight for completely crystals solution. The absorbance was read at 570nm and cell viability was calculated as:

$$\text{Cell viability} = \frac{OD_{sample} - OD_{blank}}{OD_{control} - OD_{blank}} \times 100\%$$

2.2.5 Immunofluorescence staining

2.2.5.1 Immunofluorescence staining for BMDMs

Bone marrow-derived cells were isolated and the cell concentration was adjusted to $2x10^5$/ml with complete BMDMs culture medium. 400µl cell suspension was added into each well of eight-well chamber slides. Cells were cultured for 7 days and medium was exchanged on day 3 and day 5. BMDMs were stimulated with or without 100ng/ml LPS

and incubated at different pressure (0mmHg, 20mmHg or 60mmHg) in the pressure chamber system for 24 hours.

Supernatants were discarded and adherent cells were washed 3 times with sterile 1xPBS. Cells were fixed with freshly prepared 4% paraformaldehyde (PFA) in 1x PBS (200µl/well) for 30min at RT, washed, and air dried. Cells were then blocked with 5% goat serum in 1xPerm Buffer (200µl/well) for 60min at RT and washed 3 times with 1xPerm Buffer. Cells were then incubated with primary antibodies (diluted in goat serum in 1xPerm Buffer, 200µl/well)(Table 1) overnight at 4°C. Cells incubated without primary antibodies served as blank controls.

The next day, cells were washed 3x with 1xPBS (containing 1% FBS) and incubated with secondary antibodies (diluted in 1xPBS containing 1% FBS, 200µl/well) for 30min at RT in the dark. Cells incubated without secondary antibodies served as unstained control. After 3x wash, cells were stained with Hoechst (nucleus staining, diluted in 1xPBS containing 1% FBS, 200µl/well). After 3x wash and air dried, slides were covered with Fluorescence Mounting Medium and coverglass (avoiding air bubbles). The slides were left air dried and self-sealed for 30min at RT.

Staining was observed by fluorescence microscopy using the Aptome with a specific filter set and three images were taken in different areas for each well randomly (Fig. 6).

Primary antibody [stock concentration, mg/ml]	**Dilution**	**Secondary antibody [stock concentration, mg/ml]**	**Dilution**
F4/80 [0.2]	1:500	Goat anti-rat AF488 [0.5]	1:1000
iNOS [0.2]	1:100	Goat anti-rabbit AF594 [2]	1:1000
TNF-α [0.5]	1:200	AF594 Streptavidin [0.5]	1:1400
Arg-1* [0.2]	1:200	none	none
Arg-2 [1]	1:200	Goat anti-rabbit AF488 [2]	1:1000
IL-6 [0.5]	1:200	AF594 Streptavidin [0.5]	1:1400
IL-10 [0.5]	1:200	AF594 Streptavidin [0.5]	1:1400
Fibronectin [0.14]	1:200	Goat anti-rabbit AF488 [2]	1:1000
α-SMA [0.5]	1:200	Goat anti-rabbit AF488 [2]	1:1000
Collagen IV [0.5]	1:200	Goat anti-rabbit AF488 [2]	1:1000

Table 1 Dilutions of the antibodies used in immunofluoresence stainings for BMDMs.
Dilutions of the primary and the corresponding secondary antibodies in immunofluorescence stainings for BMDMs. *Arg-1 antibody directly labeled with PE. BMDMs=bone marrow derived macrophages.

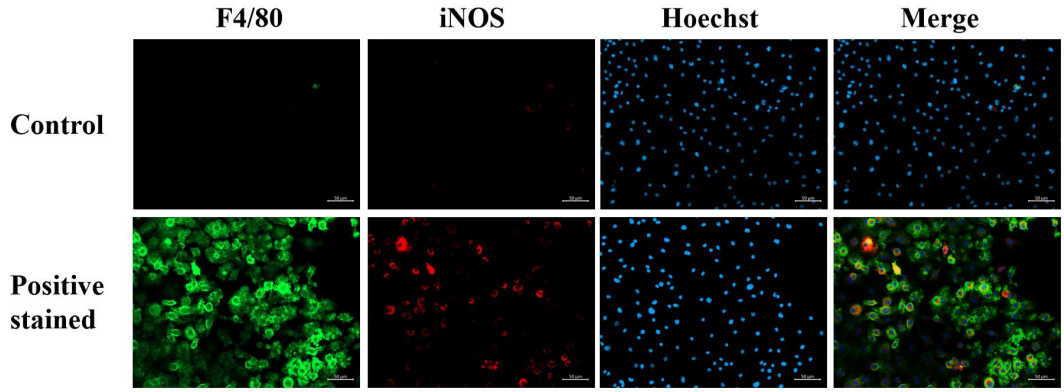

Figure 6 Representative staining of BMDMs obtained from fluorescence microscopy
BMDMs were stained with antibodies against F4/80 (green) and iNOS (red). Nucleus were stained with Hoechst (blue). Images from separate channel and merged image were shown. BMDMs=bone marrow-derived macrophages; iNOS=inducible nitric oxide synthase.

2.2.5.2 Immunofluorescence for HTM cells

Cells from passage three were harvested and adjusted to a concentration of $2x10^5$/ml with complete HTM cell culture medium. 400µl/well cell suspensions were added into eight-well chamber slides and cultured for 1 day. Culturing medium was then changed to DMEM/F12 containing 1% FBS and 1% Pen/Strep and were treated differently and incubate with different pressures (0mmHg, 20mmHg or 60mmHg) in the pressure chamber system for 24 hours.

The subsequent staining procedure was similar to BMDMs (2.2.5.1) (Table 2).

Primary antibody [stock concentration, mg/ml]	Dilution	Secondary antibody [stock concentration, mg/ml]	Dilution
Fibronectin [0.2]	1:400	Goat anti-rabbit AF488 [2]	1:1000
Myocilin [0.2]	1:200	Goat anti-rabbit AF594 [2]	1:1000
α-SMA [0.2]	1:500	Goat anti-rabbit AF594 [2]	1:1000
Collagen IV [0.2]	1:200	Goat anti-mouse FITC [2]	1:500
eNOS [0.5]	1:200	Goat anti-rabbit AF594 [2]	1:1000
iNOS [0.2]	1:100	Goat anti-rabbit AF594 [2]	1:1000
nNOS [0.5]	1:250	Goat anti-rabbit AF594 [2]	1:1000
Arg-1* [0.2]	1:200	none	none

Table 2 Dilutions of the antibodies used in immunofluoresence stainings for HTM cells.
Dilutions of the primary and the corresponding secondary antibodies in immunofluorescence stainings for HTM cells. *Arg-1 antibody directly labeled with PE. HTM=human trabecular meshwork.

2.2.6 Microscopy image acquisition and quantification

Staining was analyzed with a confocal microscope (LSM 710; Carl Zeiss). Images were acquired in single channel and merged by ZEN acquisition software (2012; Carl Zeiss). The images have not been manipulated other than contrast and brightness adjustments.

Mean fluorescence intensity (MFI) and cell numbers were analyzed by the ImageJ software (V1.8.0; National Institutes of Health) (Fig. 7) and the MFI/cell was calculated (Zhou et al. 2017). For analysis, image in Hoechst channel was opened and converted into an 8-bit image. Black and white signals were then reversed for continued analysis. The threshold of the reversed image was adjusted and all signals of nuclear were chosen in order to choose all signal of nuclear (shown in red).

After applied the settings above, signals were shown in black color. Particles were analyzed and the number of nuclear in the whole picture was determined.

The image in different signal channel was opened in ImageJ MFI was measured automatically. The MFI per cell was calculated as:

$$\text{MFI / cell} = \frac{\text{Mean fluorescence intensity}}{\text{Cell numbers}}$$

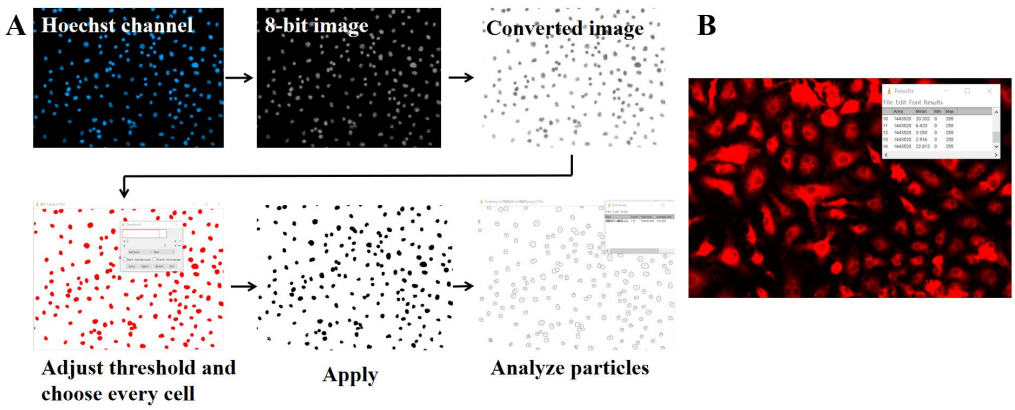

Figure 7 Fluorescence intensity per cell analyzed by ImageJ software
(A) Steps for cell counting. (B) The step for integrated density analysis.

2.2.7 Flow cytometry

2.2.7.1 Extracellular staining:

Culture medium was discarded and adherent cells were washed for 2 times with sterile 1xPBS. 2ml/dish accutase was added and plates were incubated in a standard incubator for 30min. 5ml ice cold 1xPBS/EDTA was added per dish, suspension was pipetted up

and down in order to receive a single cell suspension. The cells were transferred into a 50ml round bottom polypropylene tube.

The tube was filled up to 50ml with sterile 1xPBS. After 10min centrifugation at 1800rpm at 4°C, the supernatant was discarded and cells were resuspended with 5ml sterile 1xPBS. Cell number was calculated, Fc Block (2µl/10^6 cells) was added into the cell suspension and the cells were incubated for 5min at 4°C.

After washing (with 1xPBS) and centrifugation (10 min at 1800rpm, 4°C), cells were resuspended with sterile 1xPBS and the cell concentration was adjusted to 1x10^6 cells in 100µl. 50µl antibody staining solution (in 1xPBS) and 100µl cell suspension were mixed in round bottom Greiner tubes, incubated for 45 min at 4°C (Table 3).

After 10-min reaction, 150µl 1xFixable Viability Dye (FVD) eFlour780 (in 1xPBS) was added into the tube. Cells were washed with 600µl 1xPBS and then centrifuged at 0.5g for 10min. Cells were resuspended in 200µl 1xPBS and transferred into blue PP tube for CytoFlex analysis and results were analyzed by Kaluza software (Fig 8).

Laser	**Filters**	**Dyes**	**Marker [concentration, mg/ml]**	**Amount （µl）**	**Isotype [concentration, mg/ml]**	**Amount （µl）**
488	585/42 BP	PE	CD206 [0.2]	0.625	Rat IgG2a [0.2]	0.625
	780/60 BP	PECy7	CD86 [0.2]	0.625	Rat IgG2a [0.2]	0.625
638	660/20 BP	APC	F4/80 [0.2]	1.25	Rat IgG2a, k [0.2]	1.25
	780/60LP	eFluor 780	Fixable Viability Dye	1:2000	none	none

Table 3 Panel of extracellular staining for BMDMs in flow cytometry.
The panel of antibodies applied in extracellular staining in flow cytometry by CytoFlex analysis of BMDMs. BMDMs=bone marrow-derived macrophages.

2.2.7.2 Intracellular staining:

Before the extracellular staining (2.2.7.1), Brefeldin A solution (1:1000 in complete cell culture medium) was added into each plate, to accumulate proteins in the cells. Cells were incubated for 6 hours.

After extracellular staining of F4/80 (2.2.7.1), cells were incubated with 100µl/tube Ic

Fix Buffer over night at 4°C. The next day, cells were washed with 600µl 1xPerm Buffer (diluted in Aqua. dest) for 2 times. The antibodies for intracellular staining were prepared and diluted in 1xPerm Buffer. Cells were mixed with the antibody solution and incubated for 45min at 4°C (Table 4). After one wash with 1xPerm Buffer and centrifugation (10min at 0.5g), cells were resuspended in 200µl 1xPBS and then transferred into blue PP tubes for CytoFlex analysis. Results were analyzed by Kaluza software (Fig 8).

Laser	Filter	Dyes	Marker [concentration, mg/ml]	Amount (µl)	Isotype [concentration, mg/ml]	Amount (µl)
488	525/40 BP	AF488	IL-10 [0.5]	5	Rat IgG2b [0.5]	5
	585/42 BP	PE	Arg-1 [0.2]	10	Sheep IgG [0.2]	10
	690/50 BP	PerCP-eFluor 710	iNOS [0.2]	0.3	Rat IgG2a [0.2]	0.3
	780/60 BP	PE Cy7	TNF-α [0.2]	1.25	Rat IgG1 [0.2]	1.25
638	660/20 BP	APC	F4/80 [0.2]	1.25	Rat IgG2a,k [0.2]	1.25
	780/60 BP	eFluor 780	Fixable Viability Dye	1:2000	/	/

Table 4 Panel of intracellular staining for BMDMs in flow cytometry.
The panel of antibodies applied in intracellular staining in flow cytometry by CytoFlex analysis of BMDMs. BMDMs=bone marrow-derived macrophages.

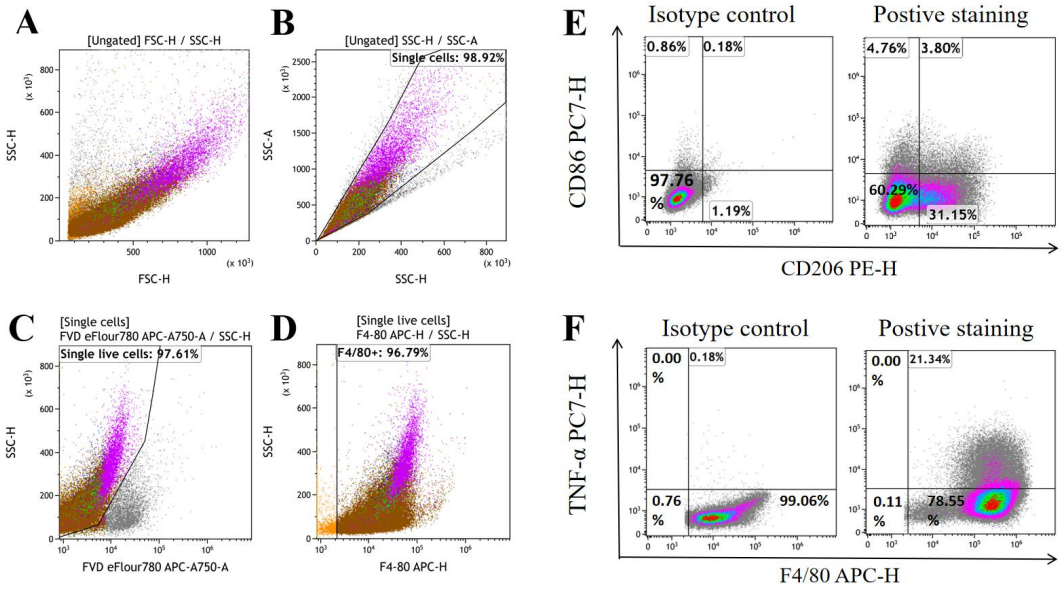

Figure 8 Representative gating strategy of Kaluza analysis

(A) Ungated events from one sample on day 7 in the SSC/FCS window. (B) Ungated events were displayed in SSC-H/SSC-A dot plot. Positive events showed single cells. (C) After gated by single cell, single live cell gate was set and positive events are depicted in the left area. (D) Dead cells were excluded, F4/80 positive events are shown in the right-side gate, which is a marker for macrophages. (E) Extracellular staining of CD86 and CD206 in BMDMs analyzed by Kaluza software. In the dot plot, after F4/80+ gating, CD86+/CD206- events were shown in the upper left area, CD86-/CD206+ events were in the bottom right area, CD86+/C206+ were in the upper right area. (F) Intracellular staining of TNF-α in BMDMs analyzed by Kaluza software. After F4/80+ gating, TNF-α+ events were displayed in the upper right area. The frequency of each population was calculated automatically by Kaluza software. BMDMs=bone marrow-derived macrophages; TNF-α=tumor necrosis factor-α.

2.2.8 Enzyme-linked Immunosorbent Assay (ELISA)

ELISA was performed to detect the amount of TNF-α, IL-6 or IL-10 (ELISA kits BioLegend, Koblenz) released by BMDMs or HTM cells in the supernatant. Cell culture supernatant was harvested from each sample and centrifuged to remove cell debris prior to analysis.

One day before running ELISA, 100µl Capture Antibody solution (in coating buffer) was added to each well of a 96-well plate. The plate was sealed with Parafilm and incubated at 4°C overnight.

After 4 times wash with 300µl/well wash buffer (0.05% Tween-20 in 1xPBS), the plate was incubated with 200µl/well assay diluent solution (in 1xPBS containing 10% FBS) in order to block non-specific binding. The plate was sealed and incubated for 1 hour at RT with shaking (500rpm with a 0.3cm circular orbit). With 4 times wash, 100µl standard dilution and supernatant from each sample were added into appropriate wells. The plate was sealed and incubated at RT for 2 hours with shaking. Detection Antibody solution (100µl/well in assay diluent solution) was added into each well after 4 times washes and incubated for 1 hour at RT with shaking.

After 4 times washing, 100µl Avidin-HRP solution (in assay diluent solution) was added to each well and incubated for 30 min at RT. The plate was then washed carefully for 5 times. TMB Substrate A and B were mixed freshly (1:1) to get the TMB substrate solution. 100µl was added into each well and incubated for 10-15min in the dark at RT. Color change was observed during the time.

When distinct blue color gradient in the standard wells was observed, 100µl/well stop solution (2N H_2SO_4) was added to stop the enzyme reaction. The absorbance was read at 450nm within 15min. The concentration of each cytokine was calculated according to the standard curve.

2.2.9 NO-test (Griess-reaction)

NO-test was performed to detect nitric oxide concentration in the supernatants from BMDMs and HTM cells. Cell culture supernatant was collected from each sample and centrifuged to remove cell debris prior to analysis. Each well of a flat bottom 96-well plate was filled with 50µl cell culture medium, sample supernatant or $NaNO_2$ standard (10mM (mmol/L), diluted in BMDMs or HTM culture medium) was added to appropriate wells, each sample was made in triplicate. 50µl 1% sulphanilic acid solution (in 4N HCl) was added into each well and incubated in the dark for 10min at RT. 50µl 1% N-(1-Naphathyl)-Ethylenediamine solution (diluted in Methanol) was added and the absorbance was read at 550nm within 15min. The concentration of NO in the supernatant was calculated according to the standard curve.

2.2.10 Arginase activity

Arginase activity assay was performed to detect the arginase activity of BMDMs and HTM cells. Arginase kit (Biotrend chemicals, Cologne) was used according to the instructions of the manufacturer.

$1x10^6$ cells per sample were collected and washed with 1xPBS for one time. After centrifugation at 1000g at 4°C for 10min, supernatant was discarded and cells lysed by 100µl of 10nM Tris-HCL (pH7.4) containing 1µM (µmol/L) pepstatin A, 1µM leupeptin and 0.4% (w/v) Triton X-100 for 10min. Cell lysates were centrifuged at 14000g for 10 min at 4°C and the supernatant was collected for arginase assay. Samples were diluted as 1:4 with water. 50µl of 1mM Urea Standard (diluted in aqua dest) or dH_2O was added to appropriate wells of a 96-well plate, and 40µl of sample (made in triplicate) was added into sample wells of the same plate. 5xSubstrate Buffer was prepared by mixing 4 vol of Arginase Buffer and 1vol of Mn Solution. 10µl/well of 5xSubstrate Buffer was

added into 3 sample wells of each group and the other wells were left without Substrate Buffer (blank control wells). The plate was incubated at 37°C for 2 hours. Urea Reagent (200µl/well) was added to each well of the 96-well plate and 5xSubstrate Buffer (10µl/well) was added to the blank control wells, incubated for 60min at RT. The optical density was read at 430nm within 15min. The arginase activity (U/L) was calculated as follows:

$$\text{Arginase activity} = \frac{OD_{sample} - OD_{blank}}{OD_{standard} - OD_{water}} \times 10.4 \times 4 \text{ (U/L)}$$

2.2.11 Statistical analysis

Statistical analyses were performed using Graph Pad Prism software version 7 (La Jolla, CA, USA). Two-way ANOVA analysis followed by Tukey's multiple comparisons test was used to determine significant differences. Results were shown as mean±standard deviation (SD). Differences were considered as statistically significant when $p < 0.05$. All experiments were repeated independently at least 3 times.

3 Results

3.1 BMDMs

3.1.1 Characterization of bone marrow-derived macrophages

Directly after isolation, bone marrow-derived cells (BMDMs) showed a round shape with clear outline, floating in the medium. Few of the cells were attached on the bottom of the petri dish. On day 1, most of the cells still showed a round shape and were in suspension. Some cells were attached to the bottom and started to develop short, thick stretches. On day 3, most of the cells were attached and showed as spindle shape, with thin and long stretches. Nearly each cell was in spindle shape and attached closely to the bottom of the plate on day 7 (Fig. 9).

Cells were then analyzed by flow cytometry. Adherent bone marrow-derived cells on day 7 were harvested and stained with an antibody targeting the murine F4/80 antigen and Fix Viability Dye (FVD) eFluor 780 as a marker for cell viability (refer to 2.2.7). Of all viable cells, 93.46±3.17% were F4/80 positive (n=6) (Fig. 8A-D), indicating that they belong to the macrophage population.

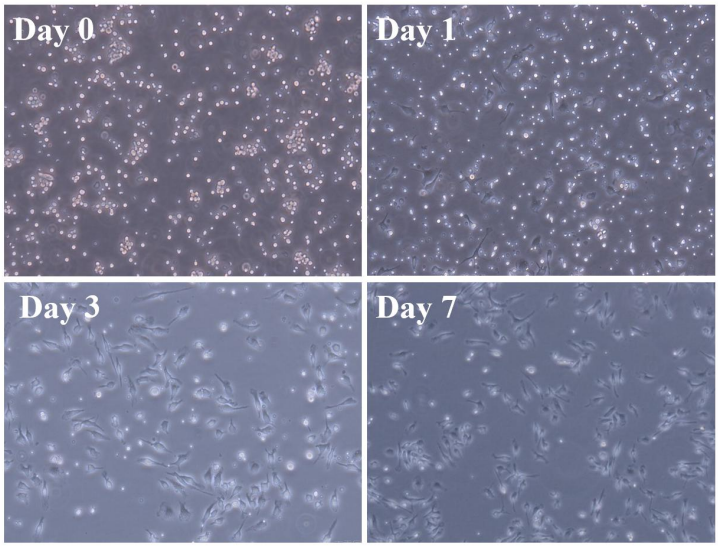

Figure 9 Morphology of bone marrow-derived cells as macrophage population after 7 days
Morphology of cultured primary bone marrow-derived cells from day 0 to day 7. BMDMs=bone marrow-derived macrophages.

3.1.2 Cell viability by MTT conversion assay

To elucidate if increased hydrostatic pressure of 20 or 60 mmHg compared to 0 mmHg

may have an influence on the viability of macrophages, MTT test was performed (refer to 2.2.4). The OD value in medium group at 0mmHg served as control and the viability was set as 100%. Cells of each group were all more than 90% viable. No significant difference in MTT conversion could be found between medium and LPS groups. BMDMs stimulated with Dex showed significantly decreased MTT conversion compared to medium groups (all p values are < 0.001) and to LPS+Dex groups at 0mmHg (p=0.0014) and 60mmHg (p=0.0247). BMDMs of the medium and LPS groups showed an increased MTT conversion after culture under higher hydrostatic pressure (20mmHg or 60mmHg) (all p values are < 0.05). With 60mmHg , the MTT conversion was also increased when macrophages were stimulated with Dex or LPS+Dex. The differences between 0mmHg and 60mmHg in each group reached the significant levels (all p values are < 0.05) (Fig. 10).

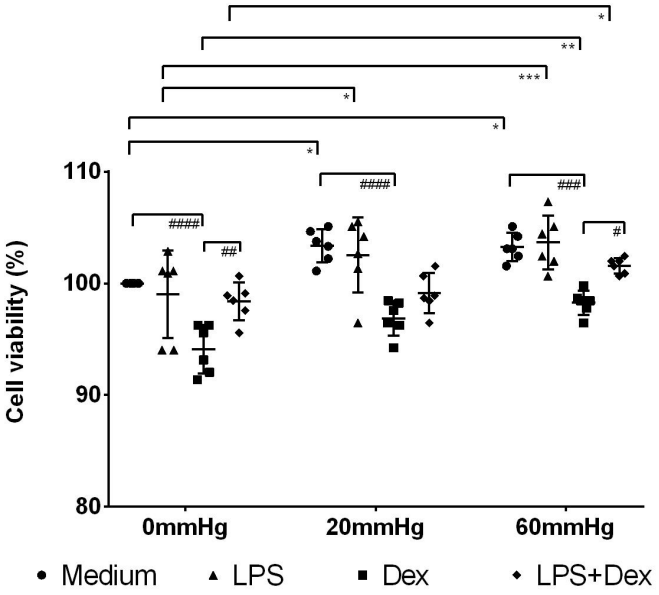

Figure 10 MTT conversion assay of BMDMs under different HP

Cell viability in (%) of medium, LPS, Dex, and LPS+Dex treated BMDMs (n=6 independent experiments). Statistical significance between different pressures (*p<0.05, **p<0.01, ***p<0.001); Statistical significance between different treatments within one pressure (#p<0.05, ##p<0.01, ###p<0.001, ####p<0.0001). LPS=lipopolysaccharide; Dex=dexamethasone; BMDMs=bone marrow-derived macrophages.

3.1.3 Cytokine expression and secretion after increased HP

To determine the role of increased HP on the cytokine expression and secretion in macrophages, BMDMs were stimulated with or without 100ng/ml LPS and cultured

under different HP (0/20/60mmHg). After 24h, the cells were analyzed according their expression of F4/80 in combination with TNF-α, IL-6, IL-10, Arg-1, Arg-2 or iNOS via fluorescence microscopy (refer to 2.2.5.1) and TNF-α, IL-10, Arg-1 and iNOS via flow cytometry (refer to 2.2.7.2).

To determine the alteration of cytokine secretion between groups, TNF-α, IL-6 and IL-10 were quantified in supernatants via ELISA (refer to 2.2.8).

3.1.3.1 TNF-α expression in BMDMs after increased HP

ImageJ analysis of immunofluorescence images shows that LPS stimulation significantly increased TNF-α (MFI/cell) in macrophages (refer to 2.2.6) compared to the macrophages of the medium controls (all p values are <0.01). Furthermore, higher HP resulted in a significantly stronger TNF-α staining (MFI/cell) in BMDMs when macrophages were activated with LPS (0mmHg group versus 60mmHg group: $p<0.0001$; 20mmHg group versus 60mmHg group: $p<0.0001$; Fig. 11A).

To confirm the results of the immunofluorescence staining, flow cytometry was performed (refer to 2.2.7.2). Cells of the medium control comprised the lowest frequency of TNF-α+ events (0.73±0.20%). Even though the frequency of TNF-α+ events raised with increasing HP, no level of significance was reached ($p>0.05$). LPS stimulation led to a significantly enhanced frequency of TNF-α+ events compared to medium control under same pressure conditions (all p values are <0.001). Comparison of LPS treated cells of 0, 20 and 60 mmHg groups showed significantly increased frequency of TNF-α+ events in 60 mmHg group (18.83±1.88%) compared to 0 mmHg (12.11±2.29%, $p=0.0033$) and 20 mmHg (13.64±2.39%, $p=0.0123$) (Fig. 11B).

Quantification of TNF-α in supernatants of BMDMs by ELISA (refer to 2.2.8) showed low level in all medium groups without significant difference under different pressures. After stimulation with LPS for 48 hours, significant more TNF-α could be measured in the supernatant compared to medium groups under all different pressures (all p values are <0.0001). Comparison of LPS treated cells of 0, 20 and 60 mmHg groups (Fig. 11C) showed significantly increased TNF-α level in 60 mmHg group (1693.86±232.68pg/ml) compared to 0 mmHg (1248.81±103.88pg/ml, $p=0.0070$) and

20 mmHg group (1117.68±80.68pg/ml, p=0.0446).

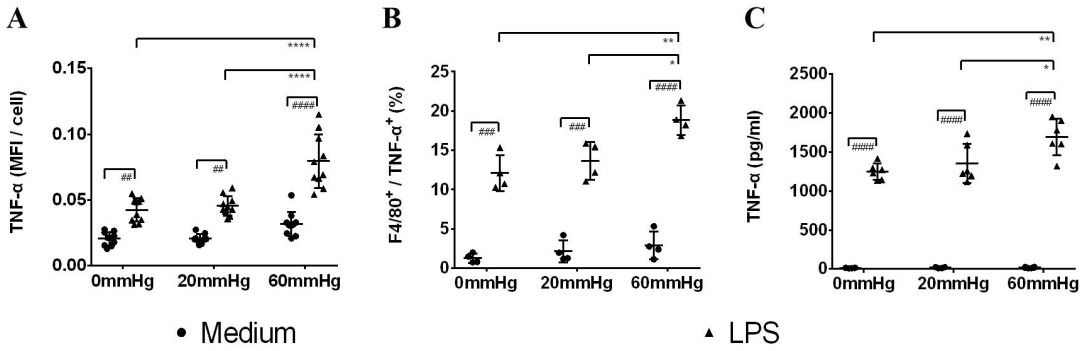

Figure 11 TNF-α expression in BMDMs after incubation under different HP

(A) MFI per cell of immunofluorescence images for TNF-α staining in medium and LPS treated BMDMs by ImageJ analysis (n=10, samples were obtained from 3 independent experiments). (B) Frequency of F4/80$^+$ / TNF-α$^+$ events (%) in medium and LPS treated BMDMs by flow cytometry (n=4 independent experiments). (C) Amount of TNF-α (pg/ml) in the supernatant from medium and LPS treated BMDMs under different HP by ELISA (n=6 independent experiments). Statistical significance between different pressures (*p<0.05, **p<0.01 and ****p<0.0001); Statistical significance between different treatments within one pressure (##p<0.01, ###p<0.001 and ####p<0.0001). TNF-α=tumor necrosis factor-α; BMDMs=bone marrow-derived macrophages; MFI=mean fluorescence intensity; LPS=lipopolysaccharide; ELISA=enzyme-linked immunosorbent assay.

3.1.3.2 Influence of increased HP on the expression and secretion of IL-6 in BMDMs

Immunofluorescence staining targeting IL-6 revealed a faint staining with a low MFI/cell in BMDM with medium. After stimulation with LPS, cells showed an increase of IL-6 (MFI/cell) (all p values are ＜0.01) with further increase at 60mmHg compared to 0 mmHg (p=0.0019) or 20 mmHg (p=0.0022; Fig. 12A).

ELISA analysis showed that IL-6 level was low in the supernatant in medium groups and the differences of IL-6 in the supernatants with medium did not meet the level of significance (p ＞ 0.05). After stimulation with LPS for 48 hours, more IL-6 could be detected in the supernatant (all p values are ＜0.0001). Compared to that in 0 mmHg group with LPS stimulation (2800.29±301.26pg/ml), significant more IL-6 was detected in the supernatant from 60 mmHg group (3593.58±70.16pg/ml, p＜0.0001). Differences between 20 mmHg (3127.73±158.50pg/ml) and 60 mmHg groups with LPS stimulation also met a significant level (p=0.0062) (Fig. 12B).

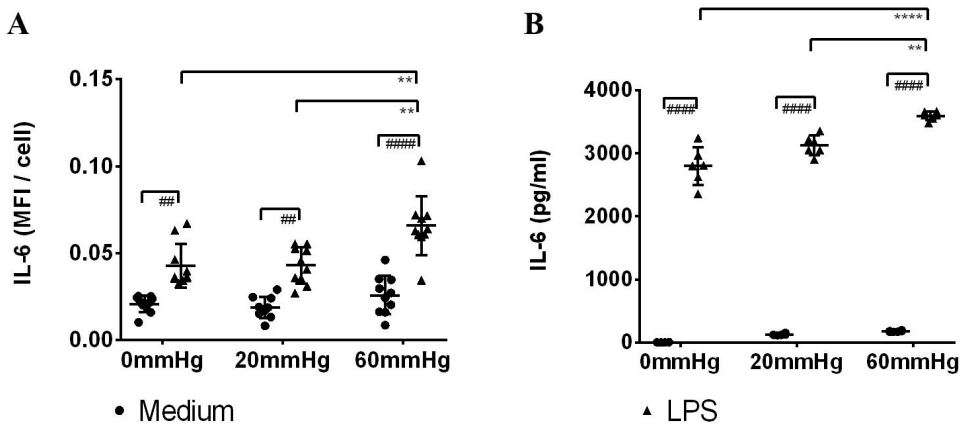

Figure 12 IL-6 expression in BMDMs under different HP

(A) MFI/cell of immunofluorescence images for IL-6 using ImageJ. BMDM were treated with medium or LPS under various HP (n=10, samples were obtained from 3 independent experiments). (B) Amount of IL-6 (pg/ml) in the supernatant from medium and LPS treated BMDMs under different HP by ELISA (n=6 independent experiments). Statistical significance between different pressures (**p<0.01 and ****p<0.0001); Statistical significance between different treatments within one pressure (##p<0.01 and ####p<0.0001). IL-6=interleukin-6; BMDMs=bone marrow-derived macrophages; MFI=mean fluorescence intensity; LPS=lipopolysaccharide; ELISA=enzyme-linked immunosorbent assay.

3.1.3.3 Expression and secretion of IL-10 by BMDMs under increased HP

Although only a low MFI/cell was shown in BMDMs with medium, the MFI/cell of IL-10 still had a slight reduction with increased HP. The difference between various pressure groups were significant (all p values are ＜0.05). After stimulation with LPS, significant increased IL-10 (MFI/cell) could be observed in BMDMs compared to medium controls (all p values are ＜0.0001). Macrophages cultured at 0mmHg with LPS stimulation showed the strongest MFI/cell. The MFI/cell of IL-10 became weaker in cells cultured under 20mmHg (p=0.0001) and the weakest MFI/cell was shown in cells at 60mmHg (p＜0.0001) (Fig. 13A).

The frequency of IL-10 positive events in medium group was lower than 1.20±0.34% and no significant differences were found among different pressure groups (p＞0.05). With LPS stimulation, there was a significantly increased frequency of F4/80+ / IL-10+ events (all p values are ＜0.01). Significant decreased frequency of IL-10+ events could be found between the 0mmHg group (2.00±0.82%) vs. 20mmHg group (1.52±0.45%, p=0.0408) and 0mmHg vs. 60mmHg group (1.38±0.67%, p=0.0116) after

LPS stimulation (Fig. 13B).

In the BMDM supernatants of medium controls, no significant differences of the amount of IL-10 under different HP could be found. After stimulation with LPS for 48 hours, IL-10 level increased significantly compared to medium controls (all p values are <0.0001) but decreased with increased HP. In LPS groups, the differences between 0 mmHg (494.46±22.80pg/ml) and 20 mmHg (454.71±27.73pg/ml, p=0.0096), 0 mmHg group and 60 mmHg (288.94±30.90pg/ml, $p<0.0001$), and 20 mmHg group and 60 mmHg also reached the level of statistical significance ($p<0.0001$)(Fig. 13C).

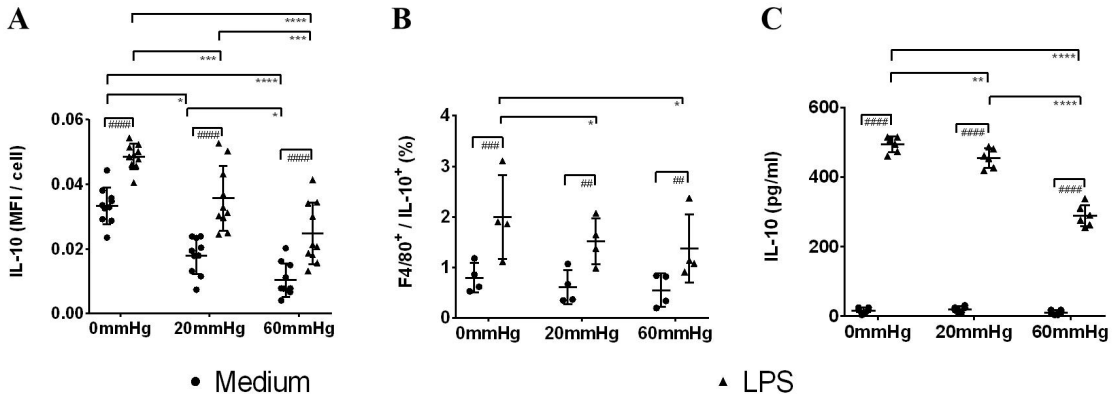

Figure 13 IL-10 expression in BMDMs under different HP

(A) MFI/cell of immunofluorescence images for IL-10 staining in medium and LPS treated BMDMs under different HP by ImageJ analysis (n=10, samples were obtained from 3 independent experiments). (B) Frequency of $F4/80^+$ / $IL\text{-}10^+$ events (%) in medium and LPS treated BMDMs under different pressures by flow cytometry (n=4 independent experiments). (C) Amount of IL-10 (pg/ml) in the supernatant from medium and LPS treated BMDMs under different HP by ELISA (n=6 independent experiments). Statistical significance between different pressures (*p<0.05, **p<0.01, ***p<0.001 and ****p<0.0001); Statistical significance between different treatments within one pressure (##p<0.01, ###p<0.001 and ####p<0.0001). IL-10=interleukin-10; BMDMs=bone marrow-derived macrophages; MFI=mean fluorescence intensity; LPS=lipopolysaccharide; ELISA=enzyme-linked immunosorbent assay.

3.1.3.4 Expression of Arg-1 and -2 in BMDMs under increased HP

Immunofluorescence staining in BMDMs from medium group showed only a faint staining for Arg-1, suggesting low expression. Arg-2 signals were in general more pronounced in BMDMs than the Arg-1 expression. In the medium group there was no significant difference of MFI/cell of Arg-1 between 0mmHg group and 20 mmHg group, however, the Arg-1 (MFI/cell) in 60 mmHg group was significantly increased compared to 0 mmHg (****$p<0.0001$). For Arg-2, no significant difference was found between

pressures in medium groups ($p > 0.05$). LPS stimulation significantly increased MFI/cell of both Arg-1 and -2 compared to medium controls (all p values are < 0.05). With LPS stimulation, the MFI/cell of Arg-1 and -2 was significantly increased with higher HP. Macrophages at 0mmHg showed the weakest MFI/cell of Arg-1 and -2 compared to that at 20mmHg or 60mmHg , and the differences reached the level of significance (all p values are < 0.05). Significant differences could also be found between 20mmHg group and 60mmHg group with LPS stimulation (all p values are < 0.001) (Fig. 14A and B).

The change in frequency of Arg-1+ events in different groups was also determined by flow cytometry (Fig. 14C). There were low F4/80+ / Arg-1+ frequencies in the medium controls and no significant difference was found between pressures ($p > 0.05$). After stimulated with LPS, significant higher F4/80+ / Arg-1 + frequency could be found than that in medium groups under the same pressure (all p values are < 0.01). The highest frequency of F4/80+ / Arg-1+ events could be found in 60mmHg group after LPS stimulation (8.01±0.53%). The difference between 0mmHg group (5.33±2.01%) vs. 60mmHg group reached the level of significance (p=0.0399).

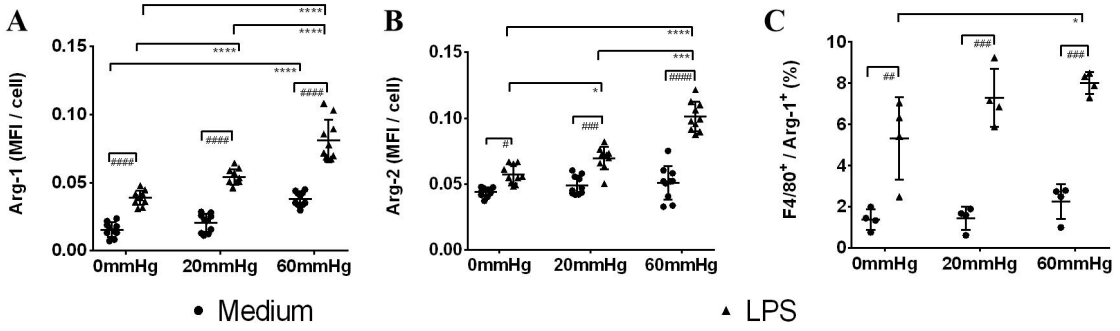

Figure 14 Arg-1 and -2 expression in BMDMs under different HP

MFI/cell of immunofluorescence images for Arg-1 (A) and Arg-2 (B) staining in medium and LPS treated BMDMs under different HP. Images were processed by ImageJ (n=10, samples were obtained from 3 independent experiments). (C) Frequency of $F4/80^+$ / $Arg\text{-}1^+$ events (%) in medium and LPS treated BMDMs under different pressures by flow cytometry (n=4 independent experiments). Statistical significance between different pressures (*p<0.05, ***p<0.001 and ****p<0.0001); Statistical significance between different treatments within one pressure (#p<0.05, ##p<0.01, ###p<0.001 and ####p<0.0001). BMDMs=bone marrow-derived macrophages; MFI=mean fluorescence intensity; LPS=lipopolysaccharide.

3.1.4 Arginase activity in BMDMs under increased HP

Primary BMDMs were stimulated with or without 100ng/ml LPS and cultured under different HP (0/20/60mmHg) for 48h. Cell lysates were used to determine arginase activity via arginase bioassay (refer to 2.2.10).

In LPS groups, significantly higher arginase activity was detected compared to medium controls (all p values are <0.0001). In medium and LPS groups, the arginase activity in macrophages decreased significantly at 20 mmHg (medium: 3.12±0.60 U/L; LPS:11.03±0.31 U/L) as compared to 0 mmHg (medium: 5.25±0.57 U/L, p=0.0245; LPS:17.93±1.92 U/L, $p<0.0001$), and 60 mmHg (medium: 5.73±0.64 U/L, p=0.0090; LPS:19.83±1.36 U/L, $p < 0.0001$). At 60mmHg with LPS stimulation, BMDMs displayed stronger arginase activity (19.83±1.36 U/L) compared to cells at 0mmHg (p=0.0405) and 20mmHg ($p<0.0001$) (Fig. 15).

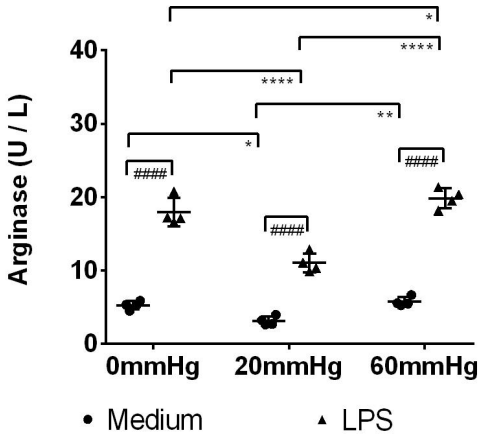

Figure 15 Arginase activity in BMDM under different HP

Arginase activity (U/L) in medium and LPS treated BMDMs under different pressures (n=4 independent experiments). Statistical significance between different pressures (*p<0.05, **p<0.001, ****p<0.0001); Statistical significance between different treatments within one pressure (####p<0.0001). BMDMs=bone marrow-derived macrophages; LPS=lipopolysaccharide.

3.1.5 Expression of iNOS under increased HP

In the unstimulated medium groups, iNOS staining was weak and the differences in iNOS (MFI/cell) in different HP groups were not significant ($p > 0.05$). After LPS stimulation, BMDMs showed a higher iNOS (MFI/cell) compared to medium controls under the same HP level (all p values are < 0.001). With LPS stimulation, iNOS (MFI/cell) decreased significantly in 20 mmHg group ($p < 0.0001$) compared to 0

mmHg, and further decreased at 60mmHg ($p < 0.0001$). The difference between 20mmHg and 60mmHg groups met the level of significance (p=0.0015) (Fig. 16A).

The medium groups showed low frequency of F4/80+ / iNOS+ events and the differences in pressures did not reach the significant levels ($p > 0.05$). However, after stimulation with LPS, higher frequency of F4/80+ / iNOS+ events was detected than in medium groups (all p values are $<$ 0.001). BMDMs cultured at 0mmHg had the highest frequency of F4/80+ / iNOS+ events (11.50±3.07%). When the pressure increased to 20mmHg, the frequency (8.97±2.43%) decreased significantly compared to that in 0mmHg, LPS stimulated group (p=0.0223). The lowest frequency of iNOS+ events in LPS groups could be found at 60 mmHg (7.49±2.66%), met the level of significance compared to LPS group at 0 mmHg (p=0.0022; Fig. 16B).

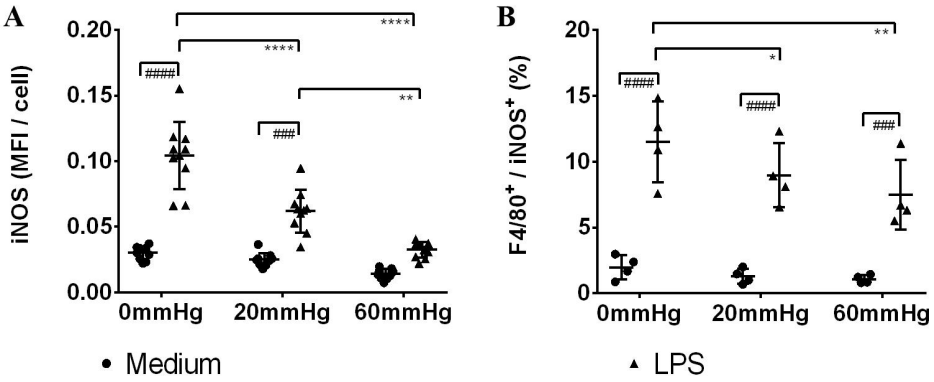

Figure 16 iNOS expression in BMDMs under different HP

(A) MFI/cell of immunofluorescence images for iNOS staining in medium and LPS treated BMDMs under different HP. Images were processed by ImageJ (n=10, samples were obtained from 3 independent experiments). (B) Frequency of $F4/80^+$ / $iNOS^+$ events (%) in medium and LPS treated BMDMs under different pressures by flow cytometry (n=4 independent experiments). Statistical significance between different pressures (*p<0.05, **p<0.01, ****p<0.0001); Statistical significance between different treatments within one pressure (###p<0.001, ####p<0.0001). iNOS=inducible nitric oxide synthase; BMDMs=bone marrow-derived macrophages; MFI=mean fluorescence intensity; LPS=lipopolysaccharide.

3.1.6 Nitric oxide (NO) production of BMDMs under increased HP

To determine whether there could be a difference in the production of NO between each group, NO-test (Griess reaction) with BMDMs supernatants were performed (refer to 2.2.9).

Low amount of NO was found in the supernatants of BMDMs of medium control,

and under different pressures of all medium groups. After LPS stimulation, the generation of NO by BMDMs was strongly increased compared to cells of the medium controls (all p values are <0.0001). LPS stimulation of BMDMs at 0mmHg results in the highest amount of NO (198.48±30.85 μM) and decreased significantly at 60 mmHg (79.55±3.79 μM, p=0.0034). Significant differences of NO levels were also found between 20 mmHg (148.70±4.13 μM) and 60 mmHg (p=0.0096; Fig. 17).

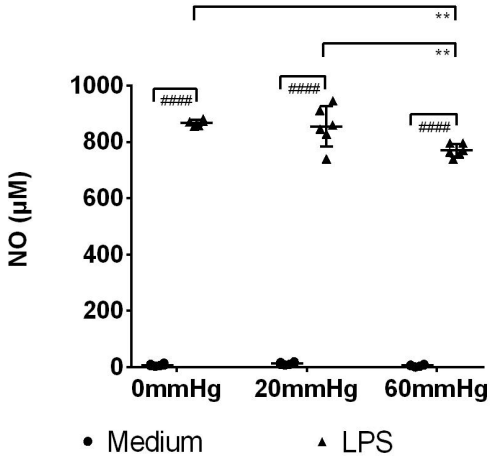

Figure 17 Production of NO of BMDMs under different HP

NO level (μM) in medium and LPS treated BMDMs under different pressures (n=6 independent experiments). Statistical significance between different pressures (**p<0.01, ****p<0.0001); Statistical significance between different treatments within one pressure (####p<0.0001). NO=nitric oxide; BMDMs=bone marrow-derived macrophages; LPS=lipopolysaccharide.

3.1.7 BMDMs polarization under different hydrostatic pressure conditions

To study the polarization of macrophages under different HP, flow cytometry analysis was performed after BMDMs were cultured with medium, 100ng/ml LPS, 200ng/ml Dex or LPS+Dex for 48h (refer to 2.2.7.1). Within the population of F4/80+ cells, the surface marker CD86 and CD206 were used to discriminate within the population of F4/80+ cells between the M1 phenotype (CD86+/CD206-), M2 (CD86-/CD206+) and intermediate M1/2 phenotype (CD86+/CD206+) as described previously (Mercalli et al. 2013). .

Higher frequency of M1 macrophages could be detected after LPS stimulation compared to medium groups (all p values are <0.0001). Macrophages treated with Dex showed a significant lower M1 frequency compared to medium control (all p values are <0.01), and LPS+Dex treated group showed lower M1 frequency than LPS

group (all p values are $<$ 0.0001). After 48-hour culturing, in medium control, Dex or LPS+Dex treated groups, no significant differences with regard to the M1 phenotype under different HP could be found. The frequency of M1 macrophage increased with higher HP in LPS groups, and the difference between 0mmHg (22.51±4.15%) and 60mmHg (28.63±2.40%) reached the level of significance (p=0.0034) (Fig. 18A).

Compared to medium controls, the frequency of M2 macrophages did not show any significant difference with LPS or LPS+Dex treatment ($p>0.05$). The frequency of M2 macrophages was significantly increased after treatment with Dex under the same HP compared to medium group (all p values are <0.001), and the LPS+Dex treated macrophages showed significant lower M2 frequency than Dex group (all p values $<$ 0.001). No significant difference was found between different pressures in medium, LPS or LPS+Dex groups. There was a significant increase of the frequency of M2 events when cells were cultured under increased HP in Dex groups, and the difference between 0mmHg (20.93±4.58%) and 60mmHg (29.00±1.88%) groups met the level of significance (p=0.0417) (Fig. 18B).

No significant difference in the frequency of intermediate population could be found between different treatments, or between different HP (Fig. 18C).

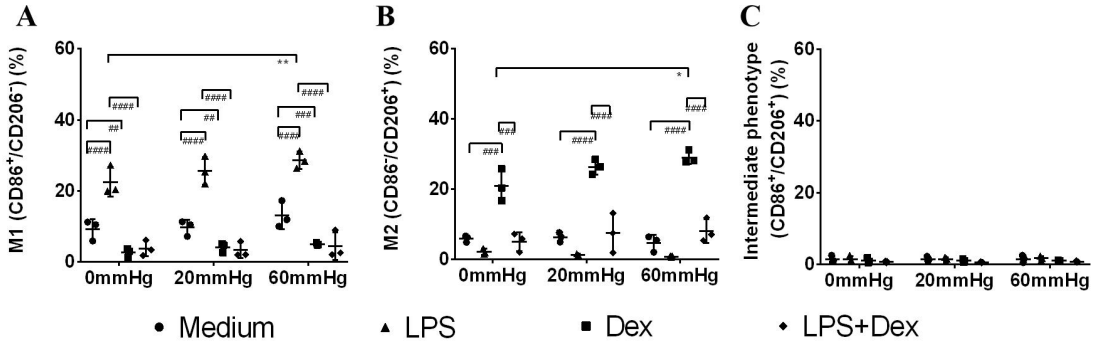

Figure 18 Frequency of M1, M2 or M1/2 macrophages under higher HP for 48h

Frequency of CD86+/CD206- (A), CD86-/CD206+ (B) and CD86+/CD206+ (C) events (%) in medium,LPS,Dex, or LPS+Dex treated BMDMs under different pressures by flow cytometry (n=3 independent experiments). Statistical significance between different pressures (*p<0.05, **p<0.01); Statistical significance between different treatments within one pressure (##p<0.01, ###p<0.001, ####p<0.0001). LPS=lipopolysaccharide, Dex=dexamethasone; BMDMs=bone marrow-derived macrophages.

3.1.8 Influence of prolonged incubation on the M1/M2 polarization of BMDMs

under increased HP

To explore whether a prolonged culture could affect M1/M2 polarization, BMDMs were treated with medium, LPS, Dex, or LPS+Dex under different HP for one week. Difference between various treatments were similar to 3.1.7. The prolongation of the culture time resulted in a decreased M1 phenotype (CD86+/CD206-) in the LPS group with increased pressure compared to that on day 2. With LPS treatment, the differences of the frequency of M1 phenotype between 0 mmHg (24.99±4.31%) and 60 mmHg (17.66±4.70%, $p < 0.0001$), 20 mmHg (23.86±4.69%) and 60 mmHg ($p < 0.0001$) both reached the level of significance. In contrast, the M2 phenotype (CD86-/CD206+) increased in the medium group, and also in Dex or LPS+Dex treated cells with increased pressure (all p values are < 0.05). In medium controls, the M2 frequency in 60mmHg group (22.13±5.46%) was significantly higher than both 0mmHg (4.36±1.56%, $p=0.0089$) and 20mmHg (7.90±6.88%, $p=0.0433$) groups. With Dex treatment, highest M2 frequency could be found when cells were cultured at 60mmHg (51.41±2.29%), which was significant higher than that in 0mmHg group (37.29±5.13%, $p=0.0454$). Similar result could be found in the LPS+Dex group. Here the M2 frequency in 60mmHg group (25.05±1.21) was significantly higher than 0mmHg group (4.27±0.87, $p=0.0024$). No significant differences were found in the M1/M2 phenotype (C86+/CD206+) (Fig. 19).

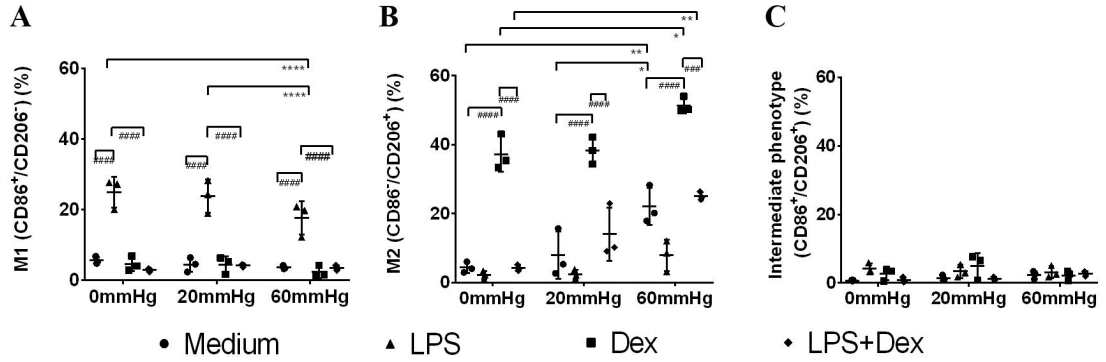

Figure 19 The polarization of M1/M2 macrophages under higher HP after 1 week

Frequency of CD86+/CD206- (A), CD86-/CD206+ (B), CD86+/CD206+ (C) events (%) in medium, LPS, Dex or LPS+Dex treated BMDMs under different pressures for 1 week (n=3 independent experiments). Statistical significance between different pressures (*p<0.05, **p<0.01, ****p<0.0001); Statistical significance between different treatments within one pressure (###p<0.001, ####p<0.0001). LPS=lipopolysaccharide; Dex=dexamethasone, BMDMs=bone marrow-derived macrophages.

3.1.9 ECM and α-SMA proteins production by macrophages under increased HP

To determine the role of increased HP on the ECM and α-SMA production by macrophages, BMDMs in the eight-well chamber slides were stimulated with medium, LPS, Dex or LPS+Dex and cultured under different HP. After 24h, the cells were fixed and immunostained with antibodies targeting fibronectin, collagen IV or α-SMA. Nuclei were stained by Hoechst dye (refer to 2.2.5.1).

After 24h, the proteins of fibronectin, collagen IV and α-SMA could be detected in BMDMs in all groups. The MFI/cell of fibronectin (Fig. 20A), collagen IV (Fig. 20B) and α-SMA (Fig. 20C) showed that, compared to medium control, weaker MFI/cell of fibronectin could be detected in LPS groups (all p values are < 0.05) and stronger MFI/cell of fibronectin, collagen IV and α-SMA staining could be detected in Dex treated macrophages (all p values are < 0.05). After stimulation of BMDMs with LPS+Dex, the MFI/cell of these three proteins was significant weaker compared to Dex groups under the same HP (all p values are <0.001).

With different pressures, LPS treated macrophages showed significantly weaker MFI/cell of fibronectin staining when cultured at 60mmHg compared to 0mmHg (p=0.0402). In Dex groups, macrophages cultured under higher HP (60mmHg) showed significantly stronger MFI/cell of fibronectin, collagen IV, and α-SMA staining compared to 0mmHg group (all p values are <0.05). The MFI/cell of α-SMA in Dex treated macrophages at 60mmHg was also significantly stronger than 20mmHg group ($p < 0.0001$). No significant difference of these three stainings was found between different pressures in medium or LPS+Dex groups.

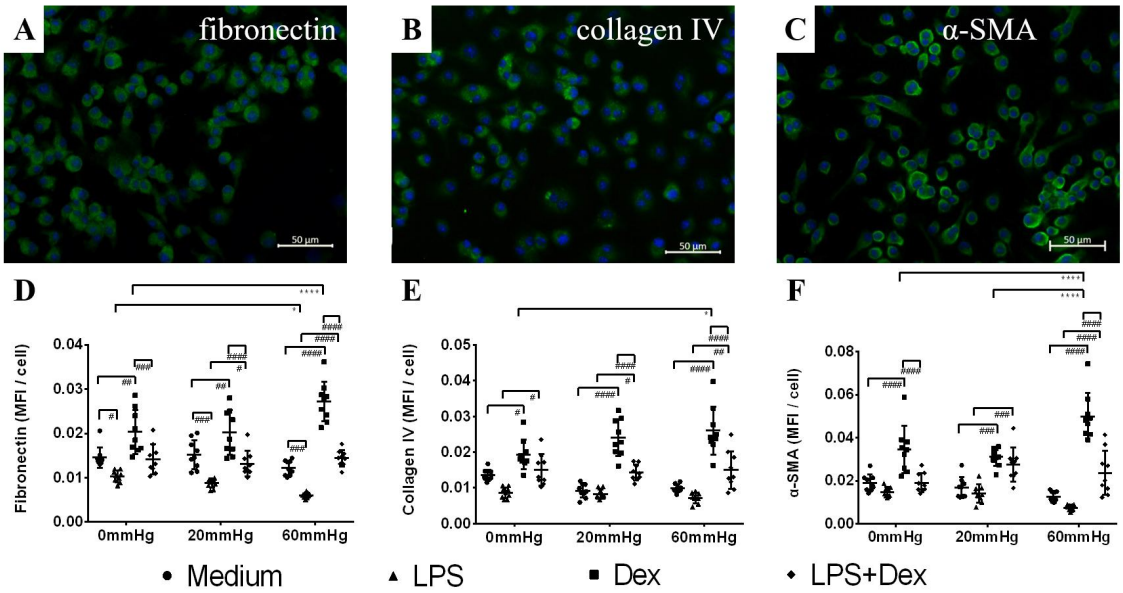

Figure 20 Expression of fibronectin, collagen IV and α-SMA proteins in BMDMs under increased HP

Representative immunofluorescence images of the expression of fibronectin (A), collagen IV (B) and α-SMA (C) in BMDMs. Scale bar=50µm. MFI/cell for fibronectin (D), collagen IV (E) and α-SMA (F) staining in medium, LPS, Dex or LPS+Dex treated BMDMs under different HP (n=9, samples were obtained from 3 independent experiments). Statistical significance between different pressures (*$p < 0.05$, ****$p < 0.0001$); Statistical significance between different treatments within one pressure (#$p < 0.05$, ##$p < 0.01$, ###$p < 0.001$, ####$p < 0.0001$). α-SMA=α smooth muscle actin; BMDMs=bone marrow-derived macrophages; MFI=mean fluorescence intensity; LPS=lipopolysaccharide; Dex=dexamethasone.

3.2 Human trabecular meshwork (HTM) cells

3.2.1 Morphology of HTM cells

HTM tissue was isolated and cultured in DMEM/F12 medium (containing 10% FBS and 1% Pen/Strep, refer to 2.2.2.3). After 2 weeks, cells started to grow out from the edge of the tissue to the bottom of the cell culture plate. The initial growth of HTM cells from the tissue is depicted in Fig. 21A. The primary cells grown from the tissue had different shapes, most of which were star-shaped. The cells possessed elliptically nuclei, a large cell body, a rich cytoplasm, and visible phagocytic particles (Fig. 21B and C). After 3 weeks of culturing, primary HTM cells were passaged as described in the 2.2.2.3. The passaged cells showed a homogeneous cell culture. After stimulation with different treatments and cultivation for 48 hours with different HP, the morphology of HTM cells did not show a visible change in the morphology.

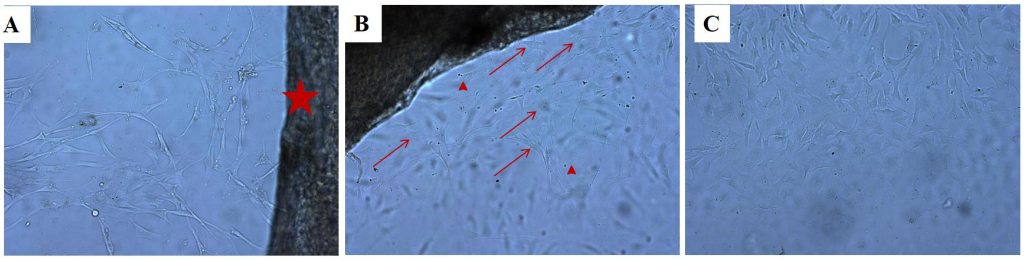

Figure 21 Morphology of HTM cells

(A) The initial growth of cells from HTM tissue after culture for 2 weeks. Cells showed protrusions. Pentagram shows the HTM tissue. (B) Primary HTM cells migrated from the tissue. Arrow shows the cell, with ellipsoidal nucleus, large cell body and rich cytoplasm. Arrowhead shows phagocytic particles in the cytoplasm. (C) Monolayer of HTM cells.

3.2.2 Identification of HTM cells

Using HTM cell isolation, contaminations by various cell types may happen, including corneal endothelium, keratocytes, sclera fibroblasts, SC outer wall endothelium or ciliary muscle cells. Because the characterization of the morphology and doubling time may not be sufficient to identify TM cells, further characterization was required. It has been reported previously that HTM cells immunostained positively against fibronectin, and collagen. Furthermore Dex-induced myocilin can be used as a marker for TM cells (Clark et al. 2001; Stamer and Clark 2017). Isolated cells were immunostained with antibodies targeting fibronectin or collagen IV. Alternatively, HTM cells were culture with or without 100nM Dex for 24 hours and were stained with myocilin antibodies. Compared to secondary antibody control, which showed no staining, isolated cells were positively stained for fibronectin. The fibronectin staining was observed in the cytoplasm, but also out of the cells. Collagen IV signals could be found in the cytoplasm of the cells. No myocilin signal was found in the cells of the medium control while after Dex treatment pronounced myocilin expression could be found in cells after 24h.

In sum, cells isolated from HTM tissues were positively immunostained for proteins fibronectin, collagen IV, and Dex-induced myocilin.

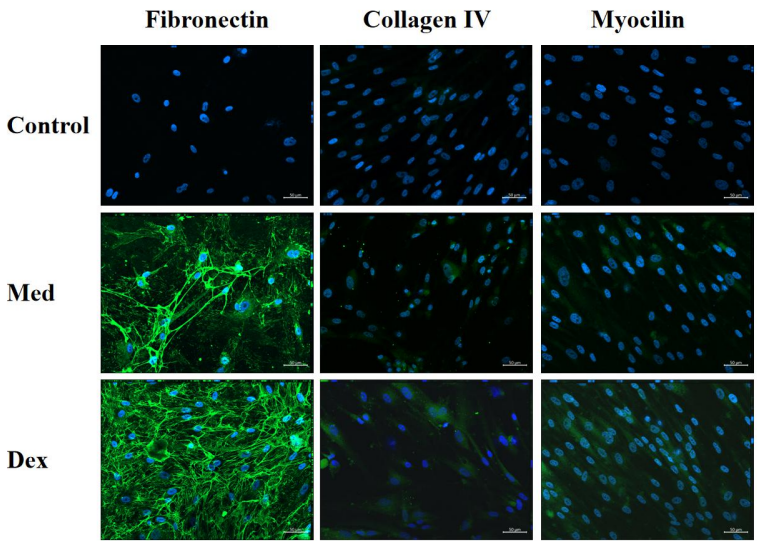

Figure 22 Fibronectin, collagen IV and myocilin expression in HTM
Isolated HTM cells were immunostained with antibodies targeting fibronectin (in AF488 channel, green), collagen IV (in AF488 channel, green) or myocilin (in AF488 channel, green). Controls were only stained with secondary antibodies. Nuclei were stained with Hoechst. Merged images were shown. Scale bar=50μm. HTM=human trabecular meshwork.

3.2.3 The viability of HTM cells under increased HP and TNF-α blocker

MTT test in HTM cells cultured with medium, 1000ng/ml Adalimumab, 100ng/ml LPS, 100nM Dex, LPS+Adalimumab or LPS+Dex and under different HP (0, 20, or 60mmHg). Medium control at 0mmHg served as control and the viability served as 100%. No significant difference was found between different treatments under the same HP level (all p values are >0.05). The Adalimumab treated group, the HTM cells showed a significantly higher MTT conversion at 60 mmHg compared to 0mmHg group (p=0.0119). No significant difference was found between different pressures in other groups.

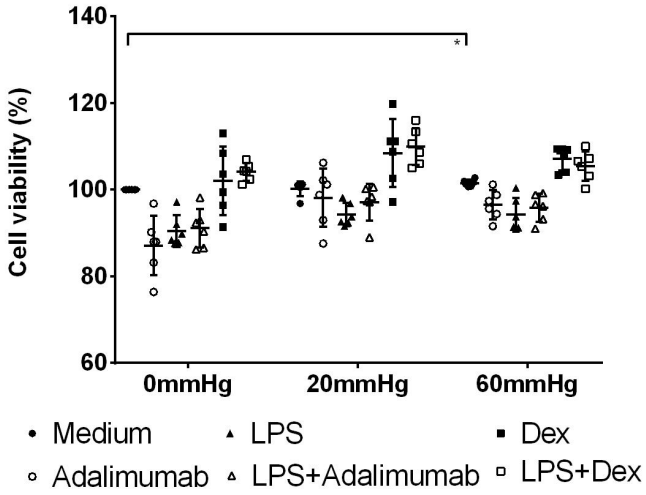

Fig. 23 Viability of HTM cells under increased HP

Cell viability in (%) of medium, Adalimumab, LPS, LPS+Adalimumab, Dex, and LPS+Dex treated HTM cells (n=6 independent experiments). Statistical significance between different pressures at *p<0.05. HTM=human trabecular meshwork; LPS=lipopolysaccharide; Dex=dexamethasone.

3.2.4 TNF-α produced by HTM cells under different HP

To determine whether HTM cells produce TNF-α and what impact the HP may have on the TNF-α production, TNF-α was quantified in supernatants of HTM cells via ELISA. The results showed that the HTM cells secreted TNF-α in the supernatant, but only a low amount regardless of the different treatments or pressures (lower than 4.05±0.38 pg/ml) (Fig. 4.2.4). No difference could be found between different treatments or pressures (all p values are ＞0.05).

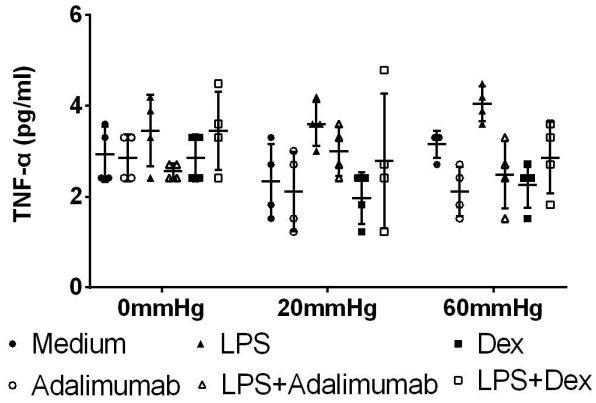

Figure 24 TNF-α in the supernatant from HTM cells under different HP as measured by ELISA

Amount of TNF-α (pg/ml) in the supernatant from medium, Adalimumab, LPS, LPS+Adalimumab, Dex or LPS+Dex treated HTM cells under different HP (n=4 independent experiments). TNF-α=tumor necrosis factor-α; HTM=human trabecular meshwork; LPS=lipopolysaccharide; Dex=dexamethasone.

3.2.5 Influence of increased HP on ECM, α-SMA and myocilin expression in HTM cells

To determine whether different treatments and / or increased HP may influence the expression of ECM, α-SMA or myocilin in HTM cells, expression of fibronectin, collagen IV, α-SMA and myocilin in HTM cells were examined (from 3 donor samples). After cultivation with medium, 1000ng/ml Adalimumab, 100ng/ml LPS, 100nM Dex, LPS+Adalimumab or LPS+Dex under different HP (0/20/60mmHg) for 48 hours, immunofluorescence staining was performed (refer to 2.2.5.2).

Compared to medium control, no significant difference in all staining was found in Adalimumab or LPS group. However, HTM cells treated with LPS+Adalimumab showed significantly stronger α-SMA (MFI/cell) compared to LPS group at 60mmHg (p=0.0358). HTM treated with Dex showed significantly stronger MFI/cell of fibronectin, α-SMA and myocilin within the same pressure (all p values are <0.001). The MFI/cell of all these four proteins in LPS+Dex treated HTM cells were weaker compared to Dex groups ($p<0.0001$). The HTM cells treated with LPS+Dex showed significantly stronger MFI/cell of myocilin than LPS groups (all p values are <0.01) (Fig 25).

No significant difference was found in the MFI/cell of fibronectin between different pressures in medium, Adalimumab, LPS, LPS+Adalimumab or LPS+Dex groups. In Dex group, HTM cells cultured at 60mmHg showed significantly stronger fibronectin (MFI/cell) staining compared to 0mmHg (p=0.0017). For collagen IV staining, HTM cells cultured at 60mmHg in medium, Adalimumab and Dex groups showed increased collagen IV (MFI/cell) compared to 0mmHg (all p values are <0.05) and 20mmHg (all p values are <0.05). In Dex groups, the MFI/cell of collagen IV in cells cultured at 20mmHg was also stronger than cells cultured at 0mmHg (p=0.0137). No significant difference of collagen IV (MFI/cell) between different pressures was found in LPS, LPS+Adalimumab or LPS+Dex groups. No significant difference of α-SMA or myocilin staining was found between different pressures in medium, Adalimmab, LPS, LPS+Adalimumab or LPS+Dex groups. Dex treated HTM cells cultured at 60mmHg showed significantly stronger MFI/cell of both α-SMA and myocilin compared to

0mmHg (all *p* values are ＜0.0001) and 20mmHg (all *p* values are ＜0.05).

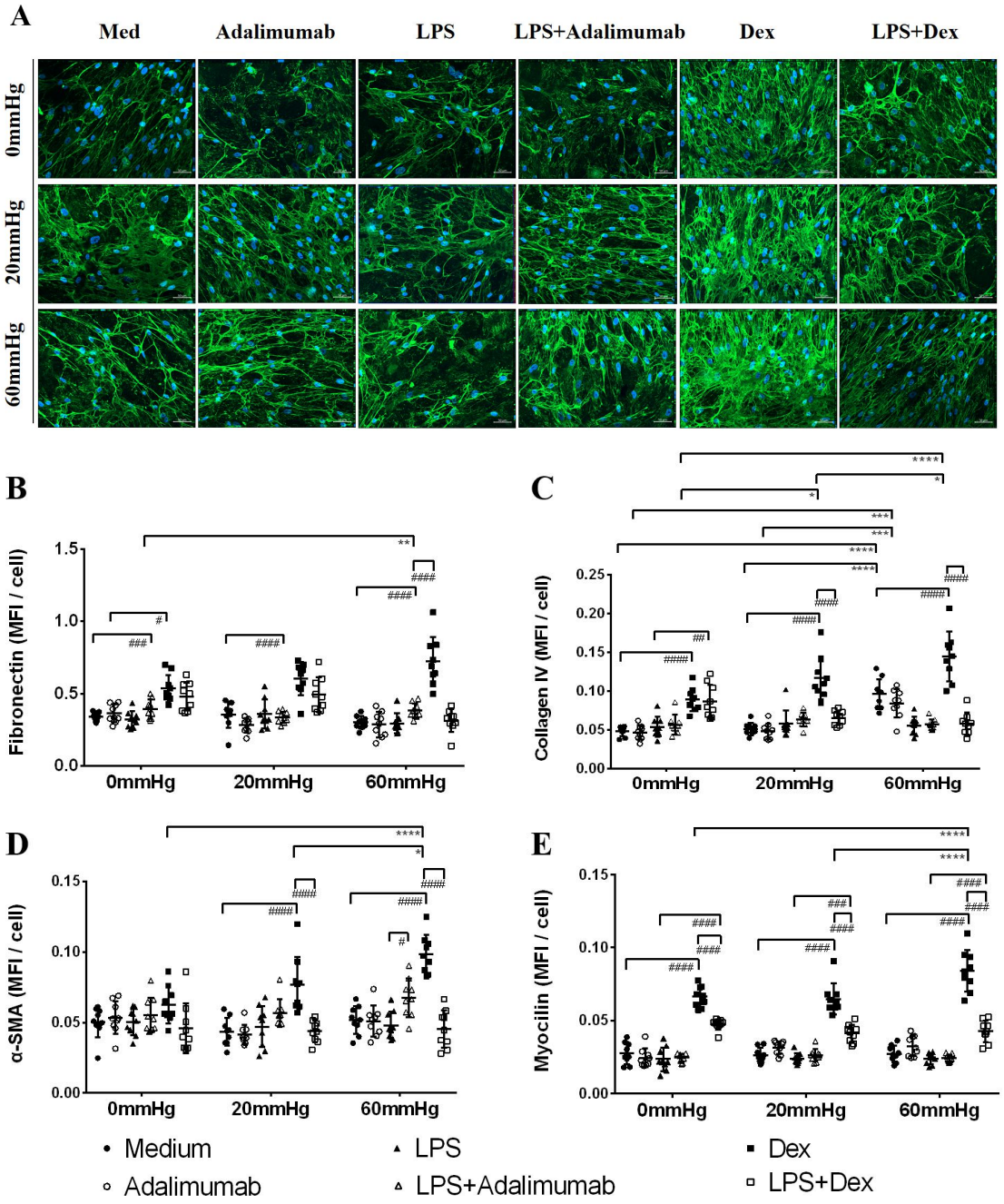

Figure 25 Expression of fibronectin, collagen IV, α-SMA and myocilin in HTM cells under increased HP

Representative images of fibronectin (in AF488 channel, green) staining (A) in HTM cells in different groups. Scale bar=50μm. MFI/cell for fibronectin (B), collagen IV (C), α-SMA (D) and myocilin (E) staining in medium, Adalimumab, LPS, LPS+Adalimumab, Dex or LPS+Dex treated HTM cells under different HP (n=9, samples were obtained from 3 independent experiments). Statistical significance between different pressures (**p*<0.05, ***p*<0.01, ****p*<0.001, *****p*<0.0001); statistical significance between different treatments within one pressure (#*p*<0.05, ##*p*<0.01, ###*p*<0.001, ####*p*<0.0001). α-SMA=α smooth muscle actin; HTM=human trabecular meshwork; MFI=mean fluorescence intensity; LPS=lipopolysaccharide; Dex=dexamethasone.

3.2.6 Influence of increased HP on NOS and Arg-1 expression in HTM cells

To observe if there is any difference in the expression of NOS and Arg-1, HTM cells were cultured with medium, 1000ng/ml Adalimumab, 100ng/ml LPS, 100nM Dex, LPS+Adalimumab or LPS+Dex under different HP for 24 hours and then stained with the iNOS, Arg-1, eNOS and nNOS antibodies (refer to 2.2.5.2).

Immunostaining showed positive eNOS, iNOS and Arg-1 signals in HTM cells in each group, but no positive nNOS signal was found (data not shown). Image J analysis (Fig. 26) showed that, compared to medium group, no significant difference was found in LPS group. The MFI/cell of eNOS, iNOS and Arg-1 staining were significantly reduced in Adalimumab and Dex groups compared to medium controls at the same pressure level (all p values are <0.05). Compared to LPS group, he HTM cells treated with LPS+Adalimumab showed decreased MFI/cell of eNOS, iNOS and Arg-1 (all p values are < 0.05). For eNOS and iNOS staining, the MFI/cell with LPS+Dex treatment were significantly weaker when compared to LPS treated group (all p values are <0.05).

Compared between different HP, no significant difference of eNOS (MFI/cell) was found in medium, LPS, Adalimumab, LPS+Adalimumab or LPS+Dex group. The eNOS (MFI/cell) in Dex group at 60mmHg was significantly weaker than 0mmHg (p=0.0220). Compared to 0mmHg, HTM cells cultured at 60mmHg showed significantly reduced iNOS staining in LPS ($p < 0.0001$) and Dex (p=0.0176) groups. The iNOS staining (MFI/cell) of cells cultured in medium at 60mmHg was significantly reduced than 20mmHg in medium (p=0.0025) and Dex (p=0.0205) groups. No significant difference of iNOS (MFI/cell) between different HP was found in other groups. Increased Arg-1 staining was shown when HTM cells were cultured at higher HP, and the differences between 0mmHg and 60mmHg in LPS (p=0.0004) and Dex (p=0.0021) groups, and between 20mmHg and 60mmHg in LPS group (p=0.0011) reached levels of significance.

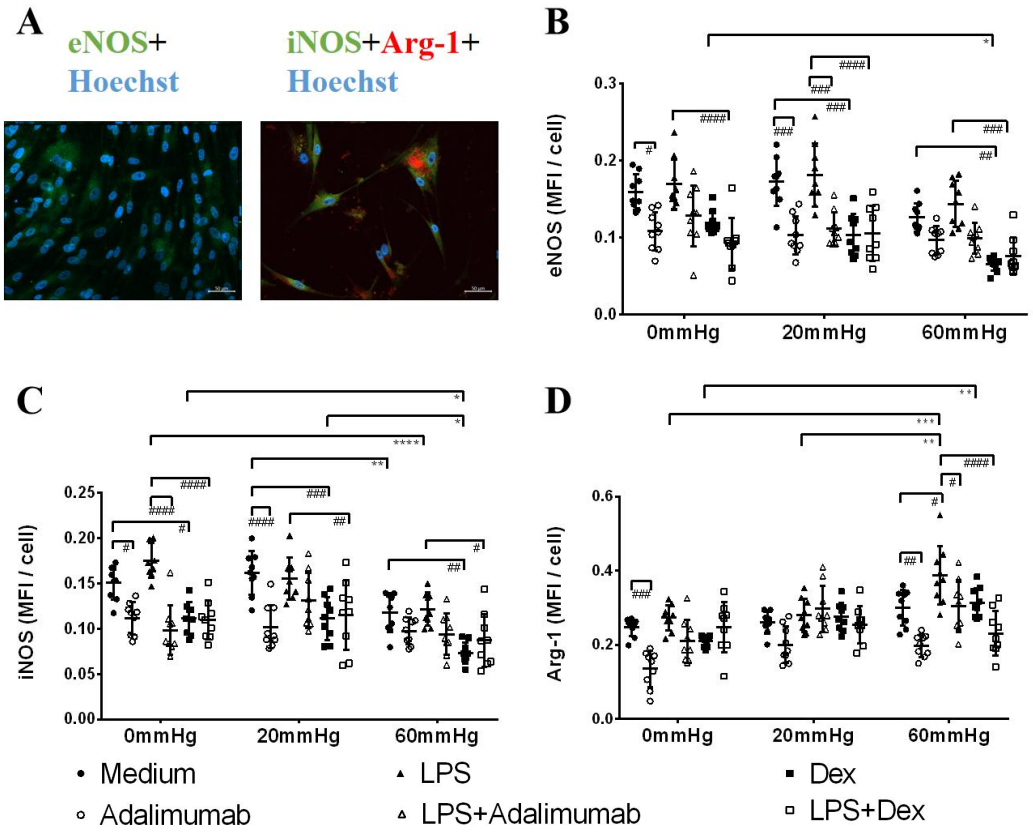

Figure 26 Expression of eNOS, iNOS, and Arg-1 in HTM cells under increased HP

(A) Representative immunofluorescence images of eNOS, iNOS or Arg-1 stainings in HTM cells. Scale bar=50μm. MFI/cell of eNOS (B), iNOS (C) and Arg-1 (D) staining in medium, Adalimumab, LPS, LPS+Adalimumab, Dex or LPS+Dex treated HTM cells under different HP (n=9, samples were obtained from 3 independent experiments). Statistical significance between different pressures (*p<0.05, **p<0.01, ***p<0.001, ****p<0.0001); statistical significance between different treatments within one pressure (#p<0.05, ##p<0.01, ###p<0.001, ####p<0.0001). eNOS=endothelial nitric oxide synthase; iNOS=inducible nitric oxide synthase; Arg-1=arginase-; HTM=human trabecular meshwork; MFI=mean fluorescence intensity; LPS=lipopolysaccharide; Dex=dexamethasone.

3.2.7 Influence of increased HP on arginase activity in HTM cells

The arginase activity in HTM cells (refer to 2.2.10) was low in medium groups (Fig. 27). At the same HP level, the arginase activity increased significantly when cells were treated with LPS (all p values are <0.05). However, Dex or Adalimumab treatment decreased the arginase activity in cells compared to medium groups ($p<0.05$). Cells with LPS+Adalimumab or LPS+Dex treatment had lower arginase activity compared to cells treated with LPS ($p<0.05$).

Compared to 0mmHg groups, the arginase activity in HTM cells increased under higher HP with each treatment. Differences of arginase activity between different

groups (Adalimumab at 0mmHg (0.46±0.20 U/L) and 60mmHg (1.18±0.13 U/L, p=0.0390), LPS at 0mmHg (1.82±0.10 U/L), and 60mmHg (2.60±0.13 U/L, p=0.0178), Dex at 0mmHg (0.38±0.11 U/L) and 60mmHg (1.08±0.23 U/L, p=0.0491)) reached the levels of significance.

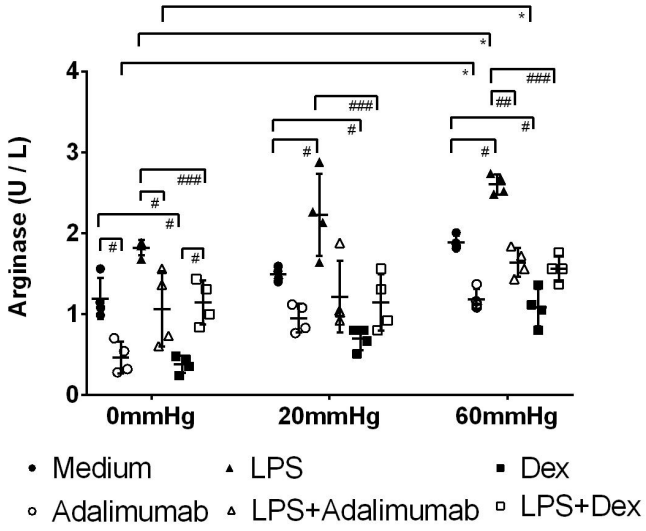

Figure 27 Arginase activity in HTM cells under increased HP

Arginase activity (U/L) in medium, Adalimumab, LPS, LPS+Adalimumab, Dex or LPS+Dex treated HTM cells under different HP (n=4 independent experiments). Statistical significance between different pressures (*p<0.05); statistical significance between different treatments within one pressure (#p<0.05, ##p<0.01, ###p<0.001). HTM=human trabecular meshwork; LPS=lipopolysaccharide; Dex=dexamethasone.

3.2.8 Influence of increased HP on NO production in HTM cells

To determine the production of NO between each group, NO-test (refer to 2.2.9) with HTM cells supernatants were performed.

HTM cells showed a rather low amount of NO in the supernatant regardless of different treatments and pressures (Fig. 28). Compared to cells in medium groups at the same HP level, no significant difference was found in NO level of LPS treated cells. The NO level decreased significantly after Adalimumab treatment at 0mmHg (0.85±0.27 μM) compared to medium control (1.35±0.39 μM, p=0.0234). The LPS+Adalimumab group showed significant decreased NO production compared to LPS group under the same pressure (all p values are ＜0.01). Under each pressure level, the HTM cell treated with Dex showed significant lower NO level than medium groups

(all p values are <0.05). Moreover, upon LPS+Dex treatments at the same HP level, the amount of NO was significant lower as compared to cells which were only LPS treated (all p values are <0.05).

Differences in NO level were found when HTM cells were cultured under different HP. With LPS treatment, compared to 0mmHg group (1.67±0.47 μM), the amount of NO decreased significantly when cells were cultured at 60mmHg (1.21±0.53 μM, p=0.0446). Significantly decreased NO level at higher HP (60mmHg) could also be found in LPS+Adalimumab and LPS+Dex groups compared to 0mmHg (all p values are <0.05).

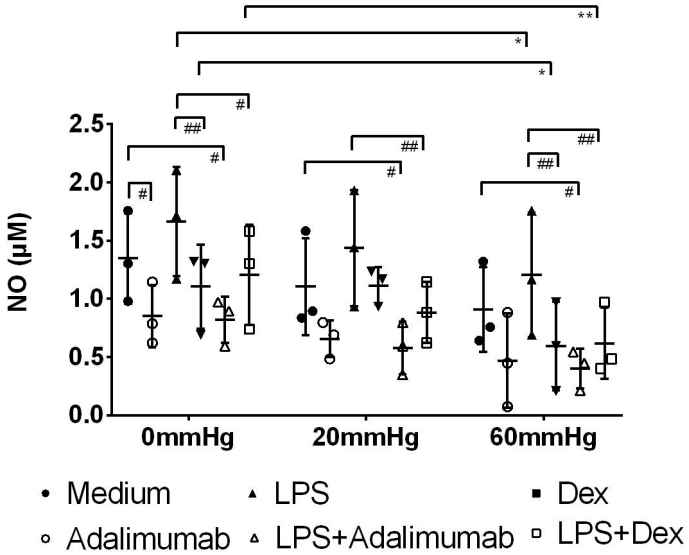

Figure 28 Production of NO of HTM cells under increased HP

NO level (μM) in medium, Adalimumab, LPS, LPS+Adalimumab, Dex or LPS+Dex treated HTM cells under different HP (n=3 independent experiments). Statistical significance between different pressures (*p<0.05); statistical significance between different treatments within one pressure (#p<0.05, ##p<0.01). NO=nitric oxide; HTM=human trabecular meshwork; LPS=lipopolysaccharide; Dex=dexamethasone.

4 Discussion

The dynamic balance between aqueous humor (AH) secretion and AH outflow is indispensable to maintain a homeostatic intraocular pressure (IOP). A disturbance in this balance may result in ocular hypertension (OHT) and subsequently to glaucoma. A continuously elevated AH outflow resistance may lead to increased IOP, which acts as a primary risk factor for the loss of retina ganglion cells (RGCs) and damage of optic nerve head (ONH) in glaucoma. Trabecular meshwork (TM) cells establish an AH outflow resistance via changes of their morphology and production of extracellular matrix (ECM) influenced by cytokines (e.g. transforming growth factor (TGF)-β1) may alter their function (Stamer and Clark 2017). According to the current understanding, IOP in the eye is regulated by mechanical distortion in the outflow pathway, which is signaled by ECM-integrin interaction to the TM cells. This results in the upregulation of matrix metalloproteinase (MMP)-2,-3, and -14 and downregulation of tissue inhibitor of metalloproteinase (TIMP)-2 in TM cells, which can regulate the ECM deposition or turnover thereby modulating the outflow facility (Bradley et al. 2001).

Cytokines modulating the TM cells are produced by ocular cells, TM cells and infiltrated immune cells, e.g., macrophages. Macrophages are resident in all parts of the eye (Chinnery et al. 2017). Infiltration of macrophages into TM has been reported in cases of ocular inflammation and experimental glaucoma, leading to the intense inflammation and damage of RGCs(Taurone et al. 2015).

Ischemia-reperfusion injury (IRI) is a pathological condition leading to tissue damage and further inflammatory response after a restricted blood supply combined with the recovery of the perfusion. Tissue damage caused by IRI is involved in the pathological processes of various diseases and organs, including myocardial infarction, ischemic stroke, acute kidney injury, and retina diseases such as age-related macular degeneration (AMD), diabetic retinopathy, central retina artery occlusion and glaucoma (Renner et al. 2017).

In retinae with IRI, shortly increased IOP compresses the blood vessels in the retina and lead to an impaired blood supply, thereby damaging the retina. The following reperfusion of the retina and the recovered oxygen supply aggravates retinal damage,

causing accelerated inflammation and RGCs death due to apoptosis (Renner et al. 2017).

The influence of increased hydrostatic pressure (HP) on macrophages and TM in increased IOP or IRI is not fully understood. In the present study, a pressure chamber system was used to culture bone marrow-derived macrophages (BMDMs) or human TM (HTM) cells under defined and reproducible conditions with various HP and various immunmodulatory treatments to analyze the immune response of macrophages and functions of TM cells. The hypothesis of the present thesis is that increased IOP and / or GCs treatment may influence the polarization of macrophages and modulate the effector responses of macrophages and TM cells und pro-and anti- inflammatory conditions, which is similar to the pathogenesis of IRI.

4.1 Cell culture of BMDMs and HTM cells under increased HP

In this study, macrophages were obtained from bone marrow-derived cells (Trouplin et al. 2013). After isolation and culture with L929 conditioned medium (containing macrophage colony stimulating factor (M-CSF)) for 1 week, cells showed characteristical morphology of macrophages with an elongated spindle shape with stretches. More than 90% of the cells were positive for the macrophage marker F4/80 (Starkey et al. 1987). Constitutive F4/80 expression was confirmed via immunofluorescence microscopy and flow cytometry, characterizing these cells as macrophages (Bauer et al. 2012).

The HTM cells in the presented study were isolated from donor corneoscleral rims which were used for human cornea transplantation as described previously (Keller et al. 2018). After two-week culturing, initial cell growth started spontaneously (refer to 2.2.2.3). Corneal keratocytes, fibroblasts, or Schlemm's canal (SC) cells may be a potential reason for unwanted contamination. Light microscopy observation revealed a similar shape of TM cells as keratocytes, scleral fibroblast or SC cells, but TM cells are wider, flatter and have more protrusions (Polansky et al. 1979; Stamer et al. 1995). Healthy HTM cells cultured *in vitro* from low passage have a shorter doubling time of 3 days or less as compared to fibroblast cells (Polansky et al. 1979). HTM cells in culture

may keep a stable morphology for weeks, while keratocytes or scleral fibroblasts change the morphology under the same conditions (Keller et al. 2018).

To strengthen the morphological identification of TM cells, cells can be positively immunostained for fibronectin, collagen IV and Dexamethasone (Dex)-induced myocilin can be used to characterize TM cells (Clark et al. 2001; Stamer and Clark 2017). In the presented study, the isolated cells could be identified as TM according to morphological characteristics, and their constitutively expression of fibronectin, collagen IV and their inducible myocilin expression upon Dex treatment.

To ensure that non-toxic concentration of lipopolysaccharide (LPS), Dex, Adalimumab were used and that the cell culture in the pressure chamber at 0, 20 and 60 mmHg did not harm to the cells, cell viability was estimated by using the MTT assay (refer to 2.2.4). Non-toxic concentrations of LPS, Dex or Adalimumab was titrated at 0 mmHg (room pressure). The medium control group at 0 mmHg was used as a standard (100% viability) and was compared to the other groups. Using the HP chamber system it was found that BMDMs and HTM cells displayed at least 90% viability regardless of the HP used. It is well known that LPS stimulation can induce various pro-inflammatory processes, e.g., tumor necrosis factor (TNF)-α mediated phagocytosis in various cells and that the application of Dex (a synthetic glucocorticoid (GC) with high immunosuppressive potency) may influence the inflammation process, e.g. phagocytotic ability and cell viability (Sonoki et al. 1997). Adalimumab is an anti-human TNF-α antibody and is able to suppress inflammatory processes and immune system, and widely used in the management of rheumatoid arthritis and non-infectious uveitis (Jaffe et al. 2016). In this study, the cell viability of BMDMs in LPS group was normalized to medium control, however, Dex groups showed significant decreased cell viability. The reduced cell viability of Dex treated cells may related to the increased outflow resistance by GCs treatment (Zhang et al. 2007). In this study, 1000ng/ml Adalimumab treated HTM cells did not show significant difference in the cell viability. This is similar to the study of Lin et al. that high concentrations (1μg/ml and 10 μg/ml) of Adalimumab did not influence the viability of human $CD4^+$ T cells (Lin et al. 2017).

To analyze the effect of increased HP on cell viability, Böhm et al. showed by using

the same pressure chamber system mentioned no alteration of cell viability in the retinal photoreceptor-derived cell line (661W) was found under different pressures (0, 20 and 40 mmHg) for 3 days (Böhm et al. 2016). Increased cell viability was shown in both BMDMs and HTM cells cultured under higher HP for 2 days in the presented study. It has been documented previously that macrophages and TM cells under transient increased pressure showed upregulated TNF-α (which can increases the nuclear factor (NF)-κB to protect cells from apoptosis) and phagocytotic ability (Liton and Gonzalez 2008), reflecting the increased cell viability.

4.2 Inflammatory response of BMDMs cultured under increased HP

The infiltration of macrophage/monocyte into the eye (optic nerve head) was found in the process of experimental model in mice. In this model, mice lacking infiltrating monocytes did not develop glaucoma (Howell et al. 2012). These results indicate that macrophages are also important in the development of glaucoma. Previous results from other investigators suggest that macrophage itself can sense the increased mechanical stress (stretch force, shear stress and HP) by activating mitogen-activated protein kinase pathway downstream of mechanosensors (e.g. voltage-gated Ca^{2+} channels and focal adhesion kinase (FAK)) and promotes inflammation by releasing various cytokines and chemokines (e.g. TNF-α, interleukin (IL)-1β, -6 and -8) (Ferrier et al. 2000; Maruyama et al. 2019).

Human alveolar macrophages and monocyte-derived macrophages under cyclic stretch demonstrated a pro-inflammatory response and a production of TNF-α, IL-6 and IL-8 (Pugin et al. 1998). However, in another study, exclusive increased mechanical stress did not induce the production of TNF-α or IL-6 in BMDMs (Maruyama et al. 2019). These findings are consistent with the results of the present study, showing that no significant different amounts of TNF-α or IL-6 could be found in medium groups after increased HP. The upregulation of TNF-α and IL-6 by BMDMs during increased mechanical stress required a further inflammatory stimulus (such as LPS) similar to results of other groups (Pugin et al. 1998). This is in line with the results in the current study. LPS stimulation provided a pro-inflammatory environment for macrophages.

After activation with LPS, BMDMs showed pro-inflammatory activation by expressing and releasing large amount of pro-inflammatory mediators like inducible nitric oxide synthase (iNOS), NO, TNF-α, and IL-6.

After cell culture under increased HP at 60mmHg for 24 or 48h, BMDMs expressed and released more TNF-α and IL-6 than at 0mmHg or 20mmHg. Murine *in vivo* models have shown that TNF-α was upregulated by increased IOP caused by obstructed AH outflow (Nakazawa et al. 2006). A similar upregulation of TNF-α was discovered in various tissues (retina, optic nerve, and vitreous) of human glaucomatous eye (Williams et al. 2017). Furthermore, open-angle glaucoma (OAG) patients were reported to have a higher TNF-α level in AH and TNF-α-308 gene polymorphism was found to be related to higher risk for glaucoma (Xin et al. 2013). Upregulated ocular TNF-α expression in the retina after OHT was found in rats, and a soluble TNF-α inhibitor (XPro1595, an engineered protein that binds selectively to soluble TNF-α and does not interact with TNF-α receptors) protected RGCs from cell death (Vargas et al. 2015). IL-6 is a pro-inflammatory cytokine secreted by macrophages and HTM cells (Moore et al. 2015). An increased expression of IL-6 was found during early stage of ONH injury caused by increased IOP in rat glaucoma models (Johnson et al. 2011). Increased secretion and transcription of TGF-β1, IL-6, IL-8, and vascular endothelial growth factor (VEGF) were also found in the HTM cells and tissues cultured under cyclic mechanical stress (Liton et al. 2005; Liton and Gonzalez 2008). Compared to healthy individuals, higher level of IL-6 along with increased TNF-α were found in TM tissues of post-mortem eyes from glaucoma patients, especially around the area of vessels and macrophages (Taurone et al. 2015). Thus, increased TNF-α and IL-6 response under increased HP found in the current study is in line with these studies.

Significant arginase (Arg)-2 expression was also found in BMDMs exposed to higher HP. In previous studies Arg-2 was found to be highly induced in M1 macrophages and was often related with inflammation and necroptosis (also termed inflammatory cell death, a caspase independent suicide mechanism) after tissue injury (Fouda et al. 2018). Higher expression of Arg-2 also indicating an increased pro-inflammatory reaction of BMDMs under increased HP.

IL-10 is an anti-inflammatory cytokine and can be expressed by macrophages. During hypertension, pro-inflammatory reaction is active and Minocycline (an anti-inflammatory antibiotic) is reported to reverse hypertension and resulted in high level of IL-10 (Harwani 2018). This is similar to the increased HP in the present study, that increased pro-inflammatory reaction but reduced IL-10 were found in BMDMs cultured under increased hydrostatic pressure for 24 or 48 hours.

The inflammatory responses of macrophages play an important role in IRI. The retina IRI process is composed by three stages: the acute phase (within several hours), the subacute phase (hours to days) and the chronic phase (days to months). The subacute phase is thought to be important in retina IRI due to the inflammatory responses, and the activation of inflammatory genes, the upregulation of inflammatory factors and infiltration of inflammatory cells may be a primary reason for the damage of retinal neurons (Song et al. 2017). Various studies reported an increased expression of TNF-α, which may be one of the main pathogenic inflammatory factors in the subacute stage in IRI, is related to impaired tissues of IRI models (Renner et al. 2017; Song et al. 2017). It is also reported that glia cells could be activated in models with increased HP or in experimental ischemia models to result in large amount of TNF-α and apoptosis of RGCs (Tezel and Wax 2000). The Bcl-2 protein family has been identified to take part in IRI (Anilkumar and Prehn 2014). In retina, after axonal damage, Bax (which promotes apoptosis) is activated and its aggregation at the outer membrane of the mitochondria lead to dysfunction of adenosine triphosphate (ATP) synthesis and reactive oxygen species (ROS) accumulation, leading to RGCs death (Nickells 2012). These primary dying RGCs can activate glia cells, which in turn are producing TNF-α, that can directly or indirectly induce apoptosis, and can increase other pro-inflammatory factors (such as IL-6 and iNOS/NO), affecting neighboring unaffected RGCs and eventually leading to the disappearance of RGCs and the loss of neural tissue. A previous study using photoreceptor cells and retinal explants under increased pressure showed upregulated high-mobility group box (HMGB)-1, toll like receptor (TLR)-2/4, Bcl-2, TNF-α, and increased IL-6 levels (Böhm et al. 2016). Excepted by the damage of RGCs and ONH, the great production of TNF-α by activated macrophages induces the

response of T-helper (Th) cells and their differentiation to Th17, which turns the acute inflammation into fibrotic reaction. ECM depositions in TM may lead to obstruction in TM outflow and continuous IOP elevation, which could result in glaucomatous damages (Taurone et al. 2015). In the present study, the increased HP induces the pro-inflammatory function in macrophages. Related studies indicated that infiltrated macrophages to the retina and the pro-inflammatory reactions response to the RGCs damage and glaucoma (Huang et al, 2007). The increased pro-inflammatory reactions of macrophages under increased pressure is resembling the data observed in retina IRI under elevated pressure (Fig 29).

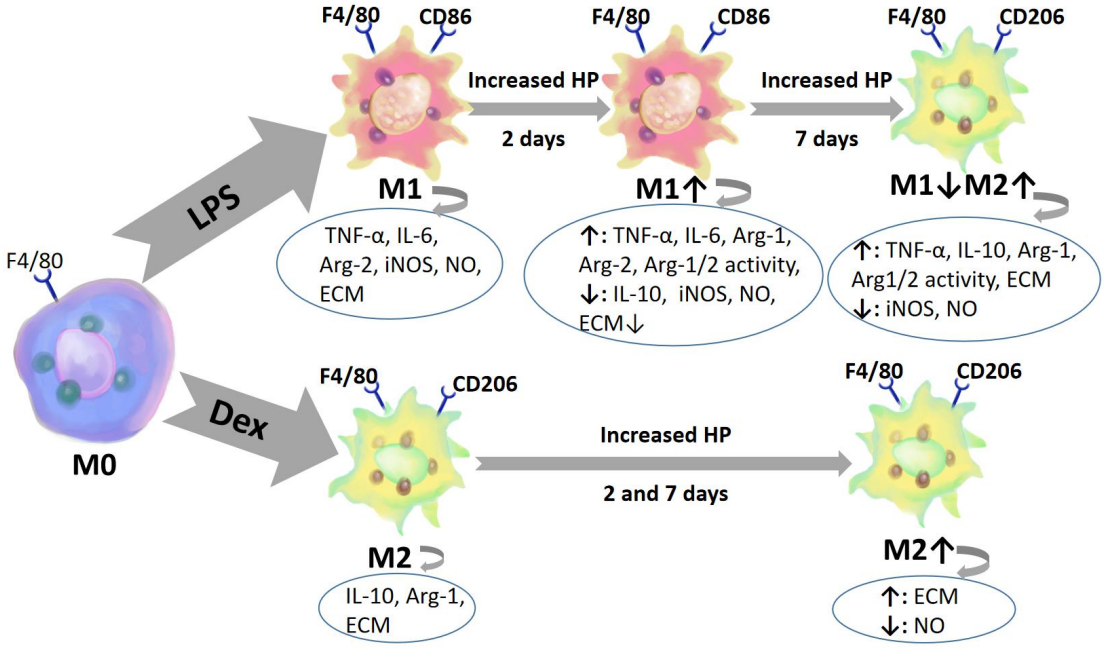

Figure 29 The polarization and inflammatory reactions of BMDMs under increased HP
BMDMs polarization under increased HP. LPS induced an M1 polarization, which were CD86+ and expressed TNF-α, IL-6, Arg-2, iNOS, released NO and produced ECM. After cultured under increased HP for 2 days, M1 phenotype was increased, with up-regulated TNF-α, IL-6, Arg-1, Arg-2 and arginase activity, while down-regulated IL-10, iNOS, NO level and ECM production. After prolonged the culture time to 7 days, BMDMs switched to M2 polarization (CD206+), with increased TNF-α, IL-10, Arg-1, arginase activity and ECM production, while decreased iNOS and NO level. Contrary to LPS group, Dex induced an M2 polarization (CD206+), which expressed IL-10, Arg-2 and produced ECM. With increased HP, M2 phenotype was up-regulated in Dex group on both day 2 and day 7, with increased ECM production and decreased NO level. BMDMs=bone marrow-derived macrophages; HP=hydrostatic pressure; LPS=lipopolysaccharides; TNF-α=tumor necrosis factor-α; IL=interleukin; Arg=arginase; iNOS=inducible nitric oxide synthase; NO=nitric oxide; ECM=extracellular matrix; Dex=dexamethasone. Macrophages were drawn by Zhiqiang Liu and permission granted.

4.3 Alteration of the arginine metabolism in BMDMs and HTM cells under increased HP

In arginine metabolism, arginase and NOS are competitive for L-arginine (Rath et al. 2014). iNOS can be expressed by macrophages (Martinez et al. 2008), as shown in the presented study. Both iNOS and endothelial nitric oxide synthase (eNOS), while not neuronal nitric oxide synthase (nNOS) were found to be expressed by HTM cells (Nathanson and McKee 1995b), which is in line with the results in the current study. Increased arginase activity can impair the synthesis and stability of iNOS, compete with iNOS for L-arginine, resulting in less NO (El-Gayar et al. 2003). NO was found to acts as an endothelium-derived relaxing factor (EDRF) in cardiovascular, respiratory and ocular tissues (TM and SC). In the eye, TM cells and endothelium within the SC respond to NO, which relax and reduce their cell volume through K cannels, thereby increasing AH outflow (Aliancy et al. 2017).

In the current study, after LPS stimulation, BMDMs and HTM cells showed an increased arginase expression, increased arginase activity, increased iNOS expression and NO level. This is consistent with a previous report showing that arginase expression/activity, iNOS expression and NO level was upregulated during interferon (IFN)-γ/LPS mediated inflammation in macrophages (El-Gayar et al. 2003; Martinez et al. 2008). There is no article provided reporting the alteration of iNOS/NO and arginase expression/activity in TM cells with LPS treatment to the best of our knowledge.

Both cell types, BMDMs and HTM cells, exhibited an upregulated arginase expression/activity, while the iNOS expression and NO level were decreased after culture under increased HP with pro-inflammatory conditions in the current study. One explanation could be the competitive relationship between arginase and iNOS. Low level of NO leads to vasospasm, and contributes in the pathologies of myocardial infarction, pulmonary hypertension, stroke, and glaucoma (Matsuo 2000). NO poverty causes TM stiffness and obstruction of AH outflow pathway (Aliancy et al. 2017). Decreased NOS expression in the TM tissues have also been discovered in enucleated eyes of glaucoma patients (Nathanson and McKee 1995a). The results of the HTM cells cultured under increased HP for 2 days in the current study are in accordance to these

previous studies. In contrast, Matsuo et al. reported an elevation of NO level and iNOS proteins when HTM cells were cultured to increased HP (Matsuo 2000). However, HTM cells in Matsuo's study experienced a spontaneous increased pressure for 400 seconds, and the elevated NO and iNOS were started to decrease at 200 seconds to the normal level, which is similar to the IOP fluctuation condition in normal eyes.

Similar as described for HTM cells, in the current study, the iNOS expression of BMDMs was decreased under higher hydrostatic pressure, which might lead to the decreased NO level. Similar findings were shown previously in hypertension, with decreased iNOS and NO level in macrophages under increased pressure (Harwani 2018).

In arginase metabolism, proline and polyamines, products from L-arginine metabolism via arginase, are regarded critically involved in tissue repair by collagen synthesis and cell proliferation. Upregulated arginase and proline/polyamines by macrophages are thought to be responsible for the increased fibrosis in hypertension and asthma (Narayanan et al. 2013). Furthermore, abnormal deposition of ECM proteins (such as collagen) and fibrotic process have been found to be critically involved in the obstruction of TM outflow (Oh et al. 2006). The increased arginase expression and activity under increased pressure in macrophages and HTM cells in the current study may be involved in the regulation of outflow pathway.

Apart from its regulation role in outflow pathway, arginase plays an important role in IRI. Upregulated arginase has been reported in IRI in cardiac tissue, kidney and liver and arginase inhibitor treatment has protective function in IRI (Gordon and Martinez 2010). As NOS is important in the apoptosis of retinal cells and retinal IRI -related diseases, arginase may play an essential role in the processes of inflammation, neurotoxicity, pathological angiogenesis, and vascular dysfunction in retina and during episodes of IRI in the retina (Narayanan et al. 2013). Arg-1 is thought to be able to suppress oxidative stress and NO production, decrease inflammation mediated by NOS/TNF-α and the following necroptosis and tissue damage, displaying a benefit role in retina IRI (Rath et al. 2014). However, Arg-2 plays a key role in I/R-induced retinal neurovascular injury by increasing oxidative stress, promoting glial cell activation and

necrosis (Shosha et al. 2016). Previous studies have shown that the Arg-1$^{-/-}$ mice had more dramatic neuronal loss and retinal thinning after IR, and PEGylated Arg-1 improved the neuronal survival in WT mice (Fouda et al. 2018). In the same study, increased inflammatory response was found in Arg-1$^{-/-}$ macrophages after LPS stimulation, while after PEGylated Arg-1 treatment inflammatory response was reduced (Fouda et al. 2018). The mRNA and protein of Arg-2 were reported to be increased in WT mice with retina IRI, and Arg-2$^{-/-}$ mice had minor RGCs loss, preserved retinal morphology and showed better inner retinal neuronal function than WT mice after retina IRI (Shosha et al. 2016). In this study, BMDMs under increased HP showed increased expression of Arg-2 and higher arginase activity with increased inflammatory response, which may be consistent with the inflammatory process in IRI. However, a moderate increased expression of Arg-1 but reduced iNOS expression and NO production in BMDMs under increased HP was also found.

Although arginase is thought to be critical important for the TM outflow and retinal IRI in glaucoma, no study showed the role of arginase in TM cells. The immunofluorescence data confirmed the existence of Arg-1 in HTM cells (Fig. 26A). Although expression was not as much pronounced as in BMDMs, increased expression and activity could also be found in HTM cells under higher HP. Therefore, arginase in TM cells could contribute to alter TM outflow facility by the fibrosis function.

Dex, as a potent anti-inflammatory drug, can significantly inhibit TNF-α-induced pro-inflammatory reactions (Castro et al. 2011). Adalimumab is an efficient TNF-α inhibitor and widely used in the treatment of rheumatoid arthritis (RA), ankylosing spondylitis and uveitis. In the presented study, the expression of Arg-1 and arginase activity were significantly decreased in LPS treated HTM with additional Dex or Adalimumab treatment. BMDMs exposed to increased HP and treated with etanercept (a fusion protein against TNF-α) also showed weaker arginase activity (data not shown). TNF-α could be a possible inducer for the activation of arginase, however, further study is needed to prove it (Fig. 30).

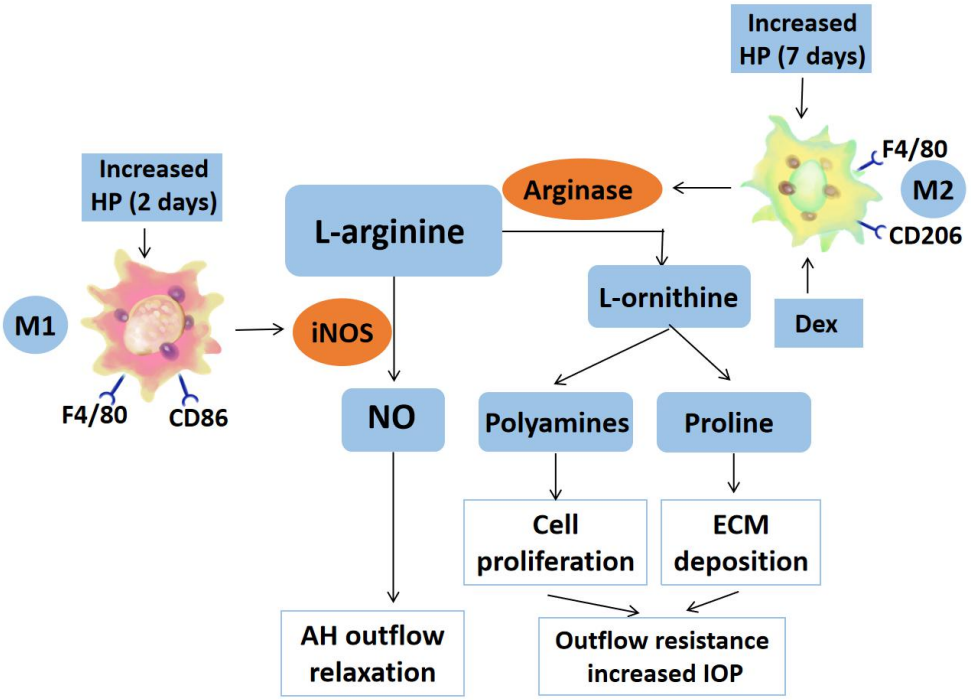

Figure 30 The alteration of the arginine metabolism in BMDMs by different polarization under increased HP

The arginine metabolism in macrophages under increased HP. After cultured under increased HP for 2 days, BMDMs polarized to M1 phenotype with highly expressed iNOS. iNOS could metabolize L-arginine and produce NO, which may relax the AH outflow pathway. After 7 days under increased HP or with Dex treatment, macrophages switched to M2 phenotype with increased arginase expression and activity. Arginase could metabolize L-arginine to L-ornithine and further to polyamines (induces cell proliferation) and proline (increases ECM deposition), which may result in upregulated outflow resistance and increased IOP. BMDMs=bone marrow-derived macrophages; HP=hydrostatic pressure; iNOS=inducible nitric oxide synthase; NO=nitric oxide; ECM=extracellular matrix; Dex=dexamethasone; AH=aqueous humor; IOP=intraocular pressure. Macrophages were drawn by Zhiqiang Liu and permission granted.

4.4 Influence of increased HP on ECM accumulation and production of α-smooth muscle actin (SMA)

The TM is a “semi-porous diaphragm” to regulate the AH outflow and IOP (Bradley et al. 2001). Decreased AH outflow facility in TM resulting to elevated IOP has been discovered in glaucoma patients, and cells in TM (TM cells and resident or infiltrated macrophages) can react to mechanical stress (increased IOP), and maintain the outflow facility (Liton and Gonzalez 2008). Apart from the morphological changes of TM, the accumulation and turnover of ECM proteins (especially by increased deposition of fibronectin, collagen, and elastin) in the outflow pathway seem to play an important role

in outflow resistance (Stamer and Clark 2017).

In the presented study, in BMDMs in medium or LPS group cultured at 60mmHg, a decreased expression of fibronectin and collagen IV compared to 0mmHg or 20mmHg groups could be determined. This is consistence with a previous study showing that macrophages exposed to increased mechanical stress can induce TNF-α, IL-1β, IL-6, resulting in increased MMP-1/2/9, which take part in ECM (collagen IV) turnover and outflow relaxation (Pugin et al. 1998). Increased TNF-α level in perfused anterior segment cultures was able to increase MMP-3 and outflow rate (Bradley et al. 2001). However, in HTM cells, no decreased ECM production was found under increased HP in the present study. Macrophages are resident cells in the TM and can infiltrate into the TM tissues (Alvarado et al. 2010). These macrophages may produce TNF-α upon increased pressure, degrade ECM, resulting in an increase outflow and maintained IOP. This is supported by the previous study showing that the treatment with laser trabeculoplasty (an IOP lowing treatment for glaucoma) can stimulate the release of TNF-α within hours (Bradley et al. 2001). Lower level of fibronectin was produced after TNF-α treatment of TM cells while MMP-2/3 expression was increased according to a microarray analysis (Chen et al. 2005).

In contrast to the decreased ECM under increased HP in BMDMs, the HTM cultured with medium at increased HP (60mmHg) for 24 hours showed significantly increased expression of collagen IV compared to that in normal HP group (20mmHg) or control groups (0mmHg). Decreased degradation and increased synthesis of collagen IV has been reported in the AH of glaucoma patients (Acott and Kelley 2008). *In vivo* studies documented over-expression of fibronectin in TM of glaucomatous eyes (Raghunathan et al. 2018). Even though, no significantly increased fibronectin expression was found in the HTM cells under increased HP in the present study, the composition of the ECM in HTM cells was induced by increased HP in the present study. However, an *ex vivo* study using perfused healthy eyes under increased pressure showed increased outflow facility and alteration of ECM in TM (Raghunathan et al. 2018). The performed increased pressure level in Raghunathan's study was 17.6mmHg compared to 8.8mmHg, which is not comparable to 60mmHg, as performed in the current study.

The relationship of ECM synthesis and IRI has been described previously. During IRI, infiltration of immune cells is closely related to inflammation and toxic effect in IR tissues, and ECM seems to be essential for the integrity of different barriers, and induction of MMPs with degraded ECM have been documented in various organs and tissues in IRI (Harwani 2018). For example, significantly decreased collagen IV and fibronectin proteins was reported in cerebral IR (Hamann et al. 1996). Similar to the brain, the retina can be protected against ischemic injury by the blood-retina barrier with ECM maintaining the normal structure of brain-retina barrier. Retina IRI has been reported to be related to the ECM alteration, which leads to retina and ONH damage (Reinhard et al. 2017). Therefore, the decreased ECM production by macrophages under higher HP may be related to the known IRI in pathogenesis of glaucoma.

After culture for 24 hours, a decreased expression of α-SMA in BMDMs exposed to increased HP was found. Even though no significant difference in α-SMA under pressure was found in HTM cells, LPS treated HTM cells showed significant decreased α-SMA expression compared to LPS+Adalimumab group at 60mmHg. α-SMA is an important protein taking part in fibrotic diseases and the upregulating α-SMA seems to play a role in tissue contraction and ocular hypertension (Raghunathan et al. 2018). The induced TNF-α level by increased pressure found in the current study could be one explanation of decreased α-SMA under increased HP. Even though there are no related studies about macrophage and TM cells to the best of our knowledge, previous study using human dermal fibroblasts indicated that TNF-α stimulation decreased the α-SMA expression and fibronectin and collagen I deposition (Goldberg et al. 2007), which is similar to the results of the present study (Fig. 31).

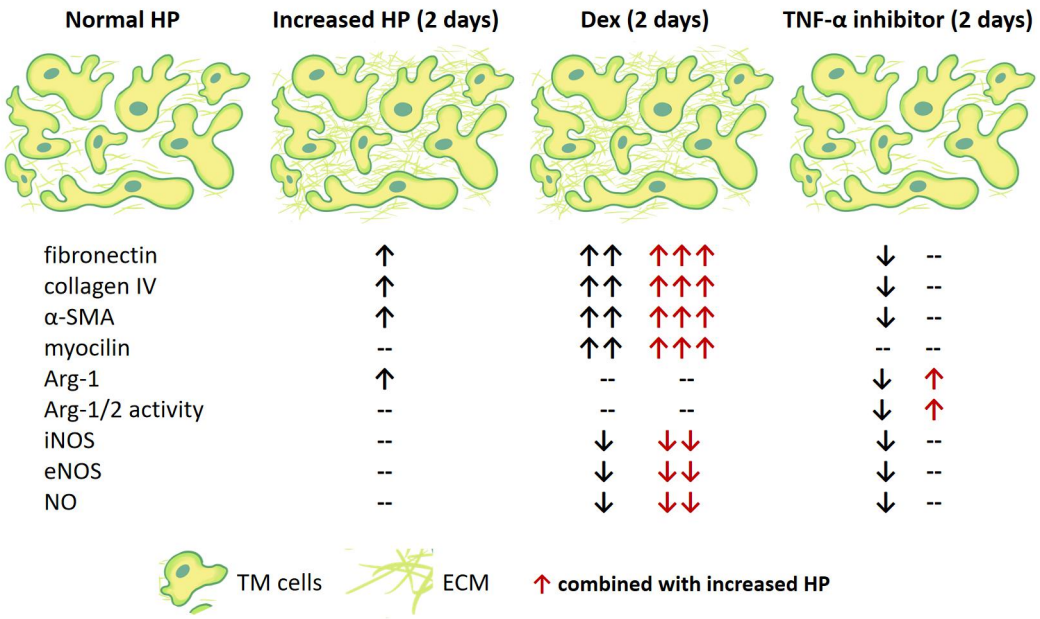

Figure 31 The alteration of HTM cells under increased HP

Under normal pressure, HTM cells produced fibronectin, collagen IV and α-SMA, express Arg-1, iNOS, eNOS and release NO. After cultured under increased HP for 2 days, HTM cells produced more fibronectin, collagen IV, α-SMA and express more Arg-1. With Dex treatment for 2 days, more ECM proteins (fibronectin and collagen IV) were produced by HTM cells. α-SMA and myocilin were up-regulated, while iNOS, eNOS and NO were decreased with Dex treatment. When Dex-treated HTM were cultured under increased HP for 2 days, the ECM deposition was further increased, α-SMA and myocilin were further up-regulated, while iNOS, eNOS and NO were further decreased. TNF-α inhibitor (Adalimumab) decreased the ECM production, α-SMA, Arg-1 and arginase activity in HTM cells, which decreased iNOS, eNOS and NO level. When co-cultured with increased HP, the Arg-1 expression and arginase activity were increased in HTM cells. HTM=human trabecular meshwork; HP=hydrostatic pressure; Dex=dexamethasone; TNF-α=tumor necrosis factor-α; α-SMA=α-smooth muscle actin; Arg=arginase; iNOS=inducible nitric oxide synthase; eNOS=endothelial nitric oxide synthase; NO=nitric oxide; ECM=extracellular matrix. Drawn by Zhiqiang Liu and permission granted.

4.5 The influence of GCs on ECM production, α-SMA or myocilin expression in BMDMs and HTM cells under increased HP

Experimental GC-induced glaucoma is widely used to mimic POAG, and GC-treated TM has been studied for decades as a model for the pathogenesis of OHT in POAG. Dex, as a synthetic GC, is widely used to study the GC-induced OHT. Furthermore, GC administration in the treatment of ocular inflammation such as uveitis can induce the ocular hypertension and secondary OAG (Din et al. 2012). GC-treated TM cells shows changes in the morphology, ECM deposition, MMPs expression, cell functions, and expression of TM related proteins (Clark et al. 2001).

In this study, Dex-treated HTM cells and BMDMs were used to study the GC-induced processes involved in OHT and glaucoma *in vitro*. Dex exposure to cultured BMDMs and HTM cells showed increased production and deposition of ECM proteins (fibronectin and collagen IV). Similar to the current results, an elevated expression of fibronectin and collagen IV was found in Dex-treated HTM cells, and in Dex-treated TM tissues, as described previously (Raghunathan et al. 2015). Some investigators have assumed that accumulation of ECM may be in part due to the decreased phagocytosis ability in TM cells by GC treatment (Stamer and Clark 2017). In TM cells GC may induce TGF-β, thereby inhibiting MMPs, and impairing ECM turnover, thus causing GC-induced ECM deposition, leading to OHT and glaucoma (Fini et al. 2017).

Apart from the increased deposition of ECM, the fibronectin sheets in Dex-treated HTM cells were denser compared to non-treated cells, which showed only diffused fibronectin (Raghunathan et al. 2018). Similar observation could be made in the present study. This assembled fibronectin and its fibril formation in Dex-treated cells, and also the cell-ECM attachments have been previously explained by upregulated integrin binding (Acott and Kelley 2008). Upregulated fibronectin-integrin binding can induce the formation of cross-link actin network (CLANs) to increase outflow resistance. This has been reported in glaucomatous eyes of primary open-angle glaucoma (POAG) and GC-induced glaucoma (Clark et al. 2001). Fibronectin itself may also perform as a scaffold and lead to the deposition and accumulation of other ECM proteins (such as collagen), to stabilize matrix and thus elevate IOP (Raghunathan et al. 2018).

Significantly increased α-SMA and myocilin expression has been shown in Dex-treated HTM cells, similar to the previous study (Raghunathan et al. 2015). The increased α-SMA level after GC treatment, and resulting increased TM cell contraction and TM stiffness may be one explanation for elevated IOP induced by GCs (Raghunathan et al. 2018). Previous studies have shown that MYOC gene and myocilin expression is associated with glaucoma and can be induced by TGF-β1 and Dex (Clark et al. 2001). The particular function of myocilin is not fully understood, but it has been documented that the intracellular increased myocilin can induce endoplasmic reticulum

(ER) stress in TM cells, causing deposition of abnormal/misfolded proteins (including ECM proteins), leading to fibrosis, thereby decreasing the outflow rate, thus increase IOP (Kasetti et al. 2017). A recent study reported that the ECM deposition in glaucomatous HTM cells treated with Dex was stiffer than that in Dex-treated normal HTM cells, with higher expression of α-SMA and myocilin (Raghunathan et al. 2018). The same study also showed that ECM derived from glaucomatous TM cells or Dex-treated HTM cells impair the ability of normal HTM cells in ECM turnover, and induce α-SMA/myocilin expression and ER stress in normal HTM cells (Raghunathan et al. 2018). These previous studies are consistent with the results in the present study that HTM cells treated with Dex produced more ECM proteins, e.g. more fibrillar fibronectin formation, increased α-SMA and myocilin expression when cultured at increased HP as compared to 0mmHg or 20mmHg. These changes in Dex-treated HTM cells may be the reason for the increased ECM deposition with increased pressure.

In this study, also Dex-treated BMDMs showed an increased ECM production in response to increased HP. It has been shown previously that GCs have strong anti-inflammatory properties, e.g. by blocking nuclear factor-kappa b (NF-κB) activation. GCs also can block the LPS or mechanical stress-mediated pro-inflammatory responses in macrophages (Pugin et al. 1998). The suppressed pro-inflammatory responses has been reported to be related to the impaired ECM turnover (Goldberg et al. 2007), which is in line with the present study.

As discussed in 4.3, arginase plays an important role in fibrotic processes. Decreased arginase-activity/expression was also shown in Dex-treated HTM cells in the present study. Furthermore, less iNOS/eNOS expression, NO production and decreased arginase expression/activity were shown in Dex groups, which may be related to the downregulated pro-inflammatory response. The iNOS/eNOS protein and NO level in Dex-treated HTM cells were further downregulated, while arginase activity was upregulated by increased HP. Arginase play an important role in fibrosis process and induce the expression of collagen (Moore et al. 2015), higher arginase activity by increased pressure may also be an explanation for higher GC susceptibility in glaucoma patients and further OHT (Fig. 29-31).

4.6 Increased HP primarily induced an M1, and secondary an M2 phenotype in macrophages

In order to modulate the immune response, macrophages can polarize into different phenotypes to response to various stimulation and signals differently. Macrophages have been classified in the M1 and M2 lineages (M1 is for Th1 activation and M2 is related to Th2 responses) (Murray et al. 2014). The classically activated macrophages (M1) can be polarized by IFN-γ and LPS and mainly have pro-inflammatory function (for host defense). The M2-macrophages are also termed "alternatively activated macrophages" encompass cells with huge differences in their biochemistry and physiology, e.g. in wound healing or regulatory function (Martinez et al. 2008).

The expressions of different surface markers and intracellular molecules can be used to identify the macrophage phenotype. M1 was identified by the highly expressed surface markers CD68, CD80, CD86, major histocompatibility complex (MHC) -II, and CC chemokine receptor (CCR) 2. M2 surface molecules were CD163, CD206, CX3CR1, and YM1/2. M1/M2 can be also classified according to the differences in cytokines and chemokine expression (Mantovani et al. 2004). Pro-inflammatory cytokines such as TNF-α, IL-1, -6, -12, -18, and -23 are secreted by M1 macrophages, while TGF-β1 and IL-10 are secreted by M2 macrophages (Gordon and Martinez 2010). In the present study, a larger proportion of CD86+/CD206- macrophages could be found in higher pressure groups (60 mmHg) after 48-hour LPS stimulation compared to 0mmHg, indicating a stronger M1 polarization with higher pressure stimulation. More expression and secretion of TNF-α and IL-6 supported the conclusion that macrophages are polarized into an M1 phenotype upon higher pressure after 48h. After a prolonged culture time of BMDMs under increased pressure for 7 days, unstimulated cells (medium group) polarized to M2, with larger proportion of CD86-/CD206+ macrophages. Similarly, larger proportion of M2 population under increased pressure was found in LPS group, although the differences between different pressures did not reach a significant level. The M1 population in LPS group was significantly decreased under increased pressure, which also indicates a M2 polarization. Larger proportion of

IL-10+ macrophages and higher IL-10 level were also found in BMDMs under higher pressure compared to normal pressure after 7 days (data not shown). BMDMs cultured under higher pressure after 7 days may polarize to M2 to display their anti-inflammatory, proangiogenetic and wound healing functions.

Macrophage polarizations by pressure stimulations has also been studied in hypertension. More CD161a+/CD68+ M1 polarization of macrophages under higher pressure condition has been reported in spontaneously hypertensive rat and the inflammatory response by M1 macrophages may be responsible for premature hypertension (Harwani et al. 2016). Other studies reported that inhibiting M1 and inducing M2 can normalize elevated blood pressure in rats with spontaneously hypertension (Harwani 2018). Although the infiltrating of macrophages, pro-inflammatory progression and the cytokines/chemokines released by macrophages are regarded to be related to neuroinflammation and the pathogenesis of glaucoma (Williams et al. 2017), the role of macrophage polarization under increased HP has not been reported previously. In the present study, BMDMs under increased pressure first polarized to M1 phenotype (after 48 hours) and then promoted a M2 polarization (7 days). Recently, the M2 marker CD163+ of macrophages has been found to be upregulated in both AH pathway and ONH of enucleated glaucomatous eyes compared to healthy group, indicates the neuro-protective role of M2 macrophages in glaucoma (Margeta et al. 2018). However, after culture of BMDMs under increased HP, no significant difference in CD163+ frequency was found (data not shown). Previous study indicated that macrophages in inflammation conditions can switch from M1 to M2 (Harwani 2018). In human eyes with POAG, increased IOP first induces acute inflammatory response, with an infiltration of immune cells and upregulation of numerous pro-inflammatory cytokines; proliferation and remolding are followed, with angiogenetic and fibrotic processes (Taurone et al. 2015). It was also reported previously in mice hypertension model that, after confirming M1 polarization in blood vessel, macrophages polarized to M2 phenotype with increased CD206 and Arg-1 expression at 7-14 days after angiotensin II infusion (Moore et al. 2015). These M2 population was associated with elevated blood pressure and fibrosis (Moore et al. 2015).

A similar M1 to M2 shifting was also reported in oxygen-induced retinopathy in mice (Zhu et al. 2017). Such changes in phenotypes may play an important role in the neuroinflammation in the eye with elevated IOP.

The arginase metabolism plays an essential role in hypertension and the polarization of macrophages and may be responsible for these altered L-arginine metabolism (Harwani 2018). Previous studies have found that M1 phenotype induces high level of iNOS and metabolize L-arginine to NO, while the M2 phenotype induces high level of Arg-1 and induces the production of ornithine, polyamines and prolines from L-arginine (Martinez et al. 2008). The NO level is indispensable for the regulation of AH outflow (Aliancy et al. 2017). Therefore, M1/M2 polarization could be important in the regulation of outflow facility and IOP via arginase metabolism as a decreased NO level, increased arginase activity in BMDMs under higher HP on both 2 days and 7 days (data from 7 days were not shown) was shown in the present study.

Dex treatment can not only suppress the pro-inflammatory response via decreasing the production of IFN-γ, TNF-α, IL-1/-6/-8, Dex also induce the production of IL-10 and TGF-β1 during immune or inflammation process. Dex may thereby induce macrophages to differentiate into an alternative activated phenotype (M2) *in vitro* (Castro et al. 2011). Under pro- inflammatory conditions (e.g. LPS stimulation), higher pressure support the induction of the pro-inflammatory response (release TNF-α and IL-6) and M1 differentiation after culture for 48 hours. However, with additional Dex treatment, enhanced expression and secretion of pro-inflammatory cytokines under increased pressure could be blocked. Macrophages exposed to Dex switched to M2 polarization and displayed larger CD86-/CD206+ population and produce more ECM (fibronectin and collagen IV) deposition after cultured under higher HP. In the eye GC treatment can lead to more ECM deposition in the outflow pathway and outflow obstruction (Clark et al. 2005; Zhang et al. 2007). The suppressed pro-inflammatory reaction and M2 polarization of macrophages in TM may be related to the outflow obstruction in GC-induced OHT, but further studies need to be done to prove this.

Fibrosis seems to be close related to GC-induced OHT (Clark et al. 2001). M2 macrophages can produce large amounts of Arg-1 and TGF-β1, and thereby contribute

to a fibrotic process (Moore et al. 2015). The increased M2 polarization of GC-exposed macrophages in the outflow pathway by higher pressure may be related to the pathogenesis of GC-induced OHT or glaucoma.

In IR, M1 macrophages accumulate after injury and can express large amount of pro-inflammatory factors (IL-1β, TNF-α, iNOS, et.al.), which is regarded to be related to tissue ischemic injury, and M2 is responsible for tissue repair with high level of IL-10, TGF-β1 and Arg-1 (Huen and Cantley 2015). In retinal IRI, inflammatory response begins from few hours until several days (generally 7 days), and chronic phase started from days and lasted for months (Song et al. 2017). Here, IL-10, as a typical M2 marker, has been reported to be upregulated 144h after starting the IRI model, and high level of TNF-α still could be detected at this time point (Song et al. 2017). The macrophage polarization as found in this study is consistent with these studies (Fig. 29 and 30).

Taken together, the present study demonstrates that higher HP upregulates macrophages to a primary pro-inflammatory reactions of M1 phenotype and shifts to a M2 related reactions under prolonged increased pressure. The plasticity of macrophages in the diversities of phenotypes and functions, together with the changes in TM cells during higher pressure may be essential to the pathogenesis of ocular hypertension and IRI during glaucoma. The M2 polarization of macrophages with Dex treatment, further upregulated M2 polarization under increased HP, together with the increased arginase activity and increased ECM deposition in macrophages and TM cells may be related to GC-induced OHT and secondary glaucoma in uveitis.

5 Summary

In the presented thesis, the influence of increased hydrostatic pressure (HP) and dexamethasone treatment on bone marrow derived macrophages (BMDMs) or human trabecular meshwork (HTM) cells was investigated. A pressure chamber system was used to culture cells at room pressure, 20 mmHg, or 60 mmHg. After culture at the different HPs for various time points (2 days or 7 days), cells were analyzed by immunofluorescence microscopy, flow cytometry, bioassay, enzyme-linked immunosorbent assay (ELISA).

BMDMs cultured under increased HP (60 mmHg) for 24 or 48 hours showed increased pro-inflammatory reactions and pronounced M1 polarization. After exposure of BMDMs to higher HP for 1 week, macrophages shifted to an M2 polarization with wound healing reaction. Moreover, dexamethasone treatment of macrophages induced a pronounced M2 polarization after 48h and 7 days. This M2 polarization could be further enlarged by increased HP.

Increased Arg-1/2 expression and activity upon increased HP or increased deposition of extracellular matrx (ECM) molecules after dexamethasone treatment may be related to the obstruction of the outflow pathway during the development of glaucoma and glucocorticoid (GC)-induced ocular hypertension (OHT)/glaucoma in uveitis.

Similar to macrophages, HTM cells showed increased deposition of ECM proteins and an increased arginase (Arg)-1 expression and activity under higher pressure (60mmHg), which increased further by dexamethasone treatment.

Modulation of the arginase and tumor necrosis factor (TNF)-α response under increase HP seem to play an important role in the function of both macrophages and HTM cells.

The promoted inflammatory process, arginase expression/activity and deposition of ECM by higher pressure in macrophages or HTM cultures seem to be closely related to the pressure-induced IRI in the eye and can be responsible for the development and deterioration of OHT or secondary glaucoma in uveitis..

6 References

1. Acharya, N.R., Tham, V.M., Esterberg, E., Borkar, D.S., Parker, J.V., Vinoya, A.C., Uchida, A. (2013): Incidence and prevalence of uveitis: results from the Pacific Ocular Inflammation Study. JAMA Ophthalmol. 131, 1405-1412.
2. Acott, T.S., Kelley, M.J. (2008): Extracellular matrix in the trabecular meshwork. Exp Eye Res. 86, 543-561.
3. Aliancy, J., Stamer, W.D., Wirostko, B. (2017): A review of nitric oxide for the treatment of glaucomatous disease. Ophthalmol Ther. 6, 221-232.
4. Alvarado, J.A., Katz, L.J., Trivedi, S., Shifera, A.S. (2010): Monocyte modulation of aqueous outflow and recruitment to the trabecular meshwork following selective laser trabeculoplasty. Arch Ophthalmol. 128, 731-737.
5. Anilkumar, U., Prehn, J.H. (2014): Anti-apoptotic BCL-2 family proteins in acute neural injury. Front Cell Neurosci. 8, 281.
6. Bauer, D., Hennig, M., Wasmuth, S., Baehler, H., Busch, M., Steuhl, K.-P., Thanos, S., Heiligenhaus, A. (2012): Amniotic membrane induces peroxisome proliferator-activated receptor-γ positive alternatively activated macrophages. Invest Ophthalmol Vis Sci. 53, 799-810.
7. Bauer, D., Kasper, M., Walscheid, K., Koch, J.M., Müther, P.S., Kirchhof, B., Heiligenhaus, A., Heinz, C. (2018): Multiplex cytokine analysis of aqueous humor in juvenile idiopathic arthritis-associated anterior uveitis with or without secondary glaucoma. Frontiers in immunology. 9, 708.
8. Böhm, M.R., Schallenberg, M., Brockhaus, K., Melkonyan, H., Thanos, S. (2016): The pro-inflammatory role of high-mobility group box 1 protein (HMGB-1) in photoreceptors and retinal explants exposed to elevated pressure. Lab Invest. 96, 409.
9. Boland, M.V., Ervin, A.-M., Friedman, D.S., Jampel, H.D., Hawkins, B.S., Vollenweider, D., Chelladurai, Y., Ward, D., Suarez-Cuervo, C., Robinson, K.A. (2013): Comparative effectiveness of treatments for open-angle glaucoma: a systematic review for the US Preventive Services Task Force. Ann Intern Med. 158, 271-279.
10. Bradley, J.M., Kelley, M.J., Rose, A., Acott, T.S. (2003): Signaling pathways used in trabecular matrix metalloproteinase response to mechanical stretch. Invest Ophthalmol Vis Sci. 44, 5174-5181.
11. Bradley, J.M., Kelley, M.J., Zhu, X., Anderssohn, A.M., Alexander, J.P., Acott, T.S. (2001): Effects of mechanical stretching on trabecular matrix metalloproteinases. Invest Ophthalmol Vis Sci. 42, 1505-1513.
12. Castro, R., Zou, J., Secombes, C.J., Martin, S.A.J.F. (2011): Cortisol modulates the induction of inflammatory gene expression in a rainbow trout macrophage cell line. Fish Shellfish Immun. 30, 215-223.
13. Chen, Y., Kelley, M., Acott, T. (2005): DNA Microarray Analysis of Gene Expression in Tabecular Meshwork Cells in Response to TNF and IL–1. Invest Ophthalmol Vis Sci. 46, 1349-1349.
14. Chinnery, H.R., McMenamin, P.G., Dando, S.J. (2017): Macrophage physiology in the eye. Pflugers Arch. 469, 501-515.

15. Chuman, H., Chuman, T., Nao-i, N., Sawada, A. (2000): The effect of L-arginine on intraocular pressure in the human eye. Curr Eye Res. 20, 511-516.
16. Civan, M.M., Macknight, A.D. (2004): The ins and outs of aqueous humour secretion. Exp Eye Res. 78, 625-631.
17. Clark, A.F., Brotchie, D., Read, A.T., Hellberg, P., English-Wright, S., Pang, I.H., Ethier, C.R., Grierson, I. (2005): Dexamethasone alters F-actin architecture and promotes cross-linked actin network formation in human trabecular meshwork tissue. Cell Motil Cytoskel. 60, 83-95.
18. Clark, A.F., Steely, H.T., Dickerson, J.E., English-Wright, S., Stropki, K., McCartney, M.D., Jacobson, N., Shepard, A.R., Clark, J.I., Matsushima, H. (2001): Glucocorticoid induction of the glaucoma gene MYOC in human and monkey trabecular meshwork cells and tissues. Invest Ophthalmol Vis Sci. 42, 1769-1780.
19. Cone, R.E., Pais, R. (2009): Anterior chamber-associated immune deviation (ACAID): an acute response to ocular insult protects from future immune-mediated damage? Ophthalmol Eye Dis. 1, OED. S2858.
20. Deschenes, J., Murray, P.I., Rao, N.A., Nussenblatt, R.B. (2008): International Uveitis Study Group (IUSG) clinical classification of uveitis. Ocul Immunol Inflamm. 16, 1-2.
21. Din, N.M., Isa, H., Taylor, S.R., Barton, K., Lightman, S.L., McCluskey, Rothova, Herbert, Heinz, Boer, d. (2012): Intraocular pressure elevation in uveitis. Expert Rev Ophthalmol. 7, 45-59.
22. El-Gayar, S., Thüring-Nahler, H., Pfeilschifter, J., Röllinghoff, M., Bogdan, C. (2003): Translational control of inducible nitric oxide synthase by IL-13 and arginine availability in inflammatory macrophages. J Immunol. 171, 4561-4568.
23. Ferrier, G., McEvoy, A., Evans, C., Andrew, J. (2000): The effect of cyclic pressure on human monocyte-derived macrophages in vitro. J Bone Joint Surg. 82, 755-759.
24. Fini, M.E., Schwartz, S.G., Gao, X., Jeong, S., Patel, N., Itakura, T., Price, M.O., Price Jr, F.W., Varma, R., Stamer, W.D. (2017): Steroid-induced ocular hypertension/glaucoma: Focus on pharmacogenomics and implications for precision medicine. Prog Retin Eye Res. 56, 58-83.
25. Fouda, A.Y., Xu, Z., Shosha, E., Lemtalsi, T., Chen, J., Toque, H.A., Tritz, R., Cui, X., Stansfield, B.K., Huo, Y. (2018): Arginase 1 promotes retinal neurovascular protection from ischemia through suppression of macrophage inflammatory responses. Cell Death Dis. 9, 1001.
26. Goldberg, M.T., Han, Y.P., Yan, C., Shaw, M.C., Garner, W.L. (2007): TNF-alpha suppresses alpha-smooth muscle actin expression in human dermal fibroblasts: an implication for abnormal wound healing. J Invest Dermatol. 127, 2645-2655.
27. Gordon, S., Martinez, F.O. (2010): Alternative activation of macrophages: mechanism and functions. Immunity. 32, 593-604.
28. Grierson, I., Lee, W.R. (1973): Erythrocyte phagocytosis in the human trabecular meshwork. Br J Ophthalmol. 57, 400-415.
29. Hamann, G.F., Okada, Y., del Zoppo, G.J. (1996): Hemorrhagic transformation and microvascular integrity during focal cerebral ischemia/reperfusion. J Cerebr Blood F Met. 16, 1373-1378.

30. Harwani, S.C. (2018): Macrophages under pressure: the role of macrophage polarization in hypertension. Transl Res. 191, 45-63.
31. Harwani, S.C., Ratcliff, J., Sutterwala, F.S., Ballas, Z.K., Meyerholz, D.K., Chapleau, M.W., Abboud, F.M. (2016): Nicotine mediates CD161a+ renal macrophage infiltration and premature hypertension in the spontaneously hypertensive rat. Circ Res. 119, 1101-1115.
32. Harwerth, R., Wheat, J., Fredette, M., Anderson, D. (2010): Linking structure and function in glaucoma. Prog Retin Eye Res. 29, 249-271.
33. Heinz, C., Koch, J.M., Zurek-Imhoff, B., Heiligenhaus, A. (2009): Prevalence of uveitic secondary glaucoma and success of nonsurgical treatment in adults and children in a tertiary referral center. Ocul Immunol Inflamm. 17, 243-248.
34. Herbert, H.M., Viswanathan, A., Jackson, H., Lightman, S.L. (2004): Risk factors for elevated intraocular pressure in uveitis. J Glaucoma. 13, 96-99.
35. Howell, G.R., Soto, I., Zhu, X., Ryan, M., Macalinao, D.G., Sousa, G.L., Caddle, L.B., MacNicoll, K.H., Barbay, J.M., Porciatti, V. et al. (2012): Radiation treatment inhibits monocyte entry into the optic nerve head and prevents neuronal damage in a mouse model of glaucoma. The Journal of Clinical Investigation. 122, 1246-1261.
36. Huang, Y., Li, Z., van Rooijen, N., Wang, N., Pang, C.P., Cui, Q. (2007): Different responses of macrophages in retinal ganglion cell survival after acute ocular hypertension in rats with different autoimmune backgrounds. Exp Eye Res. 85, 659-666.
37. Huen, S.C., Cantley, L.G. (2015): Macrophage-mediated injury and repair after ischemic kidney injury. Pediatr Nephrol. 30, 199-209.
38. Jabs, D.A., Nussenblatt, R.B., Rosenbaum, J.T., Group., S.o.U.N.S.W. (2005): Standardization of uveitis nomenclature for reporting clinical data. Results of the First International Workshop. Am J Ophthalmol. 140, 509-516.
39. Jaffe, G.J., Dick, A.D., Brézin, A.P., Nguyen, Q.D., Thorne, J.E., Kestelyn, P., Barisani-Asenbauer, T., Franco, P., Heiligenhaus, A., Scales, D. (2016): Adalimumab in patients with active noninfectious uveitis. N Engl J Med. 375, 932-943.
40. Johnson, E.C., Doser, T.A., Cepurna, W.O., Dyck, J.A., Jia, L., Guo, Y., Lambert, W.S., Morrison, J.C. (2011): Cell proliferation and interleukin-6–type cytokine signaling are implicated by gene expression responses in early optic nerve head injury in rat glaucoma. Invest Ophthalmol Vis Sci. 52, 504-518.
41. Kasetti, R.B., Maddineni, P., Millar, J.C., Clark, A.F., Zode, G.S. (2017): Increased synthesis and deposition of extracellular matrix proteins leads to endoplasmic reticulum stress in the trabecular meshwork. Sci Rep. 7, 14951.
42. Keller, K.E., Bhattacharya, S.K., Borrás, T., Brunner, T.M., Chansangpetch, S., Clark, A.F., Dismuke, W.M., Du, Y., Elliott, M.H., Ethier, C.R. (2018): Consensus recommendations for trabecular meshwork cell isolation, characterization and culture. Exp Eye Res. 171, 164-173.
43. Kelley, M., Rose, A., Keller, K., Hessle, H., Samples, J., Acott, T. (2009): Stem cells in the trabecular meshwork: present and future promises. Exp Eye Res. 88, 747-751.
44. Kim, B.-Y., Son, Y., Lee, J., Choi, J., Kim, C.D., Bae, S.S., Eo, S.-K., Kim, K. (2017): Dexamethasone inhibits activation of monocytes/macrophages in a milieu rich in 27-oxygenated cholesterol. PloS one. 12, e0189643.

45. Kwon, Y.H., Fingert, J.H., Kuehn, M.H., Alward, W.L. (2009): Primary Open-Angle Glaucoma. N Engl J Med. 360, 1113-1124.
46. Lin, Y.-C., Lin, Y.-C., Wu, C.-C., Huang, M.-Y., Tsai, W.-C., Hung, C.-H., Kuo, P.-L. (2017): The immunomodulatory effects of TNF-α inhibitors on human Th17 cells via RORγt histone acetylation. Oncotarget. 8, 7559.
47. Liton, P.B., Gonzalez, P. (2008): Stress response of the trabecular meshwork. J Glaucoma. 17, 378.
48. Liton, P.B., Luna, C., Bodman, M., Hong, A., Epstein, D.L., Gonzalez, P. (2005): Induction of IL-6 expression by mechanical stress in the trabecular meshwork. Biochem Biophys Res Commun. 337, 1229-1236.
49. Mantovani, A., Sica, A., Sozzani, S., Allavena, P., Vecchi, A., Locati, M. (2004): The chemokine system in diverse forms of macrophage activation and polarization. Trends Immunol. 25, 677-686.
50. Margeta, M.A., Lad, E.M., Proia, A.D. (2018): CD163+ macrophages infiltrate axon bundles of postmortem optic nerves with glaucoma. Graefes Arch Clin Exp Ophthalmol. 256, 2449-2456.
51. Martinez, F.O., Sica, A., Mantovani, A., Locati, M. (2008): Macrophage activation and polarization. Front Biosci. 13, 453-461.
52. Maruyama, K., Nemoto, E., Yamada, S. (2019): Mechanical regulation of macrophage function-cyclic tensile force inhibits NLRP3 inflammasome-dependent IL-1β secretion in murine macrophages. Inflamm Regen. 39, 3.
53. Matsuo, T. (2000): Basal nitric oxide production is enhanced by hydraulic pressure in cultured human trabecular cells. Br J Ophthalmol. 84, 631-635.
54. Mercalli, A., Calavita, I., Dugnani, E., Citro, A., Cantarelli, E., Nano, R., Melzi, R., Maffi, P., Secchi, A., Sordi, V. (2013): Rapamycin unbalances the polarization of human macrophages to M 1. Immunology. 140, 179-190.
55. Moore, J.P., Vinh, A., Tuck, K.L., Sakkal, S., Krishnan, S.M., Chan, C.T., Lieu, M., Samuel, C.S., Diep, H., Kemp-Harper, B.K. (2015): M2 macrophage accumulation in the aortic wall during angiotensin II infusion in mice is associated with fibrosis, elastin loss, and elevated blood pressure. Am J Physiol Heart Circ Physiol. 309, H906-H917.
56. Murray, P.J., Allen, J.E., Biswas, S.K., Fisher, E.A., Gilroy, D.W., Goerdt, S., Gordon, S., Hamilton, J.A., Ivashkiv, L.B., Lawrence, T. (2014): Macrophage activation and polarization: nomenclature and experimental guidelines. Immunity. 41, 14-20.
57. Nakazawa, T., Nakazawa, C., Matsubara, A., Noda, K., Hisatomi, T., She, H., Michaud, N., Hafezi-Moghadam, A., Miller, J.W., Benowitz, L.I. (2006): Tumor necrosis factor-α mediates oligodendrocyte death and delayed retinal ganglion cell loss in a mouse model of glaucoma. J Neurosci. 26, 12633-12641.
58. Narayanan, S.P., Rojas, M., Suwanpradid, J., Toque, H.A., Caldwell, R.W., Caldwell, R.B. (2013): Arginase in retinopathy. Prog Retin Eye Res. 36, 260-280.
59. Nathanson, J.A., McKee, M. (1995a): Alterations of ocular nitric oxide synthase in human glaucoma. Invest Ophthalmol Vis Sci. 36, 1774-1784.
60. Nathanson, J.A., McKee, M. (1995b): Identification of an extensive system of nitric oxide-producing cells in the ciliary muscle and outflow pathway of the human eye. Invest Ophthalmol Vis Sci. 36, 1765-1773.

61. Nickells, R.W. (2007): From ocular hypertension to ganglion cell death: a theoretical sequence of events leading to glaucoma. Can J Ophthalmol. 42, 278-287.
62. Nickells, R.W. (2012): The cell and molecular biology of glaucoma: mechanisms of retinal ganglion cell death. Invest Ophthalmol Vis Sci. 53, 2476-2481.
63. Oh, D.-J., Martin, J.L., Williams, A.J., Russell, P., Birk, D.E., Rhee, D.J. (2006): Effect of latanoprost on the expression of matrix metalloproteinases and their tissue inhibitors in human trabecular meshwork cells. Invest Ophthalmol Vis Sci. 47, 3887-3895.
64. Overby, D.R., Stamer, W.D., Johnson, M. (2009): The changing paradigm of outflow resistance generation: towards synergistic models of the JCT and inner wall endothelium. Exp Eye Res. 88, 656-670.
65. Paul, C.V., Fred, E., Douglas, E.G., E. Kenneth, S., Allen, B., Bruce, E.P., Marshall, N.C., Howard, W. (2000): The Advanced Glaucoma Intervention Study (AGIS): 7. The relationship between control of intraocular pressure and visual field deterioration. Am J Ophthalmol. 130, 429-440.
66. Polansky, J.R., Weinreb, R.N., Baxter, J.D., Alvarado, J. (1979): Human trabecular cells. I. Establishment in tissue culture and growth characteristics. Invest Ophthalmol Vis Sci. 18, 1043-1049.
67. Pouvreau, I., Zech, J.-C., Thillaye-Goldenberg, B., Naud, M.-C., Van Rooijen, N., de Kozak, Y.J.J.o.n. (1998): Effect of macrophage depletion by liposomes containing dichloromethylene-diphosphonate on endotoxin-induced uveitis. 86, 171-181.
68. Pugin, J., Dunn, I., Jolliet, P., Tassaux, D., Magnenat, J.-L., Nicod, L.P., Chevrolet, J.-C. (1998): Activation of human macrophages by mechanical ventilation in vitro. Am J Physiol Lung Cell Mol Physiol. 275, L1040-L1050.
69. Raghunathan, V.K., Benoit, J., Kasetti, R., Zode, G., Salemi, M., Phinney, B.S., Keller, K.E., Staverosky, J.A., Murphy, C.J., Acott, T. (2018): Glaucomatous cell derived matrices differentially modulate non-glaucomatous trabecular meshwork cellular behavior. Acta Biomater. 71, 444-459.
70. Raghunathan, V.K., Morgan, J.T., Park, S.A., Weber, D., Phinney, B.S., Murphy, C.J., Russell, P. (2015): Dexamethasone stiffens trabecular meshwork, trabecular meshwork cells, and matrix. Invest Ophthalmol Vis Sci. 56, 4447-4459.
71. Rath, M., Müller, I., Kropf, P., Closs, E.I., Munder, M. (2014): Metabolism via arginase or nitric oxide synthase: two competing arginine pathways in macrophages. Frontiers in immunology. 5, 532.
72. Reinhard, J., Renner, M., Wiemann, S., Shakoor, D.A., Stute, G., Dick, H.B., Faissner, A., Joachim, S.C. (2017): Ischemic injury leads to extracellular matrix alterations in retina and optic nerve. Sci Rep. 7, 43470.
73. Renner, M., Stute, G., Alzureiqi, M., Reinhard, J., Wiemann, S., Schmid, H., Faissner, A., Dick, H.B., Joachim, S.C. (2017): Optic nerve degeneration after retinal ischemia/reperfusion in a rodent model. Front Cell Neurosci. 11, 254.
74. Rothova, A., Suttorp-van Schulten, M., Treffers, W.F., Kijlstra, A. (1996): Causes and frequency of blindness in patients with intraocular inflammatory disease. Br J Ophthalmol. 80, 332-336.

75. Rulli, E., Biagioli, E., Riva, I., Gambirasio, G., De Simone, I., Floriani, I., Quaranta, L. (2013): Efficacy and safety of trabeculectomy vs nonpenetrating surgical procedures: a systematic review and meta-analysis. JAMA Ophthalmol. 131, 1573-1582.
76. Shifera, A.S., Trivedi, S., Chau, P., Bonnemaison, L.H., Iguchi, R., Alvarado, J.A. (2010): Constitutive secretion of chemokines by cultured human trabecular meshwork cells. Exp Eye Res. 91, 42-47.
77. Shosha, E., Xu, Z., Yokota, H., Saul, A., Rojas, M., Caldwell, R.W., Caldwell, R.B., Narayanan, S.P. (2016): Arginase 2 promotes neurovascular degeneration during ischemia/reperfusion injury. Cell Death Dis. 7, e2483.
78. Song, Q., Liu, D., Zhang, H., Yi, L., Huo, M. (2017): Expression of inflammatory cytokines in retina ischemia-reperfusion injury rats. Biomed Res. 28, 3066-3071.
79. Sonoki, T., Nagasaki, A., Gotoh, T., Takiguchi, M., Takeya, M., Matsuzaki, H., Mori, M. (1997): Coinduction of nitric-oxide synthase and arginase I in cultured rat peritoneal macrophages and rat tissues in vivo by lipopolysaccharide. J Biol Chem. 272, 3689-3693.
80. Soto, I., Howell, G.R. (2014): The complex role of neuroinflammation in glaucoma. CSH Perspect Med. 4, a017269.
81. Stamer, W.D., Clark, A.F. (2017): The many faces of the trabecular meshwork cell. Exp Eye Res. 158, 112-123.
82. Stamer, W.D., Seftor, R.E., Williams, S.K., Samaha, H.A., Snyder, R.W. (1995): Isolation and culture of human trabecular meshwork cells by extracellular matrix digestion. Curr Eye Res. 14, 611-617.
83. Starkey, P., Turley, L., Gordon, S. (1987): The mouse macrophage-specific glycoprotein defined by monoclonal antibody F4/80: characterization, biosynthesis and demonstration of a rat analogue. Immunology. 60, 117.
84. Taurone, S., Ripandelli, G., Pacella, E., Bianchi, E., Plateroti, A.M., De Vito, S., Plateroti, P., Grippaudo, F.R., Cavallotti, C., Artico, M. (2015): Potential regulatory molecules in the human trabecular meshwork of patients with glaucoma: immunohistochemical profile of a number of inflammatory cytokines. Mol Med Rep. 11, 1384-1390.
85. Tezel, G., Wax, M.B. (2000): Increased production of tumor necrosis factor-α by glial cells exposed to simulated ischemia or elevated hydrostatic pressure induces apoptosis in cocultured retinal ganglion cells. J Neurosci. 20, 8693-8700.
86. Tham, Y.-C., Li, X., Wong, T.Y., Quigley, H.A., Aung, T., Cheng, C.-Y. (2014): Global prevalence of glaucoma and projections of glaucoma burden through 2040: a systematic review and meta-analysis. Ophthalmology. 121, 2081-2090.
87. Trouplin, V., Boucherit, N., Gorvel, L., Conti, F., Mottola, G., Ghigo, E. (2013): Bone marrow-derived macrophage production. J Vis Exp. e50966.
88. Vargas, J.L.C., Osswald, I.K., Unsain, N., Aurousseau, M.R., Barker, P.A., Bowie, D., Di Polo, A. (2015): Soluble tumor necrosis factor alpha promotes retinal ganglion cell death in glaucoma via calcium-permeable AMPA receptor activation. J Neurosci. 35, 12088-12102.
89. Williams, P.A., Marsh-Armstrong, N., Howell, G.R., Bosco, A., Danias, J., Simon, J., Di Polo, A., Kuehn, M.H., Przedborski, S., Raff, M. (2017): Neuroinflammation in glaucoma: A new opportunity. Exp Eye Res. 157, 20-27.

90. Xin, X., Gao, L., Wu, T., Sun, F. (2013): Roles of tumor necrosis factor alpha gene polymorphisms, tumor necrosis factor alpha level in aqueous humor, and the risks of open angle glaucoma: a meta-analysis. Mol Vis. 19, 526.
91. Yasuda, M., Takayama, K., Kanda, T., Taguchi, M., Someya, H., Takeuchi, M. (2017): Comparison of intraocular pressure-lowering effects of ripasudil hydrochloride hydrate for inflammatory and corticosteroid-induced ocular hypertension. PloS one. 12, e0185305.
92. Zhang, X., Goncalves, R., Mosser, D.M. (2008): The isolation and characterization of murine macrophages. Curr Protoc Immunol. 83, 14.11. 11-14.11. 14.
93. Zhang, X., Loewen, N., Tan, O., Greenfield, D.S., Schuman, J.S., Varma, R., Huang, D., Francis, B., Parrish II, R.K., Kishor, K.S. (2016): Predicting development of glaucomatous visual field conversion using baseline Fourier-domain optical coherence tomography. Am J Ophthalmol. 163, 29-37.
94. Zhang, X., Ognibene, C.M., Clark, A.F., Yorio, T. (2007): Dexamethasone inhibition of trabecular meshwork cell phagocytosis and its modulation by glucocorticoid receptor β. Exp Eye Res. 84, 275-284.
95. Zhou, R., Caspi, R.R. (2010): Ocular immune privilege. F1000 Biol Rep. 2, 3.
96. Zhou, T., Huang, Z., Sun, X., Zhu, X., Zhou, L., Li, M., Cheng, B., Liu, X., He, C. (2017): Microglia polarization with M1/M2 phenotype changes in rd1 mouse model of retinal degeneration. Front Neuroanat. 11, 77.
97. Zhu, Y., Zhang, L., Lu, Q., Gao, Y., Cai, Y., Sui, A., Su, T., Shen, X., Xie, B. (2017): Identification of different macrophage subpopulations with distinct activities in a mouse model of oxygen-induced retinopathy. Int J Mol Med. 40, 281-292.

7 List of figures and tables

Figures

Tables

8.List of Abbreaviations

Abbreviations	Full name
AC	anterior chamber
ACG	angle closure glaucoma
AH	aqueous humor
AMD	age-related macular degeneration
Arg	arginase
α-SMA	α-smooth muscle actin
BMDMs	bone marrow-derived macrophages
CCR	chemokine receptor
CME	cystoid macular edema
CXCL	chemokine ligand
Dex	dexamethasone
DMSO	demethylsulfoxid
ECM	extracellular matrix
EDRF	endothelium derivative relaxing factor
EDTA	ethylendiamintetraacetat
ELISA	enzyme-linked immunosorbent assay
eNOS	endothelial nitric oxide synthase
ER	endoplasmic reticulum
FBS	fetal bovine serum
GCs	glucocorticoids
HP	hydrostatic pressure
HTM	human trabecular meshwork
IFN	interferon
IL	interlukin
iNOS	inducible nitric oxide synthase
IOP	Intraocular pressure
IRI	Inschemia reperfusion injury

JCT	juxtacanalicular
LPS	lipopolysaccharide
MCP	monocyte chemoattractant protein
M-CSF	macrophage colony-stimulating factor
MFI	mean fluorescence intensity
MHC	major histocompatibility complex
MMPs	matrix metalloproteinase
NF-κB	nuclear factor-kappa b
nNOS	neuronal nitric oxide synthase
NO	nitric oxide
OAG	open-angle glaucoma
OCT	optical coherence tomography
OHT	ocular hypertension
ONH	optical nerve head
PACG	primary angle-closure glaucoma
PBS	phosphate-buffered saline
Pen / Strep	Penicillin / Streptomycin
POAG	primary open-angle glaucoma
RGCs	retinal ganglion cells
ROS	reactive oxygen species
SC	schlemm's canal
SOAG	secondary open angle glaucoma
TGF-β	tumor transforming factor-β
TIMP	tissue inhibitor of metalloproteinase
TLR	Toll-like receptor
TM	trabecular meshwork
TNF-α	tumor necrosis factor-α
UG	uveitis glaucoma
VEGF	vascular endothelial growth factor

9 Acknowledgement

I would like to wholeheartedly thank all those who have given me support during my M.D.

First and foremost, I want to thank my supervisor Professor Heinz, who provide me many precious opportunities and constant support during my M.D. He acted as role models to me not only academically but also in life. He gave me many supports and help in academics, and the valuable suggestions. He has shown me, both consciously or unconsciously, how basic and clinical ophthalmology research should be carried out. Without his dedication, motivation and energy to push the boundaries of ophthalmology, this study and many others not covered in this thesis would undoubtedly never had achieved fruition.

I would like to thank to Dr Dirk Bauer and Dr Maren Kasper. In fact, it was Dirk who first suggested and kickstarted the work of this thesis. He developed the model of macrophages under hydrostatic pressure used in this thesis and his works have provided a solid foundation for my work. Dirk and Maren provided precious advice on the experimental design. They taught me to develop good programming habits, volumes of knowledge and techniques covered by this thesis, and helped me a lot with my thesis writing. I would not have been able to complete this study without their help and care.

I would also like to thank all the other members of the Ophtha-Lab that I had the pleasure of working with. Professor Heiligenhaus, Dr Susanne Wasmuth, Dr Martin Busch, Dr Karoline Walscheid, Björn Laffer, Dr Lena Wildschütz, Tida Viola Jalilvand and Kevin Gilhaus shared the experimental and clinical expertise and providing precious advice. I also want to thank all the members for looking after me with such kindness and patience in Germany. We celebrated birthdays and special days together, visited good restaurants, played with puppies and told all the funny (and not-so-funny) jokes. I felt like been loved and been in a family.

I must say thank to Professor Yanning Yang, who is my supervisor in Wuhan University during my Master, for her kind help. I also want to thank all the members in the St. Franziskus Hospital that I had the pleasure of talking with. I am very thankful for all my friends, in both China and Germany, for their care and love.

I am indebted to my motherland for raising me, and the China Scholarship Council (CSC), for providing financial support.

Of course, thanks must go to my parents. My parents do not speak English or German and have no idea what macrophage is, but they tried their best to support and encourage me to do what I want. Without their constant support, I would never have had a chance to start and finish a M.D or even to come to study in Germany. They give me the courage and freedom to see a world of infinite possibilities.

I want to thank my boyfriend, Zhiqiang Liu. He drew the figures in the introduction and discussion sessions of this thesis for me. Although he is not an ophthalmologist or scientist, he always listens to me talking about my work with patient and interest. Although he is not in Germany with me, he always concerns about me in all aspects. Without his encouragement and love, it would have been impossible for me to go through the two and a half years without any regrets.

Finally, I would like to thank myself for being with me the whole time.

These were the happiest three years I have had. While challenging, it was undoubtly exciting. Thank you to everyone I have met along the way. 谢谢!

10 Curriculum Vitae

This curriculum vitae is not included in the online version for data protection reasons.